

**US Army Corps  
of Engineers.**

Engineer Research and  
Development Center

*Coastal Inlets Research Program*

**Shinnecock Inlet, New York, Site Investigation  
Report 3, Selected Field Data Report for 1997,  
1998, 1999 Velocity and Sediment Surveys**

Thad C. Pratt and Donald K. Stauble

February 2001

20010404 065

The contents of this report are not to be used for advertising, publication, or promotional purposes. Citation of trade names does not constitute an official endorsement or approval of the use of such commercial products.

The findings of this report are not to be construed as an official Department of the Army position, unless so designated by other authorized documents.



PRINTED ON RECYCLED PAPER

# **Shinnecock Inlet, New York, Site Investigation**

## **Report 3, Selected Field Data Report for 1997, 1998, 1999 Velocity and Sediment Surveys**

by Thad C. Pratt, Donald K. Stauble

Coastal and Hydraulics Laboratory  
U.S. Army Engineer Research and Development Center  
3909 Halls Ferry Road  
Vicksburg, MS 39180-6199

Final report

Approved for public release; distribution is unlimited

# Contents

---

Preface .....	v
1—Introduction.....	1
Background .....	1
Geology and Geomorphology.....	2
Purpose.....	3
Approach.....	3
2—Data Presentation .....	4
ADCP Velocity Data 1997,1998,1999 .....	4
Equipment .....	4
Method .....	4
Location.....	5
Sediment Data .....	5
3—Data Analysis .....	8
ADCP Velocity Data 1997,1998,1999 .....	8
1997 Survey.....	8
1998 Survey.....	8
1999 Survey.....	9
Sediment Data .....	9
Flood shoal .....	9
Throat .....	11
Ebb shoal .....	11
Adjacent beaches.....	13
4—Summary .....	15
ADCP Velocity Data 1997,1998,1999 .....	15
1997 Survey.....	15
1998 Survey.....	15
1999 Survey.....	16
Sediment Data .....	16
References.....	18

**Figures 1-16**

**Tables 1-4**

**Plates 1-27**

**SF 298**

# Preface

---

This study was conducted by the U.S. Army Engineer Research and Development Center (ERDC) (formerly U. S. Army Engineer Waterways Experiment Station (WES)), Coastal and Hydraulics Laboratory (CHL), Estuaries and Hydroscience Division (E&HD). The Inlet Field Investigation Work Unit 32931 provided funding for this study, Coastal Inlets Research Program (CIRP). Mr. Thad C. Pratt was the CIRP Principal Investigator, Dr. Nicholas Kraus was the Technical Manager, and Mr. E. Clark McNair was the CHL Program Manager for CIRP. Messrs. John Bianco, Charles Chesnutt, and Dr. Barry W. Holliday were the program monitors at Headquarters, U.S. Army Corps of Engineers. The U.S. Army Engineer District (USAED), New York, provided additional support for data collection and studies at Shinnecock Inlet.

Work was performed under the general supervision of Dr. Robert T. McAdory, Chief, Tidal Hydraulics Branch, E&HD; Dr. William H. McAnally, Chief, E&HD; Dr. Joan Pope, Chief, Coastal Evaluation and Design Branch (CE&DB), CHL; Mr. Charles C. Calhoun, former Assistant Director, CHL; and Dr. James R. Houston, former Director, CHL. The data collection program was designed by Mr. Pratt and Dr. Donald K. Stauble, CE&DB. The data were collected by Dr. Stauble; Messrs. Pratt and Howard A. Benson, E&HD; Dr. Adelle Militello, Coastal Hydraulics Branch, CHL; Ms. Kerry Donahue, USAED, New York; and Dr. William Grosskopf and staff of Offshore & Coastal Technologies, Inc. Data reduction was performed by Dr. Stauble; Ms. Marian Howze, contract student; Mr. Daryl S. Cook, contractor with Digital Information & Mapping Company; and Ms. Clara J. Coleman, E&HD. This report was prepared by Mr. Pratt and Dr. Stauble with graphical and editing assistance by Mr. Cook and Ms. Coleman.

The authors acknowledge the assistance and advice generously provided by their co-worker, Dr. Nicholas Kraus. Ms. Lynn Bocamazo and Ms. Diane Rahoy recovered much of the historical data from the archives at the USAED, New York, and provided valuable technical assistance. Other data were supplied by Messrs. Fred Anders and Mohabir Persaud, New York State Department of State; Mr. Jay Tanski, New York Sea Grant; and Mr. W. Gray Smith, Moffatt & Nichol Engineers.

At the time of publication of this report, Dr. James R. Houston was Director of ERDC, and COL James S. Weller, EN, was Commander.

*The contents of this report are not to be used for advertising, publication, or promotional purposes. Citation of trade names does not constitute an official endorsement or approval of the use of such commercial products.*

# 1 Introduction

---

## Background

Shinnecock Inlet is the easternmost of six tidal inlets in the barrier island chain that runs along the south shore of Long Island, NY (Figure 1). The barrier islands and spits enclose a series of coastal bays and tidal marshes. Shinnecock Inlet is located in Suffolk County, 153 km by sea east of the Battery, at Manhattan, and 60 km southwest of Montauk Point. Two rubble-mound jetties constructed in the early 1950s stabilize the inlet. A Federal navigation channel connects the Atlantic Ocean to Shinnecock Bay, through which boaters can access the Long Island Intracoastal Waterway. Shinnecock Bay is an irregularly shaped body 14.5 km long (east-west) and 0.6 to 4.5 km wide, with water depths mostly less than 2 m. The bay is connected by the Quogue and Quantuck Canals to Moriches Bay to the west and by the Shinnecock Canal to Peconic Bay on the north. Several small creeks drain into the northern side of the bay, including Penniman, Stone, Phillips, and Weesuck. These creeks do not provide much freshwater input. The total water surface area of Shinnecock Bay is about 4,100 hectares (10,240 acres). A fish-handling facility is located just west of the inlet on the north side of the barrier. The commercial fishing fleet depends upon Shinnecock Inlet for access to offshore fishing grounds because the only alternate route is Moriches Inlet, several hours distant.

During the last two decades, the beach west of the west jetty has eroded severely, and the highway has been over-washed during many winter storms. In addition, Shinnecock is notorious for being one of the most dangerous inlets on the East Coast because of waves and turbulence. Several boaters, therefore, have been killed in accidents. Both jetties have needed repair, and scour holes over 20 m deep have needed filling.

Several New York District-sponsored tidal inlet current monitoring studies have been conducted at Shinnecock Inlet since 1992 to monitor scour hole formation and development. These efforts complement the Fire Island to Montauk Point Reformulation Study (FIMPRS), which is examining coastal processes, shore protection, and flood damage reduction alternatives from Fire Island Inlet eastward to Montauk Point. The Coastal Inlets Research Program (CIRP) sponsored a field-monitoring program at Shinnecock Inlet during 1997, 1998, and 1999. The fieldwork included current measurements and sediment sampling in the channel, the Atlantic Ocean, and Shinnecock Bay.

## Geology and Geomorphology

Long Island is the southern boundary of Pleistocene glacial advance on the eastern end of the North American continent. Two end moraines mark this boundary and form the physiographic backbone of Long Island. The southernmost moraine, the Ronkonkoma Moraine, extends parallel to the Connecticut mainland and forms the southern peninsula of eastern Long Island and outcrops in cliffs at Montauk Point (Williams 1976). The shoreline of eastern Long Island is composed of a headland cliff coast with pocket beaches at Montauk Point west for around 30 km to a bluff-backed coast at the town of East Hampton. West of East Hampton to the town of Southampton (18 km), the coast is called the ponds region (Morang, in preparation) and is characterized by a low-relief, sandy headland attached beach with numerous coastal ponds. These ponds are occasionally open to the ocean via inlets, particularly during storm events, but the inlets close off due to longshore drift during fair-weather conditions. At Southampton a narrow, low-relief barrier spit extends west from the mainland shore 6 km to Shinnecock Inlet. West of Shinnecock Inlet to Moriches Inlet (24 km) the shoreline is composed of a narrow, low-relief barrier island. Historic maps dating back to colonial times show that there have been periodic inlet openings along this barrier spit/island area (Cialone and Stauble 1998).

The present day Shinnecock Inlet was formed by a hurricane on 21 September 1938 which breached the then barrier spit into Shinnecock Bay. Local and Federal interests have constructed two jetties to maintain the inlet at its present location. Various modifications and additions to the structures and dredging events have occurred over time to stabilize the inlet and navigation channel (Cialone and Stauble 1998). Ebb shoal morphology and other studies (Colony 1932; Krinsley et al. 1964; Warnke and Stauble 1971) indicate that the net drift is to the west along the Long Island coast.

A detailed history of the geomorphic evolution of the inlet since its formation can be found in Morang (1999). The most recent bathymetry of Shinnecock Inlet was collected by the Scanning Hydrographic Operational Airborne Lidar Survey (SHOALS) on 28 May 1998. The SHOALS lidar bathymetry (Irish et al. 1995) is limited by depth and water clarity. Areas of the throat where there are scour holes were too deep for the SHOALS to penetrate and were missing from the survey. The New York District did a standard Fathometer survey of the navigation channel through the throat of the inlet from one of their survey boats on 4-6 March 1998. The digital data from both surveys were combined into TERRAMODEL GIS software and geo-rectified using a vertical datum of National Geodetic Vertical Datum (NGVD) 1929 (All depths herein cited are in meters, referenced to the NGVD 1929). The combined bathymetry was contoured at a 0.6-m interval (Figure 2). A digital terrain model (DTM) was constructed to provide a three-dimensional view of the inlet bathymetry (Figure 3). The morphological features of the inlet include the ebb shoal on the ocean side. This ebb shoal has an asymmetrical downdrift (to the west) offset and is bisected by a dredged navigational channel that cuts across the crest of the ebb shoal. The main mass of the ebb shoal is opposite Tiana Beach where the shoal attaches to the beach to the west of the inlet in the vicinity of the County park. The attachment point can be seen where the shoreline protrudes seaward. The

throat section between the two jetties has two scour holes, one on the ocean side next to the end of the west jetty and one on the bay side next to the east jetty. A linear shoal cuts across the throat from the west bay side to the east ocean side. The oblong flood shoal is located immediately on the bay side of the throat. Due to the close proximity of the flood shoal to the throat, the navigation channel splits into east and west channels that curve around the edges of the flood shoal. The flood shoal has several shallow flood channels that flow through the shoal into Shinnecock Bay, along with several sand flats that are exposed at low tide.

## Purpose

The purpose of this report is to assemble and document field-collected current measurements and sediment sample data collected at Shinnecock Inlet in one volume. The main objective of the current measurements was to obtain tidal current profiles and distributions across the inlet channel with particular emphasis on scour hole locations. Additional data were collected at back-barrier channels immediately north of the inlet. Data were collected for specific time periods to capture physical phenomena observed at the site.

Collection and comparison of these current data to bathymetric data collected by the New York District will help to calibrate and verify tidal circulation, hydrodynamic, and wave simulation models presently being developed at the U.S. Army Engineer Research and Development Center (ERDC), Coastal and Hydraulics Laboratory (CHL). These current data will also help to examine the relationship between current patterns and scour hole formation.

## Approach

The individual surveys were conducted with adherence to accepted scientific and engineering principles to provide technically correct, defensible results. The studies were constructed to incorporate existing information from previous studies whenever possible to provide better understanding of the data collected. Current measurements were made using an Acoustic Doppler Current Profiler (ADCP). This instrument was mounted over the side of the vessel and submerged sufficiently under the water to keep the instrument face below the surface during rough conditions. The survey lines were located prior to running the field collection. The district supplied ERDC-CHL with a digital .DGN file depicting the shoreline and jetty location for line layout and navigation purposes. The individual lines were laid out inside and outside the jetty depending on the problem being addressed in each survey. HYPACK navigation software was used in conjunction with Differential Global Positioning System (GPS), to maintain line repeatability throughout the survey. This software was also used to locate sample point locations for the bed material samples which were collected using a bucket dredge sampler throughout the whole system.

## 2 Data Presentation

---

### ADCP Velocity Data 1997, 1998, 1999

#### Equipment

For the 1997, 1998, and 1999 field experiments, tidal currents were measured with a 1200-kHz and a 600-kHz acoustic frequency BroadBand Acoustic Doppler Current Profiler (BroadBand ADCP) manufactured by RD Instruments of San Diego, CA. These instruments measure current velocities by transmitting pulses of sound and measuring the Doppler shift of the reflected sound off of matter suspended in the water. This method assumes that the particles are moving at the same velocity as the water. By time-gating the returned signal and knowing the speed of sound in water, the BroadBand ADCP associates different periods in the returned signal with different ranges of depth (bins). The water velocity for these depth bins can then be calculated. The TRANSECT software program provided by RD Instruments, in conjunction with a laptop computer, enabled the raw current data to be interfaced with the Differential Global Positioning System (DGPS). This software can replay the raw data and convert it to ASCII format.

The ADCPs have a vertical resolution of 0.5 m. The measurements are made remotely at regular intervals of time and space throughout the water column, thus generating a cross-sectional current profile. An additional advantage of the BroadBand ADCP is that the survey boat does not need to be stationary during the measurement. The instrument subtracts vessel motion from the raw data to produce earth-referenced current vectors. Thus, the survey mobility was greatly increased with the application of the BroadBand ADCP.

#### Method

The ADCPs were mounted on the side of the collection platform using specially designed mounts that allow use with varying hull configurations. The vessels used in the three surveys varied in type and size. The instrument was mounted to the gunnel of the boat and secured forward and aft with mooring lines. The level of the instrument in the water column was adjusted to keep the instrument face below the water surface. A blanking distance was set for each instrument based on the frequency used. The bin size was set for 50 cm. The bin

size is the discrete length of the water column into which the velocity profile is divided. The profile is a series of measurement points one bin size apart for the entire water column. The instrument collects the velocity data at a fixed sampling rate, which is a function of the depth of water and the time of travel of the acoustic signal. At this site, the instrument was collecting a velocity profile every 6 sec.

The starting and ending position data were recorded in HYPACK (hydrographic survey package) for processing the velocity data for further use. Each line was repeated during the separate surveys on an hourly basis. This was done to capture the peak velocities for ebb and flood flows at the inlet. The area of focus was different for each of the surveys.

### **Location**

Figures 4-7 show the ADCP transect lines for each of the respective surveys. The 1997 survey was focused on the channel inside the jetty structures and the channel immediately in front of the fishing fleet dock area. The 1998 survey was also focused on the same area as the 1997 survey, but additional lines were added to capture the conditions at the tip of the east jetty. Additional ADCP transect lines were added outside the inlet west of the west jetty to capture conditions during maximum flood and ebb flows through the inlet. These lines were run perpendicular to the shore in an attempt to capture large-scale eddy patterns believed to exist west of the west jetty. The 1999 survey was focused on a completely different area. The transect lines were laid out on the ocean side of the jetties parallel to each other for a distance of 1,219.20 m from the end of the jetty.

### **Sediment Data**

A set of 116 sediment samples was collected at Shinnecock Inlet from 20-23 July 1998 to identify the grain-size distribution pattern and sediment pathways. Differential GPS was used to locate surface grab samples, which were collected by boat using a bucket dredge on the ebb and flood shoals and in the inlet throat. Surface grab samples were collected with a hand-held scoop on both the updrift and downdrift beaches and on some of the flood shoal, which was exposed at low tide. These samples represent the present day surface sediment distribution. Several patterns of sampling were applied, depending on the area of the inlet. Figure 8 shows the sediment sample positions and Table 1 lists location and statistical data on the samples and use the same notation as presented in the following station descriptions. Bathymetry in Figure 8 is from a SHOALS survey collected 28 May 1998 by helicopter. This data set was augmented with a hydrographic survey collected by boat from the New York District on 5-6 March 1998. SHOALS data are depth limited by water clarity, and scour holes within the inlet throat and areas on the seaward end of the ebb shoal were below the limit of the laser beam penetration (approximately-12.19 m on this particular SHOALS survey). Track lines from the boat survey were merged in TERRAMODEL with the SHOALS data in these areas.

On the ebb shoal a radial pattern was sampled extending from the throat seaward over the back face, crest, and front face of the shoal on five radial lines for a total of 28 samples. Line E (east transect) contained three samples and paralleled the east beach. Line SE (southeast transect) had five samples. Line CL (the center line of the inlet channel) contained six samples, and Line SW (southwest transect) had five samples. Line W (west transect) paralleled the west beach and contained seven samples. Sample W6 was collected off the transect line due to breakers over the ebb shoal in the designated sampling position. Two samples were also collected on a line landward of the west transect in a basin near the west beach (WB1 and WB2), to characterize the sediment deposited in a depression next to the west beach near the west jetty inside the ebb shoal.

Two samples were taken on each of five transect lines across the inlet throat between the east and west jetties for a total of 10 samples. These channel samples were designated as CH A1 through E2 and represented varied throat morphology including two scour holes (CHB2 and CHD1) and a throat shoal on the western side of the channel (CHC2).

Samples were collected in two environments in the area of the bay side flood shoal. Two deeper bay side channels designated as flood shoal tidal channels are used for navigation into Shinnecock Bay and are located around the front side of the flood shoal. Within the East Flood Channel, four samples were collected by boat along the approximate center line of the channel (FCE), and four samples were collected along the center line of the West Flood Channel (FCW). A sample was also collected in the vicinity of the confluence of the East and West Flood Channels in the center line of the inlet throat (FCCL) for a total of nine samples. FCCL was located in an area of mussel beds and was composed of mainly small mussel shells, with some sediment. Samples were collected along three transect lines over the roughly circular-shaped flood tidal shoal, much of which is exposed at low tide, and were designated as Line 1 (FS1-1 to FS1-9) on the ocean side, Line 2 (FS2-1 to FS2-6) across the center of the shoal, and Line 3 (FS3-1 to FS3-6) on the bay side of the flood shoal. A total of 21 samples were collected on the flood shoal. Some of the flood shoal samples were collected from the boat with the bucket dredge, and some in the shallowest areas were collected with a hand scoop by wading in shallow water or walking on dry sand.

Inlet adjacent beaches were also sampled along New York State profile lines, at the high tide (HT), mid tide (MT), low tide (LT) and in the nearshore (OS1) and occasionally (OS2) located approximately 15.2 to 30.5 m seaward of the mid tide sample at time of low tide. These samples were collected by hand scoop and located with a portable differential GPS. Seventeen grab samples were collected between the east jetty and 2,438 m east of the inlet east jetty along Southampton Beach on profile lines P01, P02, P04, and P05 (P designation is for the Ponds Reach). Thirty-one grab samples were collected from the west jetty to 3,048 m to the west along Tiana Beach along seven profile lines W36, W38, W39, W40, W41, W42, and W44 (W is designation for the Westhampton Reach). This brackets the area of ebb shoal attachment to the west beach. Four additional beach samples were collected at the mid tide location at four sites beginning at Montauk Point near profile M34 (around 58 km to the east), Ditch Plains, 366 m east of profile M36 (around 50 km to the east), and at the now closed Mecox

Inlet, 121 m east of profile P20 (14 km to the east) and one site 24 km to the west of Shinnecock Inlet located at the east jetty of Moriches Inlet, 182 m west of profile M1. These samples provide a regional look at beach sediment distributions from the glacially derived cliffs at Montauk Point in the net downdrift direction to the west. The beach at the base of the lighthouse at Montauk Point was mainly a coarse gravel beach, while the other three samples were composed of sand-size material.

# 3 Data Analysis

---

## ADCP Velocity Data 1997, 1998, 1999

### 1997 Survey

The 1997 survey was focused on the interior channel between the jetties as shown in Figure 4. The survey was conducted on 3 December 1997, from 0800 hours through 1400 hours eastern standard time (EST). Ten ADCP transects were collected on the hour during the survey period. The data were processed using the starting and ending points of each line to spatially reference each velocity profile. The spatially referenced data were then imported into HyPAS (Hydraulic Processes Analysis System) (Pratt and Cook, in preparation) software inside ArcView. The data were then depth-averaged to make the plots (Plates 1-7). The data were plotted in vector format in cm/sec. The velocity vectors ranged from 0 to 216 cm/sec for both flood and ebb flows. Table 2 summarizes the physical parameters for each transect-time, total area, average velocity, velocity direction, and discharge.

### 1998 Survey

The 1998 survey was again focused on the interior channel between the two jetties with the addition of a line at the south end of the east jetty and a repositioning of some of the interior lines as shown in Figure 5. The surveys were conducted on 20-22 July 1998. On 20 July, a single line was run across the tide gate that opens into Peconic Bay. Discharges ranged from 20 to 145 cu m/sec. Table 3 summarizes the physical parameters measured at the tide gate range and at an additional transect that was run parallel to the Ponquogue Bridge. Table 3 also summarizes all of the physical parameters measured at the other two surveys inside the inlet structure and west of the west jetty during the 1998 survey. Additional lines were collected west of the west jetty to capture large-scale eddies believed to exist during flood and ebb flows. These additional lines were collected during max ebb and flood flows on 21 July. Plates 8 and 9 are depth-averaged velocity vectors plotted in plan view depicting the eddy patterns. The lines on the interior of the jetty and past the end of the east jetty were collected on 22 July between 0700 hours and 1800 hours EST. Figure 6 depicts the location of the lines for the ADCP survey. Plates 10-21 are

plots of the depth-averaged velocity vectors collected during this survey. The velocities ranged from 0 to 265 cm/sec throughout the flood and ebb flows.

### **1999 Survey**

The 1999 survey was focused on the ocean side of the jetties. The lines were laid out parallel to each other for a distance of 1,219.20 m from the end of the jetty. The intent of the survey was to measure the velocity jet as it left the structures during ebb flow and to capture the velocity jet as it developed and changed during the tidal cycle. Figure 7 shows how the lines were laid out for the ADCP survey conducted on 28-29 July 1999. The survey was conducted with two boats equipped with ADCPs and GPS gear to measure positions. The survey was started at 2100 hours on 28 July and completed at 0200 hours on 29 July. Plates 22-27 are plots of the depth-averaged velocity data collected during this survey. The flow velocities ranged from 0 to 160 cm/sec during maximum ebb flow. Table 4 summarizes the physical parameters measured during the two-boat survey.

## **Sediment Data**

All samples were sieved at quarter-phi ( $\phi$ ) intervals. Phi units are equal to  $-\log_2$  times the sediment diameter in millimeters. Sediment statistics were calculated using the method of moments (Friedman and Sanders 1978). Mean and standard deviation values were calculated for each sediment sample. Shinnecock Inlet had a wide range of mean grain sizes, ranging from the coarse sand to fine sand size range, with some shell and gravel size components. Finer silt material was present on the low energy bay side of the flood shoal, while coarse gravel components were present in the higher energy environments of the inlet throat and in the surf zone along the adjacent beaches. Generally, the samples with coarser gravel, shell, and sands have poorer sorting. Table 1 provides data on sample location and sediment statistics.

### **Flood shoal**

The distribution of grain sizes within the inlet environment is complex. The circular shape of the flood shoal with ebb and flood channels and sediment lobes is shown in Figure 9 of an aerial photograph taken 10 April 1997. The east and west flood channel can be seen flowing around the flood shoal. The flood shoal is divided into two areas with the main body of the shoal directly behind the inlet throat. It is composed of a broad flood ramp in front and the tidal flat in the rear composed of tidal channels and flood and ebb spillover lobes. A narrow deeper channel (dark color on aerial photo) is oriented almost north-south and extends from the flood ramp all the way to the ebb shield at the back side of the shoal. To the west of the main flood shoal is a circular sand body attached to Warner Islands, a vegetated island that is supratidal. Non-vegetated intertidal sand flats with various bed forms and elevations, some of which are exposed at low water, comprise this western shoal feature.

Figure 10 shows the mean grain size distribution plotted as a contour map. The sediment distribution on the flood shoal indicates that a coarser lobe of sand is present directly landward of the inlet throat. The coarsest material was composed of whole and broken shell material from the mussel bed directly landward of the split in the east and west flood shoal channels. Relatively coarse material is present on the ocean side of the flood shoal, and the east and west flood channels. This material is also present in the narrow, shallow central channel, forming an inverted "V" shape as outlined by the  $1.5 \phi$  (0.354 mm) contour. These areas contain material between  $-1.5$  to  $1.0 \phi$  (2.83 to 0.50 mm) composed of quartz sand, gravel, and shell material. To the northwest edge of this "V", the sediment progressively gets finer toward Shinnecock Bay. Sediment in the grass beds behind the shoal are finer than  $2.00 \phi$  (0.25 mm). Surface sediments on the north and west of the "V" on the circular sand flats are composed of medium to fine sands between  $1.50$  to  $2.00 \phi$  (0.354 to 0.25 mm).

A sediment study of the inlet conducted in 1970 (McCormick 1971) showed that the flood shoal at that time was bisected by a central channel that created an east and west flood shoal. The flood shoal was divided into four lobes (a western lobe, eastern lobe, northern lobe, and a small crescent-shaped lobe between the east and west lobes). The main east and west flood channels were also present but were not sampled. McCormick's (1971) sediment sampling area covered a smaller area of the flood shoal region than the present study. Sediment samples were collected from these flood shoal areas, but not from the deeper channels. The general trend was for sands closer to the inlet to be coarser and decrease to the north into the bay (McCormick 1971). The finest material (finer than  $1.5 \phi$ , 0.354 mm) was found in the shallower interior sections of the sand flats. The coarser material (1.5 to  $1.0 \phi$ , 0.354 to 0.5 mm) occurred on the deeper areas of the ocean side of the lobes. While McCormick's (1971) study was restricted to a smaller area of shoal edge and flats adjacent to the inlet throat, the grain sizes (1.3 to  $1.7 \phi$ , 0.41 to 0.31 mm) are within the range of the present study (0.95 to  $2.92 \phi$ , 0.52 to 0.13 mm), which covers a wider area of the flood shoal including deeper channels (coarser sands) and bay side sea grass beds (finer sands). The central channel of 1970 has filled and the present day sand has become coarser in that inverted "V" area. The coarser sands in the front of the flood shoal, the inverted "V" and the east and west flood channels indicate that flows are stronger in these areas. The finer material settles out on the sides of the "V" area of the shoal and in the interior grass beds, where the tidal velocities slow. The west channel sand is coarse along the entire length sampled, as compared to the east channel which, while coarse near the inlet, rapidly fines to the north as it enters Shinnecock Bay. Depth appears to play a role in the sediment distribution, but this difference in east and west channel mean grain size is probably more related to flow strength. Both channels have been dredged in the past and have depths to -6.1 to -7.6 m. McCormick (1971) presents tidal current data which indicates that in the early 1970s, flow into the west channel was more flood dominated (maximum 1.2 m/s flood and 0.9 m/s ebb) than into the east channel (maximum 0.98 m/sec, on both ebb and flood), which was more ebb dominated. Present ADCP readings did not cover the east channel so comparisons of flow characteristics could not be made, but the fine means of the bay side east channel suggest that lower flow rates are found in the east channel.

## Throat

The largest variability in sediment size distribution was found in the throat section between the jetties. The bathymetry indicates a deep hole (-13.4 m) close to the east jetty on the bay side. Figure 11 shows the details of the throat bathymetry and sediment distribution. Sample CHD1, a coarse sand (0.58  $\phi$ , 0.67 mm), and sample CHC1, a fine gravel (-1.47  $\phi$ , 2.77 mm), were collected in the vicinity of this scour hole. A shoal is present on the west side of the throat with a northwest-southeast orientation, extending about half way across the throat width. Sample CHC2, a coarse sand (0.89  $\phi$ , 0.45 mm), was collected on its crest. The deepest scour hole is in the vicinity of the ocean tip of the west jetty and reaches a depth of around -14.6 m. Sample CHB2 was collected in the vicinity of this hole and was a very coarse sand (-0.47  $\phi$ , 1.39 mm).

Samples CHD2 and CHE2, both medium sands (1.16  $\phi$ , 0.45 mm and 1.00  $\phi$ , 0.50 mm respectively) collected on the west side of the bayward end of the throat, were the finest material found between the jetties. ADCP transects collected in this study indicate that the flow velocities on flood are low in this west side as the flow enters the bay. The highest flow across this transect occurs on the east side over the bayward scour hole in the vicinity of sample CHD1 and begins to fan out over sample CHE1, a coarse sand (0.16  $\phi$ , 0.90 mm).

Turbulent conditions occur about one-third of the way into the inlet on the ocean side, especially on ebb flow when standing waves are often present as the outgoing tidal flow interacts with the incoming waves. The coarsest sands collected in the throat are found under this area (CHB1, a coarse sand with a mean of 0.26  $\phi$  (0.83 mm), along with CHB2 and CHC1), and contain up to 40 percent gravel-size material. Samples CHA1, a coarse sand (0.99  $\phi$ , 0.53 mm), and CHA2, a medium sand (1.29  $\phi$ , 0.41 mm), were collected seaward of the west jetty, but still landward of the longer east jetty. Again circulation appears to play more of a role than depth in sediment grain size distribution in the throat area.

Sediment samples collected in 1970 by McCormick (1971) show a pattern of coarsest material down the center line of the throat, with mean values coarser than -0.25  $\phi$  (1.19 mm). The sediment mean grain size became finer (to around 1.50  $\phi$ , 0.354 mm) toward both jetties. No mention of scour holes was made in McCormick (1971), and the mean grain-size pattern may reflect a more uniform inlet channel with the deepest part along the center line of the throat. The present pattern of cross-throat mean grain size reflects the more complex present bathymetry, dominated by the two scour holes and the western throat shoal.

## Ebb shoal

The ebb shoal at Shinnecock Inlet is a crescentic feature with a downdrift westward asymmetry. The present shoal extends south from the east jetty some 914 m into the Atlantic Ocean (Figure 8). The eastern edge of the shoal can be identified by the oceanward deflection of the straight and parallel shoreface

contours about 304.8 m east of the east jetty. The contours return to a straight and parallel nature some 1,524 m west of the west jetty, where the ebb shoal attaches to the beach, for a total alongshore width of 1,828 m.

The present sediment distribution is characterized by coarser material 0 to 1.5  $\phi$  (1.0 to 0.354 mm) on the back side of the shoal crest, in the vicinity of the jetty tips, and in the basin to the west of the throat (Figure 10) which corresponds to the depth greater than -3 m as shown in Figure 8. The area outlined by the 1.5- $\phi$  contour line corresponds to the back side of the ebb shoal and contains the coarser material. The ebb shoal crest is not continuous in its crescentic shape around the ebb shoal, but is bisected by a deeper channel extending directly seaward of the inlet jetties. The material coarser than 1.5  $\phi$  (0.354 mm) includes an area that extends seaward through this area of deeper depths. The crest of the ebb shoal (identified by the area shallower than the -3.1-m contour on the east and west side of this channel) corresponds to the area with a mean grain size range between 1.5 and 2.0  $\phi$  (0.354 and 0.25 mm). The front face of the shoal that slopes seaward from around the -3.1-m contour to the -10-m contour has a mean grain size range between 2.0 and 2.5  $\phi$  (0.25 and 0.177 mm). The shelf, defined as the area seaward of the -6-m contour off the adjacent beaches and deeper than the -10-m contour in front of the ebb shoal, corresponds to a mean grain size finer than 2.5  $\phi$  (0.177 mm).

Previous sediment studies in 1970 by McCormick (1971) in the vicinity of the ebb shoal indicate that the shoal was much smaller in area at that time and appeared to be crescent shaped around the entire width of the ebb shoal. Based on grain size contours (since no bathymetry was available for that time period), the ebb shoal was around 914 m in alongshore width and extended at least 610 m into the Atlantic Ocean. A similar mean grain-size distribution was present within this reduced area, where the coarsest means were found immediately seaward of the jetties in the back shoal (coarser than 1.0  $\phi$ , 0.5 mm). The coarse material extended in a small band to the west immediately behind the shoal crest at that time, but did not extend to the west beach. Material finer than 2.0  $\phi$  (0.25 mm) was present west of the west jetty tip. From the limited sampling of McCormick (1971) in the area of the ebb shoal, the sediment became progressively finer from 1.0 to 2.0  $\phi$  (0.5 to 0.25 mm) from the back shoal basin seaward to the crest of the shoal. His mean grain-size map of the ebb shoal showed a crescentic pattern in this seaward finning across the ebb shoal.

The present day mean grain-size distribution is similar to the 1970 pattern on the ebb shoal, but the mean isopleths are further seaward and cover a larger area, indicating a growth in the ebb shoal, both seaward and downdrift to the west. From 1955 to 1985 the shoal growth rate was approximately 76,500 m<sup>3</sup>/yr (Cialone and Stauble 1998). The coarsest material is found on the back slope of the shoal (present study includes the western basin, where fine material was found in 1970) and at the mouth of the jetties. The mean grain-size distribution gets progressively finer in the seaward direction over the shoal crest and front slope out onto the nearshore shelf. Dredging of the ebb shoal directly off the inlet throat occurred in 1984, and in a designated deposition basin over the ebb shoal in 1990 (510,753 m<sup>3</sup>), 1993 (363,185 m<sup>3</sup>) (Cialone and Stauble 1998), 1997

(191,150 m<sup>3</sup>) (Morang, in preparation), and most recently in 1998 just before the present sediment sampling (26,761 m<sup>3</sup>). As a result of this dredging, the crescentic shape of the 1970 shoal crest has been bisected and coarser material is now found in the area between the east and west shoal crest.

One 12-m and four 6.1-m cores were taken on the east side of the ebb shoal in November 1996 (Alpine 1997). Grain-size data from selected depths within the cores were also reported. Figure 12 shows the locations of the cores, and Figure 13 are logs of the cores. Two of the cores were collected along the -5-m contour mean lower low tide (mllw). Cores 20b and 20a and a-r (lower half of core 20a) were collected along the eastern shoal ocean crest edge and show medium sand with layers of coarser gravel size material at depth. The mean of the surface samples in both cores are similar to the means of the grab samples of this study. Three of the cores (including the 12-m core) were collected around the -6.7-m contour. Cores 20d, 40, and 20c were collected along the front face of the ebb shoal. The surface sample from cores 20d and 20c were anomalously coarse compared with the surface grab samples in the area, but the surface sample from core 40 was similar to the surrounding fine sand surface grab means. The main body of the eastern section of the ebb shoal is composed of medium to coarse sands with some layers of fine sand and gravel beds. Cores 20d and 40 penetrated a mud layer around -11 to -12 m. The long core indicates that this mud deposit is at least 6 m thick. This mud layer indicates that the base of the ebb shoal is around -11 m deep.

### **Adjacent beaches**

The adjacent beaches east and west of the inlet have experienced erosion since dredging of the ebb shoal (Cialone and Stauble 1998). Prior to ebb shoal dredging, the east beach had been accretional and had impounded sand at the east jetty, producing an updrift offset to the inlet. At the time of sediment sampling the east beach had a 1.0 to 1.5-m scarp in the vicinity of the east jetty.

The west beach has eroded, forming an embayment between the west jetty and the area of ebb shoal attachment, which is presently visible as a protuberance in the shoreline centered around 1,219 m west of the west jetty (Figures 8 and 9). Beach-fill material has been placed by Federal, state, and local interests in the eroded area generally between profiles W41 and W44 since 1984 to prevent serious overwash and island breaching and to protect the harbor infrastructure and access road, located on the bay side of the island. Exact records of fill volumes and dates were difficult to find but Morang (in preparation) lists 11 fill events since 1984 to 11 July 1998 that have placed around 795,184 m<sup>3</sup> of sand from various borrow areas on this west beach area.

Sediment samples were collected at the high tide (HT), mid tide (MT) and low tide (LT) area to provide a representative sediment distribution of the beach foreshore area and one or two samples in the nearshore averaging 3.2 to 18.3 m distance offshore of low tide to depict the nearshore sediment distribution. The collection of nearshore samples (listed in Table 1 as OS1 and on profiles W36, W39, and P03, an OS2 sample) varied in seaward distance depending on the

beach slope. The shortest distance offshore was on profiles P01 and P03, which had the steepest nearshore slope, and the longest distance offshore was at profiles W40 and W41, which had the flattest nearshore slope associated with the shoreface attachment of the ebb shoal. On profile W38 a ridge and runnel feature was present, and a sample was collected from the ridge crest (RC).

There was a high degree of variability in the sediment distributions of the individual samples due to the presence of gravel and shell material at some of the sample locations. The beach sand means ranged from gravel to medium sand. In general, the coarsest material was found in the low tide area, where the uprush and backwash turbulently interact with the incoming surf. The finest material was generally found in the nearshore samples, with the high tide and mid tide sample means falling in between. Exceptions to that rule were found on the east beach where all the samples from high tide to nearshore contained a large percentage of coarse gravel and shell material, making the east beach samples coarser than the west beach. The finest material was found at profile W38 on the west beach just downdrift of ebb shoal attachment. At that profile the sediment was well sorted, medium sand from high tide grading to fine sand in the nearshore. The highest variability in individual samples was found on this west beach. These beaches have been under the influence of ebb shoal attachment, storm erosion, repeated beach fills, and possible drift reversal west of the ebb shoal attachment, which have caused a wide variety of different wave and current processes to be active along this stretch of coast.

To reduce some of the variability in characterizing the adjacent beach samples, mathematical composites were computed from the one-fourth  $\phi$  sample distributions. The profile composite contained the mathematical average of the HT, MT, LT, and OS1 samples. Figure 14 shows a plot of the composite mean grain size relative to distance east and west of the inlet. The beach samples become increasingly coarser toward the east jetty, the direction of net westerly longshore drift. The coarse gravel size material is a lag deposit with an original source from the nearby glacial till material found in the Ronkonkoma moraine. Storm waves have eroded the east beach leaving the coarse material behind, forming a steep beach with .5- to 1.5-m-high erosional scarps. The most prominent scarp is found on the beaches closest to the east jetty.

The west beach composite means show the influence of the asymmetrical ebb shoal offshore of these profiles. The finest composite means are found at profile W44 (adjacent to the west jetty) and downdrift of the attachment point of the ebb shoal at profile locations W39, W38, and W36. These beaches have in general flatter slopes, particularly in the area of shoal attachment. Finer material from the ebb shoal may be transported around the shoal and be deposited on these western beaches. The coarsest means on the west beach were found on the east (updrift) side of the shoal attachment, in the area of profiles W40, W41, and W42. This is the location of the numerous beach-fill placements. A localized drift reversal, due to wave refraction around the ebb shoal and the erosive nature of these profiles, results in deposition of only coarse material on these beaches and a winnowing out of the finer sediments which are most likely transported to the east to profile W44.

# 4 Summary

---

## ADCP Velocity Data 1997, 1998, 1999

### 1997 Survey

The 1997 survey was focused on the interior channel between the jetties. Velocities reached 216 cm/sec during the tidal cycle. On flood tide, the flow through the jetties seemed to align itself with the jetties until the entrance to the bay. At the point of entry into the bay, a smaller portion of the flow diverted to the east, but the majority of the flow went over the flood shoal and to the west in front of the fishing fleet area. On ebb tide, the flow comes from the west with the greatest velocity and splits off the northwest corner of the west jetty. A jet of water moves across the channel and impinges the east jetty. A scour hole seems to have developed on the east jetty where the jet impinges the structure. The location of the lines did not allow for capturing the flow around the end of the west jetty on the ocean side. In future surveys, the line locations need to be slightly adjusted to capture the flow as it enters the jetty structures.

### 1998 Survey

The 1998 survey was again focused on the interior channel between the two jetties with the addition of a line at the south end of the east jetty and a repositioning of some of the interior lines. Additional lines were collected west of the west jetty to capture large-scale eddies believed to exist during flood and ebb flows. These additional lines were collected during maximum ebb and flood flows. The eddy patterns seem to rotate in the same direction for flood and ebb flows. The eddy has a clockwise rotation pattern moving from the west to the east along the shore. The eddy pattern is not as evident during flood flow, but the flow pattern along the shoreline is the same for both conditions. The flow moves out along the west jetty. On ebb flow, the velocities follow the jet out of the inlet, but on flood flow, the water flows south along the west jetty and turns sharply east around the end of the west jetty into the inlet. The end of the west jetty has subsequently scoured in response to the large velocities present. The data collected on the interior of the structures capture flows as they develop through different tidal conditions. The velocities ranged from 0 to 265 cm/sec throughout the flood and ebb tide. The accretion zones along the west jetty are most likely caused by the eddy patterns that developed during ebb and flood flows. Flow separated off the northwest side of the west jetty and caused a

clockwise eddy pattern along the jetty that slowed the flow down. The slower flow allows the sand to fall out. On flood flow, the velocities separate along the west jetty and cause an eddy pattern to develop in the same area as the ebb flow. At both stages of the tide a slower velocity region exists along the west jetty where accretion is occurring.

### 1999 Survey

The 1999 survey focused on the ocean side of the jetties. The lines were laid out parallel to each other for a distance of 1,219.20 m from the end of the jetty. The intent of the survey was to measure the velocity jet as it left the structures during ebb flow. The intent was to capture the velocity jet as it developed and changed during the ebb cycle. The flow velocities ranged from 0 to 160 cm/sec during maximum ebb flow. The velocity jet developed on the east side of the inlet as the ebb flow developed. The jet seemed to start on the east side and migrate westward as the distance increased from the end of the jetties. As maximum ebb flow developed, the jet was still greater along the east jetty and it migrated westward as the distance increased from the end of the jetty. The jet followed the direction of the navigation channel cut through the ebb shoal. Once the flow got past the ebb shoal, the jet was indistinguishable.

### Sediment Data

Analysis of the grain size distributions of the sediments at Shinnecock Inlet indicate a wide variety in depositional environments around the inlet. Size and composition of material range from gravel size quartz material and shells to fine sand and silt. Coarse material was found in the high energy areas of the throat where waves interact with the ebb and flood tidal currents, and the sediment is characteristically poor to very poorly sorted (well graded). Other coarse gravel, shell, and sand material was found in both the east and west flood shoal navigation channels and in the intertidal areas of the east beach and inside the shoal attachment area of the west beach. The source of the coarse gravel is reworked glacial till material from the nearby terminal moraine deposits. The shell material is mostly from bivalves, and small fractions were found in all environments. Sample FCCL was collected from a particularly dense *Mytilus edulis* bed (located on the bay side of the inlet throat).

The finest material was found on the bay side of the flood shoal, mostly in seagrass beds and other low energy environments of the shallow Shinnecock Bay. Little wave and tidal current activity must be present for the deposit of this fine material. This is especially true as the thick seagrass baffles the current flow behind the flood shoal. Additional fine sand was found on the seaward edge of the ebb shoal at depths greater than -10 m. These fine-grained deposits were also well sorted (poorly graded).

The majority of the sediment mean grain sizes fall in the sand size range between 0 to 3  $\phi$  (1.0 to 0.125 mm). The sorting is well to moderate. Figure 15 illustrates the distribution pattern of each inlet sample group on a mean versus

sorting plot. The coarser, more poorly sorted samples were collected from the east beach, west beach, and throat channel. Four of the flood channel samples had medium sand means, but were poorly sorted, being composed of a wider range of material including some gravel and shell material. The grouping of the majority of the sample mean and sorting values fell in the moderately well sorted, medium sand range, but shows some distinctive characteristics based on where they were collected. The sorting ranged from well to moderate, and the mean size showed the transition from relatively coarse sands on the east beach overlapping the throat channel samples to the medium sands of the ebb shoal backshoal area and the east beach. The finer mean sizes were found on the ebb shoal crest, front face and shelf, and on the bayward side of the flood shoal and flood channels.

The coarsest material was found on the east beach (average mean  $-0.63 \phi$ , 1.55 mm) followed by the throat channel (average mean  $0.43 \phi$ , 0.74 mm) and the east and west flood shoal channels (average mean  $0.91 \phi$ , 0.53 mm). Finer material was found on the west beach (average mean  $1.23 \phi$ , 0.43 mm), ebb shoal (average mean  $1.53 \phi$ , 0.35 mm), and the finest material was on the flood shoal (average mean  $1.69 \phi$ , 0.31 mm).

The sediment grain-size distributions reflected the depositional processes active at the inlet. Each sediment sample represented the material that is allowed to be deposited in that particular environment. Figure 16 shows the relationship between sediment particle mean grain-size distribution, bathymetry, and depth-averaged ebb velocities. The ebb velocities were a composite of several days of data at similar stages of the tide. The transport energy was a function of the interaction of wave and tidal current energy. The restricted area increased ebb and flood currents in the throat and back side of the ebb shoal. The interaction of incoming waves and tidal currents created turbulent flow conditions in the inlet causing scour hole formation on the tip of the west jetty. The scour hole on the north end of the east jetty seemed to be caused mainly by an ebb flow jet that came off the northwest corner of the west jetty. Only the coarser material could settle out in the most turbulent areas while finer material settled out in the more protected west throat shoal area. A lower energy zone existed along the west jetty behind the inflection point in the channel. This condition seemed to exist for both flood and ebb flows, thus causing a shoaling area to develop. The swash processes along the adjacent beach also restricted the size of material that may settle out. Wave refraction around the ebb shoal differentiated the sediment distribution over the ebb shoal and the attachment area of the west beach. The clockwise eddy pattern west of the west jetty on both flood and ebb flows coupled with the wave processes at the inlet entrance caused the erosion of the beach west of the west jetty. The beach sediments reflected this erosional pattern with fine material along the west jetty and coarser material west of the west jetty before the shoal attachment point. The center of the embayment scour hole exhibited coarser material as expected. As the flood flow left the inlet structures and entered the bay, a finning toward the north occurred. The flows lost energy over the flood shoal dropping heavier material first and carrying finer material farther into the bay. The flood shoal had an inverted "V" shape caused by a remnant channel through the center of the shoal.

# References

---

Alpine Ocean Seismic Survey, Inc. (1997). "Vibracore sampling at Jones and Shinnecock Inlets, Long Island, New York." Prepared for New York State Department of State, Division of Coastal Resources and Waterfront Revitalization, Albany, NY.

Cialone, M. A., and Stauble D. K. (1998). "Historic findings on ebb shoal mining," *Journal of Coastal Research*, 14(2), 537-563.

Colony, R. J. (1932). "Source of sands of the south shore of Long Island and the coast of New Jersey," *Journal of Sedimentary Petrology*, 2, 150-159.

Friedman, G. M., and Sanders, J. E. (1978). *Principals of sedimentology*. John Wiley and Sons, New York, NY.

Irish, J. L., Parsons, L. E., and Lillycrop, W. J. (1995). "Detailed bathymetry of four Florida inlets," *Proceedings of the 8<sup>th</sup> National Conference on Beach Preservation Technology*, FSBPA, Tallahassee, FL, 234-258.

Krinsley, D. H., Takahashi, T., Silberman, M. L., and Newman, W. S. (1964). "Transportation of sand grains along the Atlantic shore of Long Island, New York: an application of electron microscopy," *Marine Geology*, 2, 100-120.

McCormick, C. L. (1971). "Sediment distribution of the ebb and flood tidal deltas, Shinnecock Inlet, Report 3," Submitted to the Town of Southampton, NY, 34.

Morang, A. (in preparation). "Atlantic coast of New York monitoring project, Report 1, analysis of beach profiles, 1995-1996," U.S. Army Engineer Research and Development Center, Vicksburg, MS.

Morang, A. (1999). "Shinnecock inlet, New York, site investigation, Report 1: morphology and historical behavior," Coastal Inlets Research Program, Technical Report CHL-99-32, U.S. Army Engineer Waterways Experiment Station, Vicksburg, MS.

Pratt, T. C., and Cook, D. S. (2000). "HyPAS user's manual: a hydraulic processes analysis system, an extension for ArcView GIS, version 4.0.1," Coastal Inlets Research Program, Technical Report, U.S. Army Engineer Research and Development Center, Vicksburg, MS.

Warnke, D. A., and Stauble, D. K. (1971). "An application of reflected-light differential-interference microscopy: beach studies in eastern Long Island," *Sedimentology*, 17, 103-114.

Williams, S. J. (1976). "Geomorphology, shallow subbottom structure, and sediments of the Atlantic inner continental shelf off Long Island, New York," Technical Paper No. 76-2, U.S. Army Engineer Waterways Experiment Station, Vicksburg, MS.



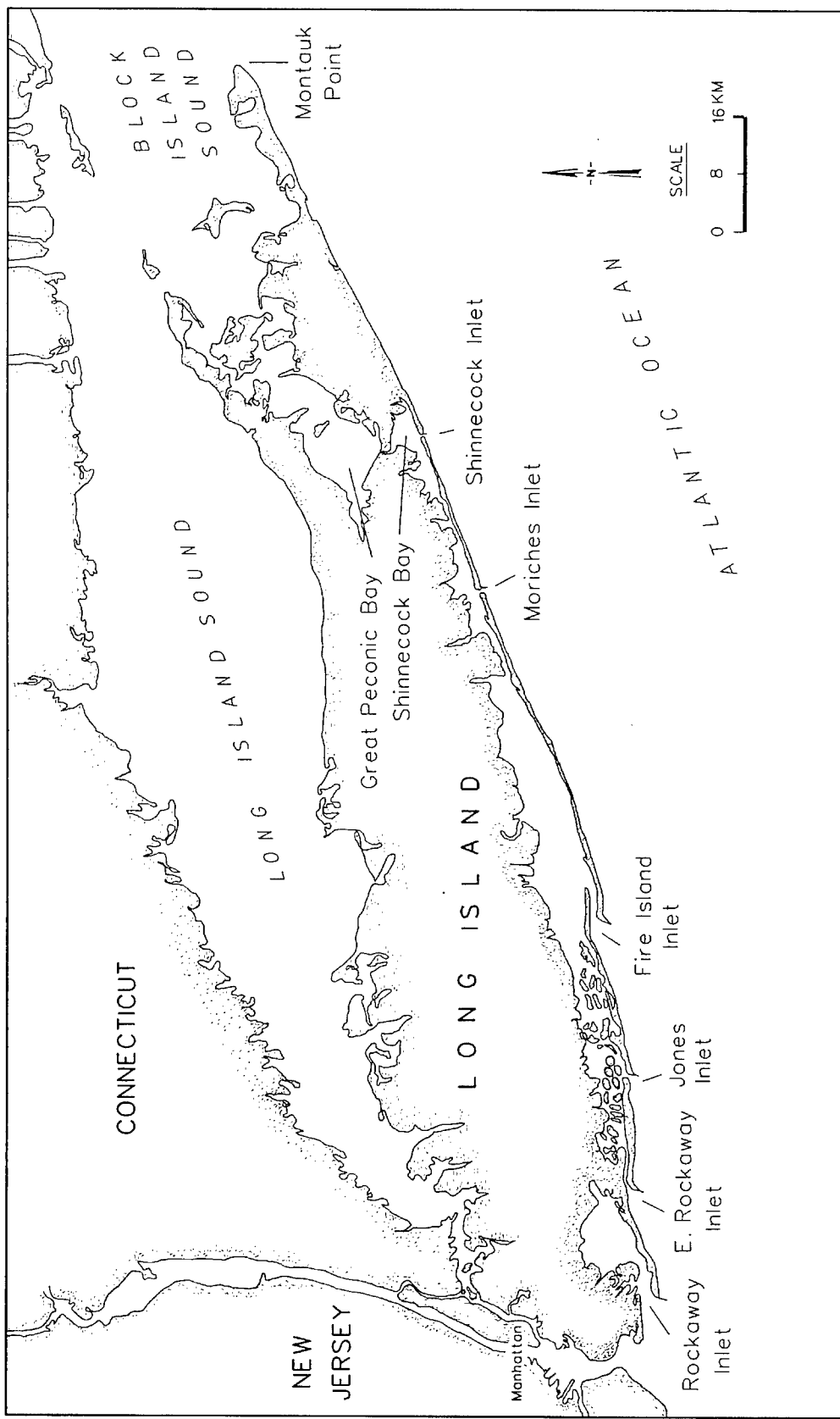


Figure 1. Shinnecock Inlet location map

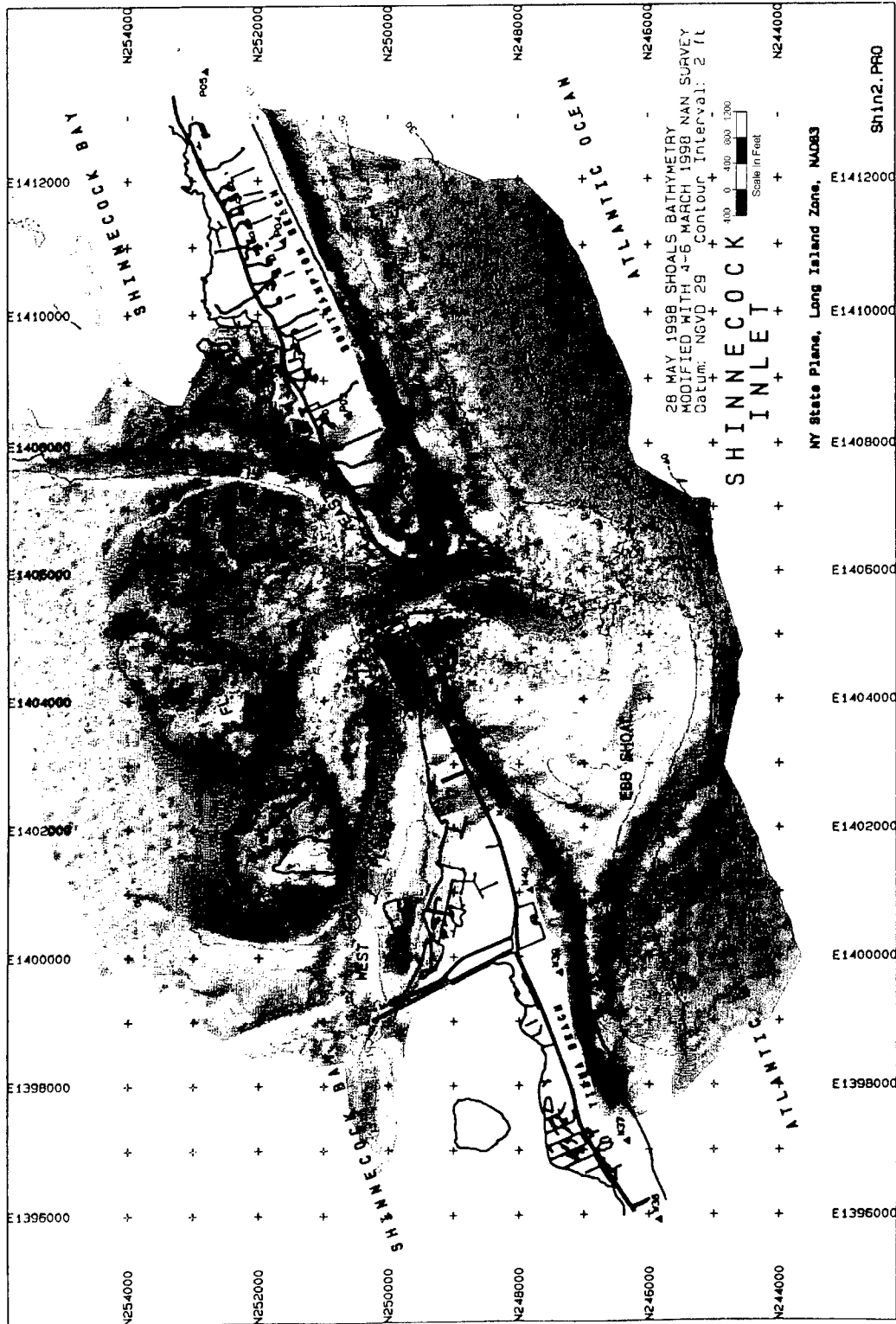


Figure 2. Bathymetry map of Shinnecock Inlet, Long Island, NY. Bathymetry from 28 May SHOALS survey, supplemented with data from 4-6 March 1998 New York District survey (To convert feet to meters, multiply by 0.3048)



Figure 3. Oblique view of bathymetry of Shinnecock Inlet, Long Island, NY from Figure 2, showing configuration of ebb and flood shoals, scour holes in throat, and channels around flood shoal

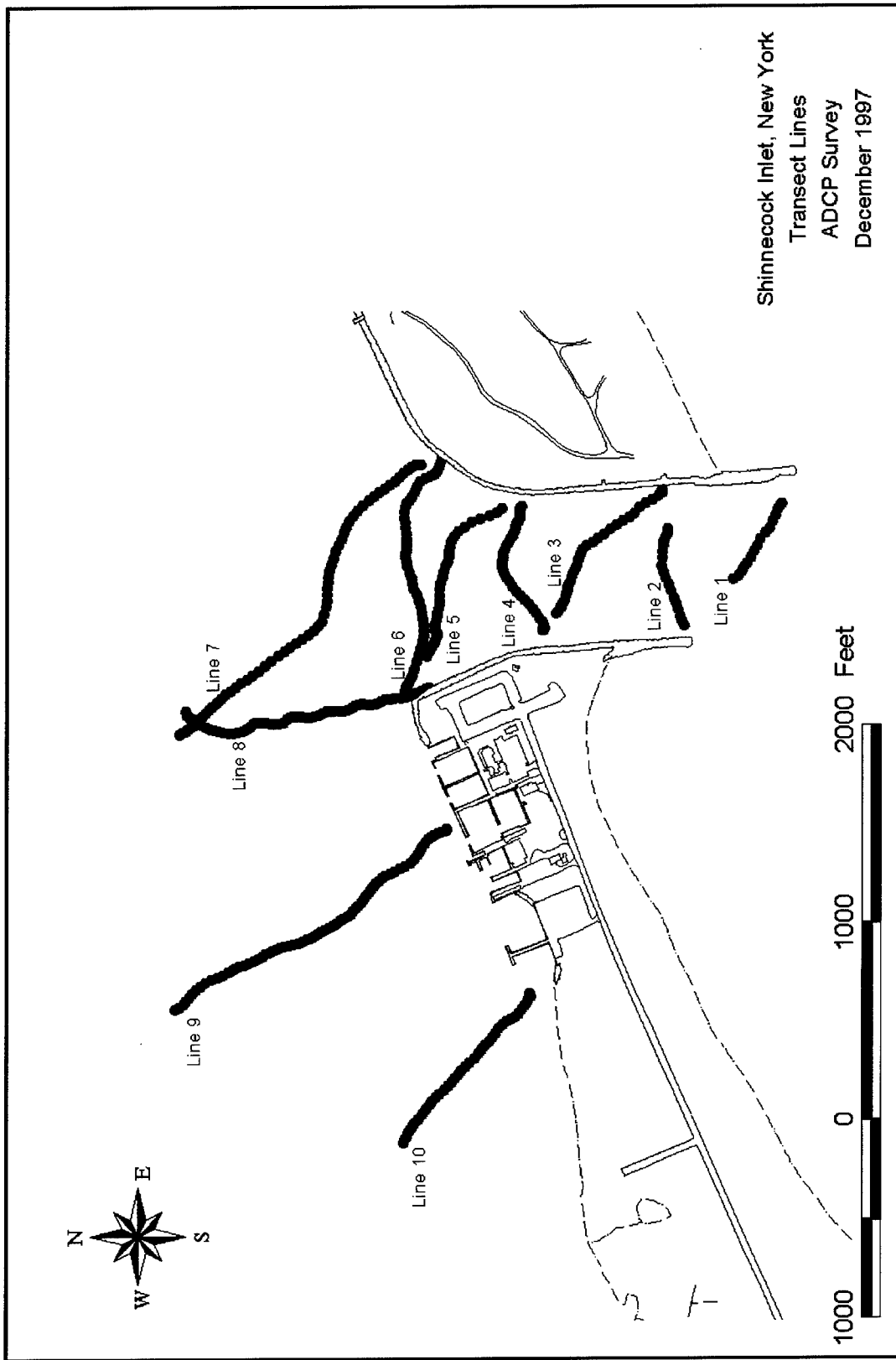


Figure 4. 1997 ADCP transect location map (To convert feet to meters, multiply by 0.3048)

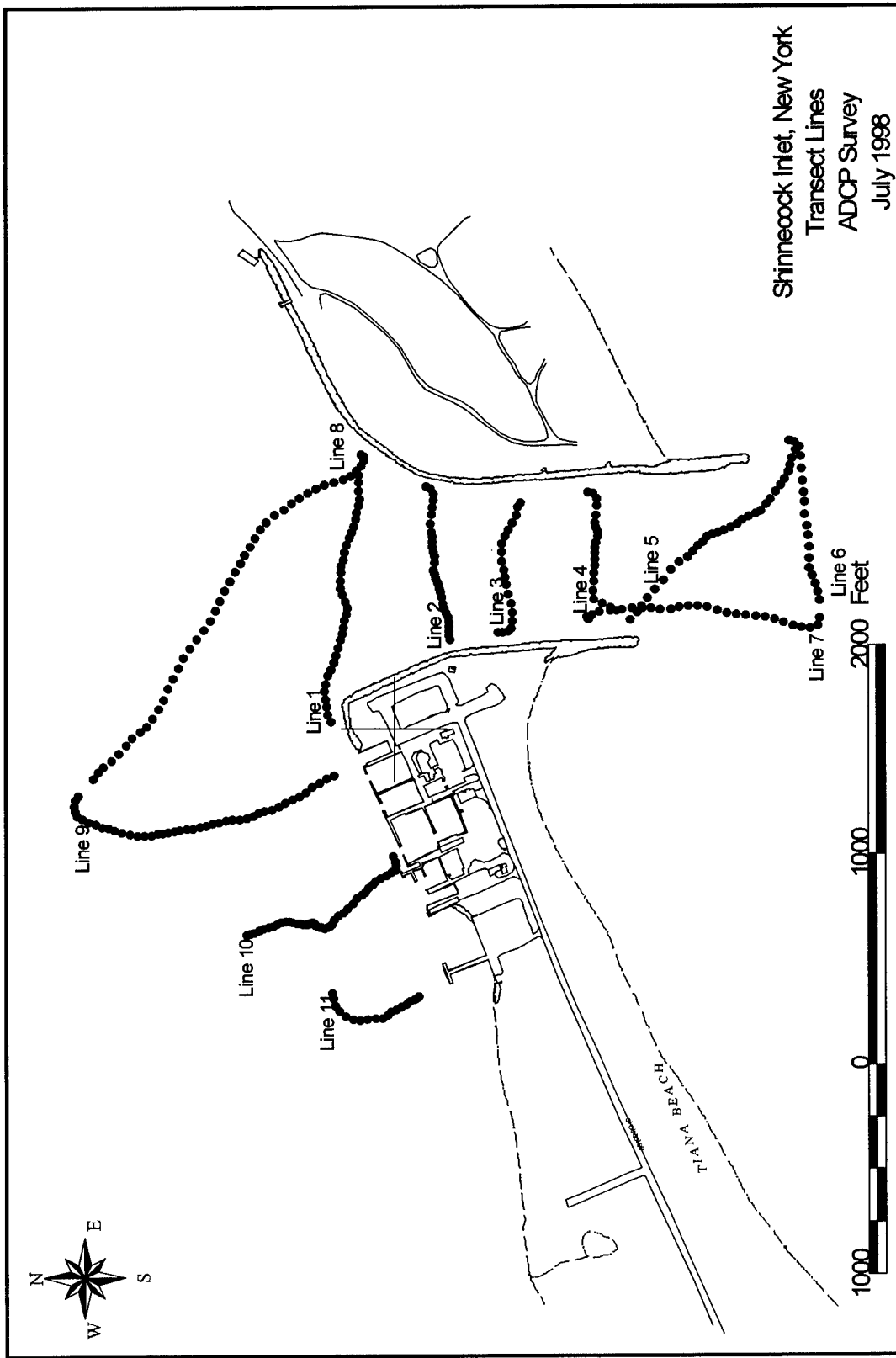


Figure 5. 1998 ADCP transect location map inside the inlet

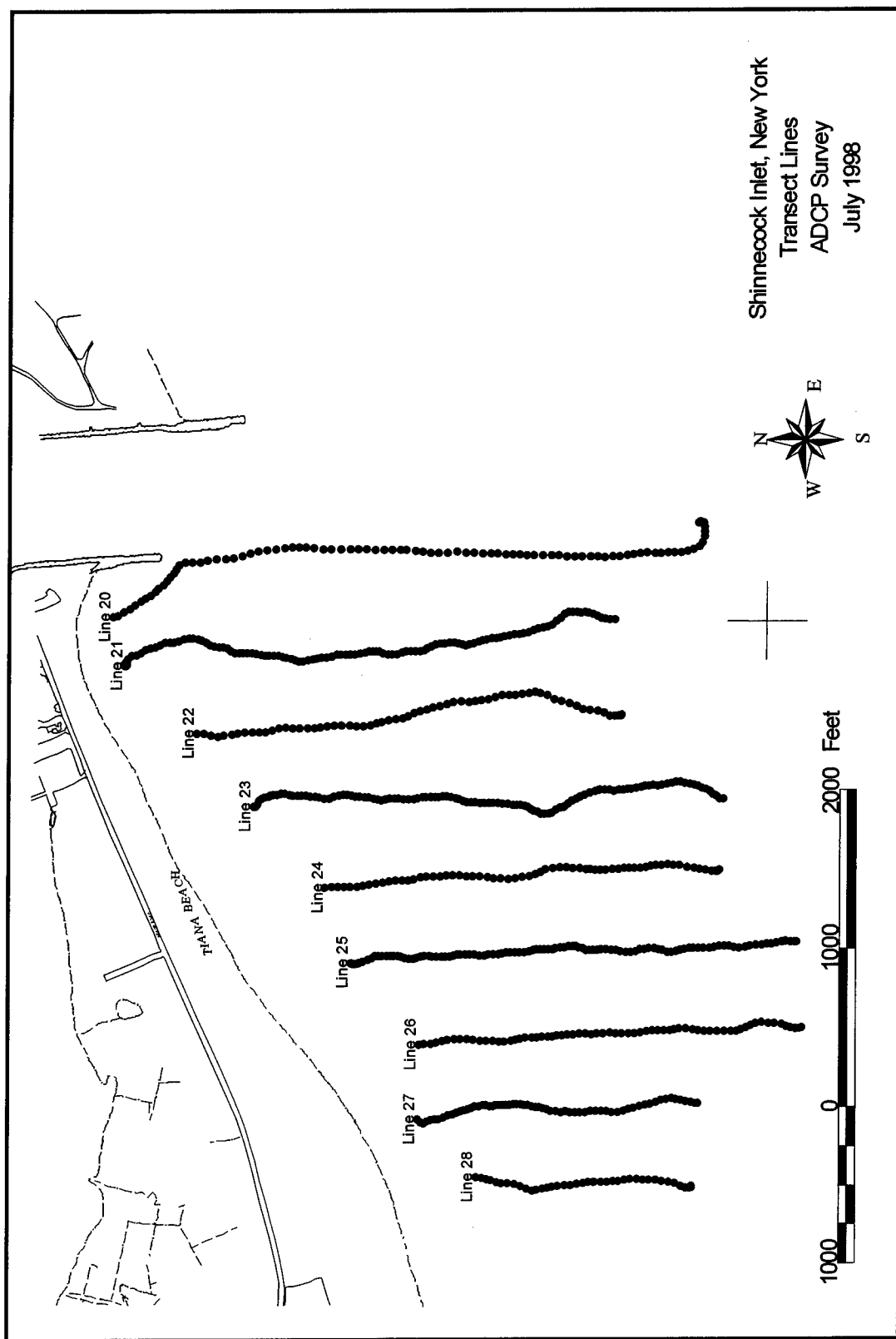


Figure 6. 1998 ADCP transect location map outside the inlet to the west of the west jetty

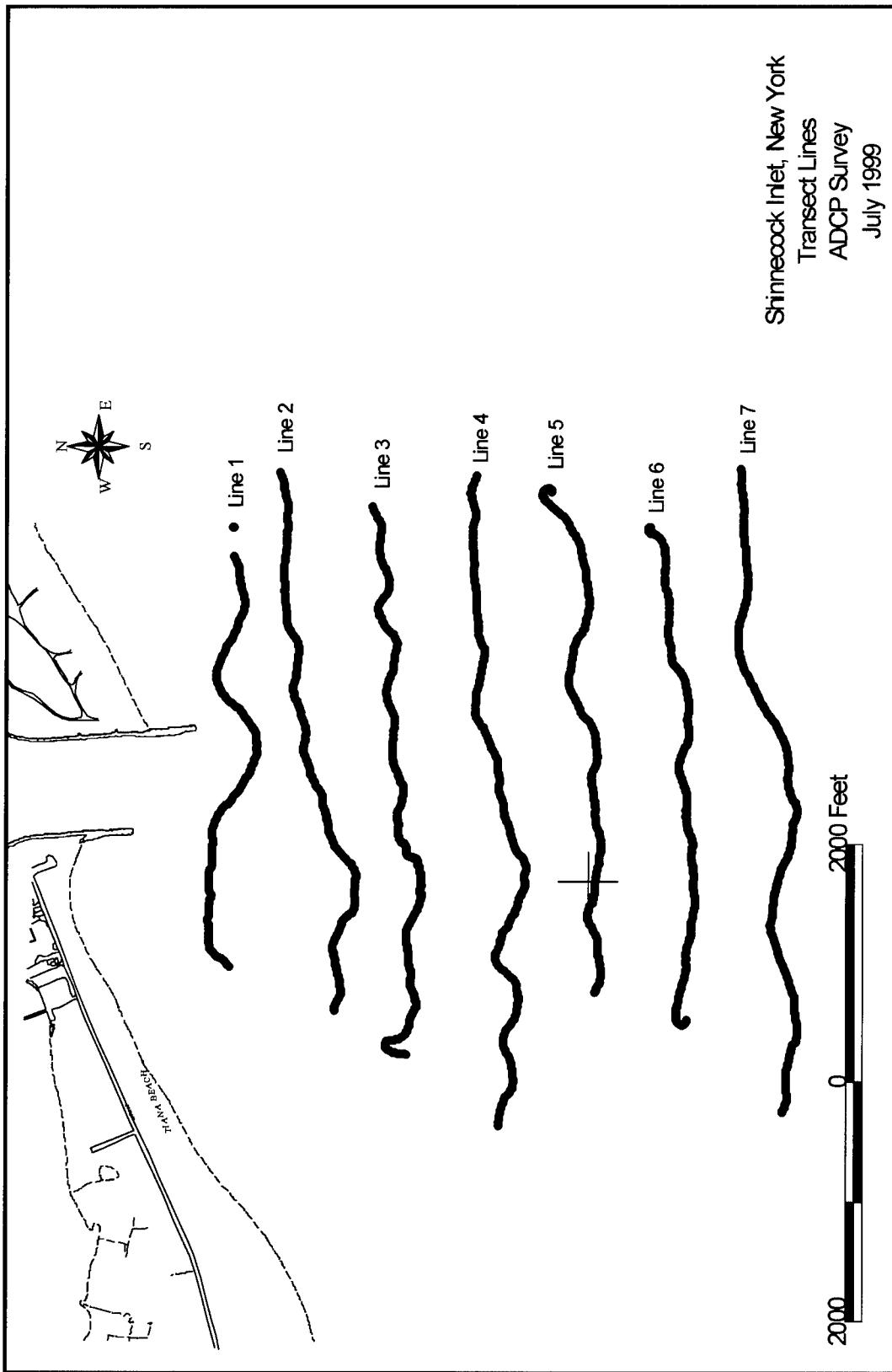


Figure 7. 1999 ADCP transect location map outside the inlet over the flood shoal

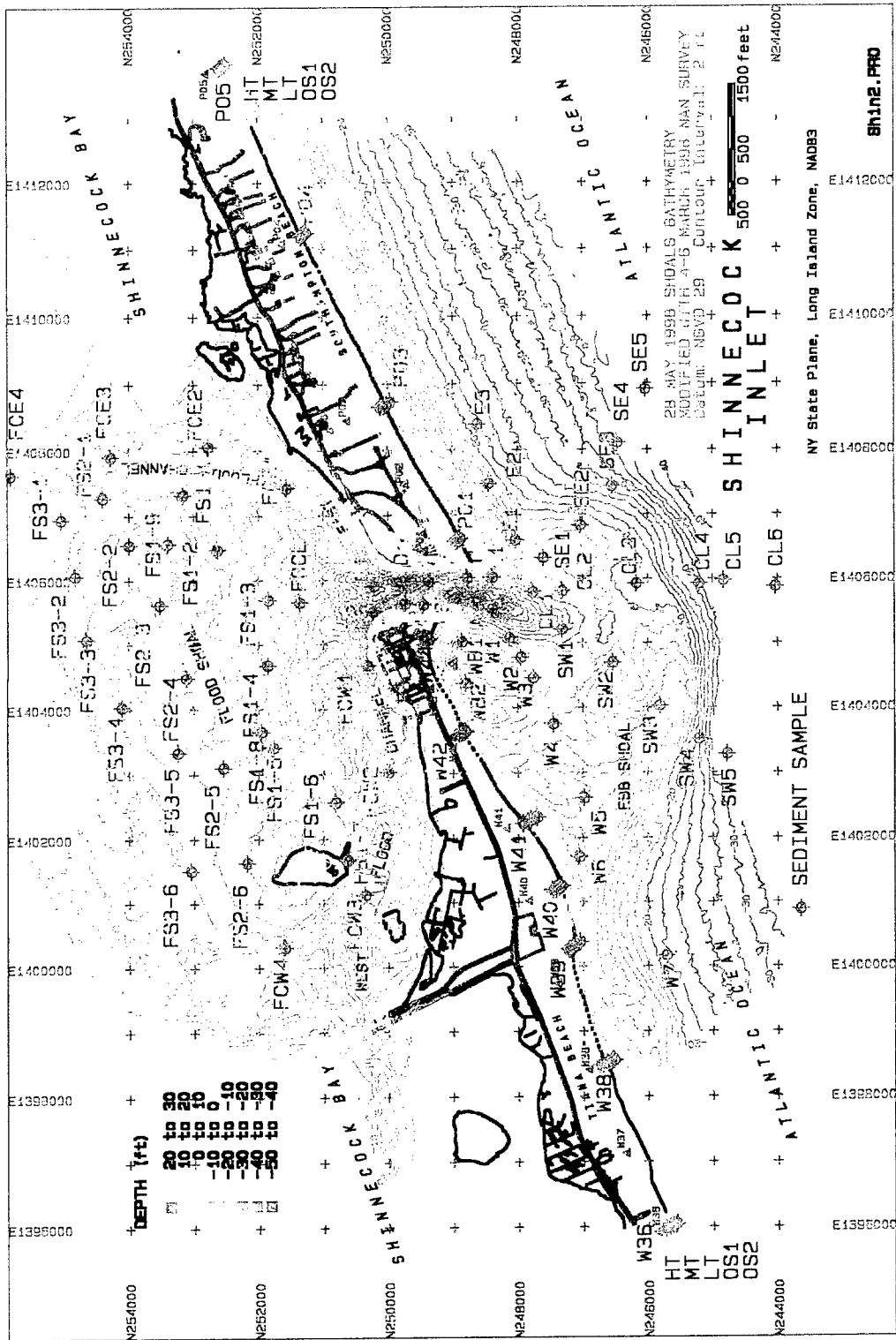


Figure 8. Location of sediment samples at Shinnecock Inlet, Long Island, NY. Bathymetry from 28 May SHOALS survey, supplemented with data from 4-6 March 1998 New York District survey



Figure 9. Aerial photo mosaic of Shinnecock Inlet 10 April 1997 showing the flood shoal and channel distribution

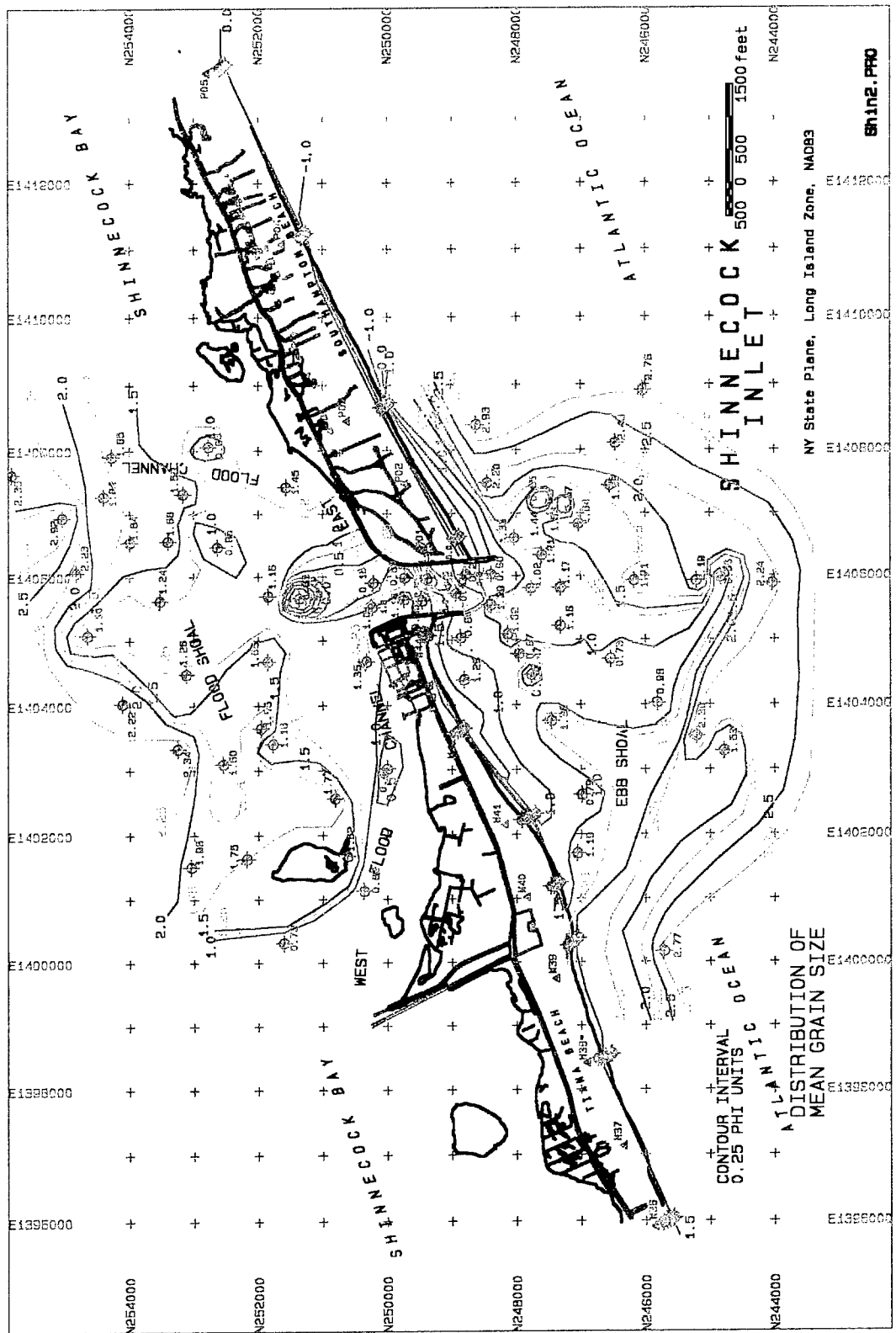
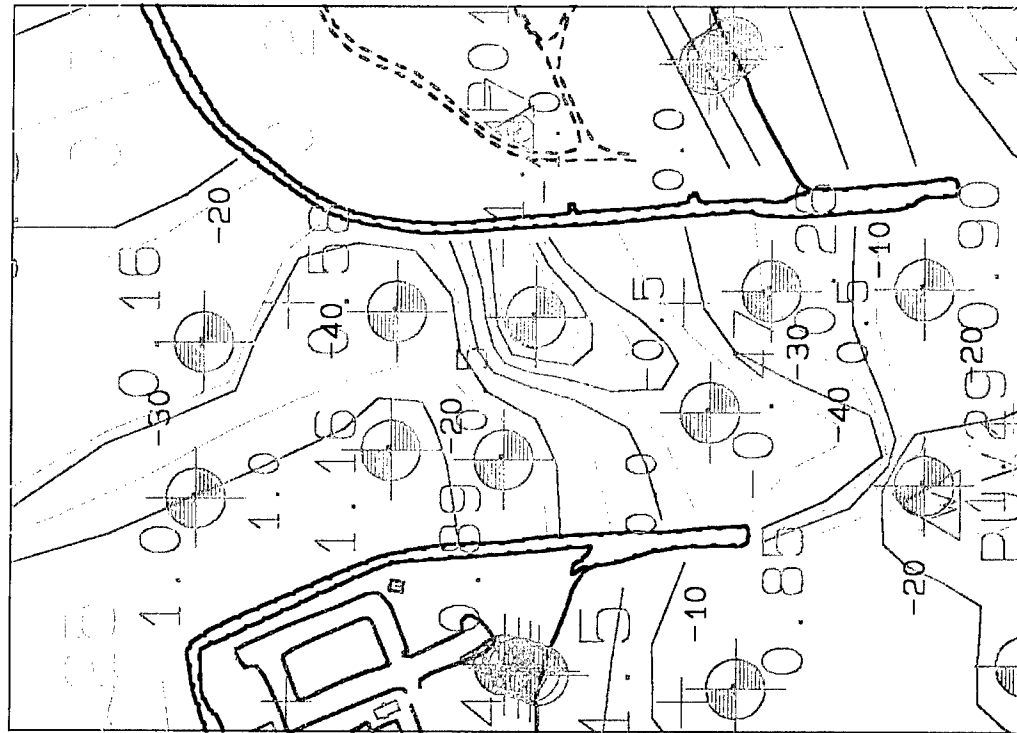
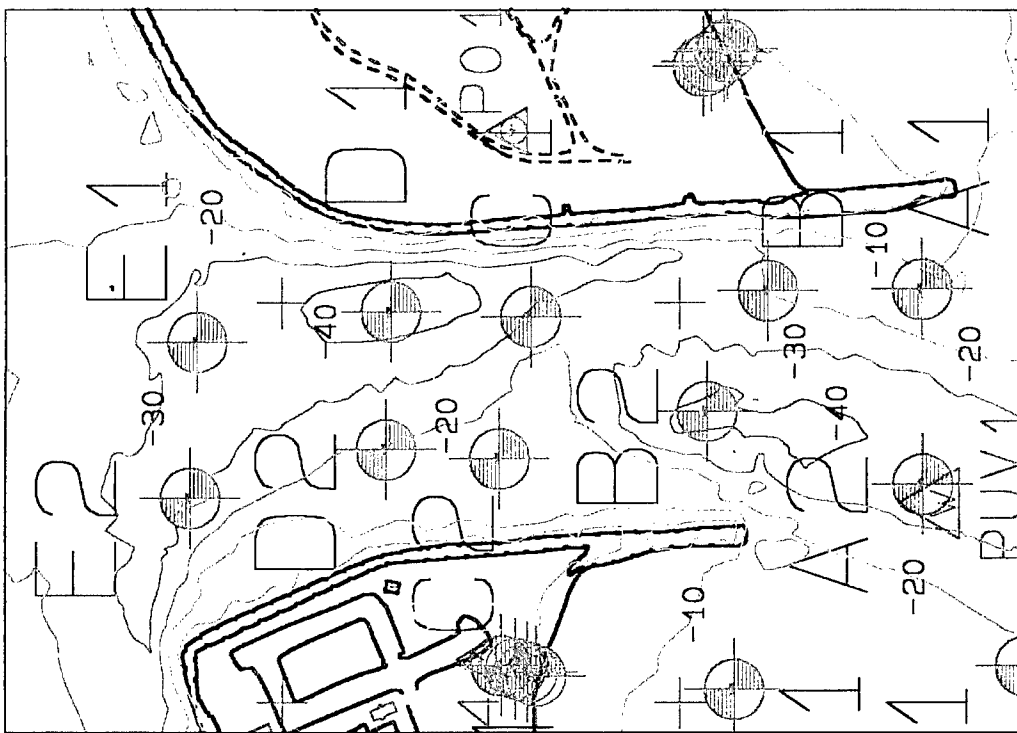


Figure 10. Distribution of mean grain size at Shinnecock Inlet



b. Mean grain size distribution (contours in one-fourth phi units)



a. Sample location and bathymetry (ft NGVD)

Figure 11. Detail of the throat

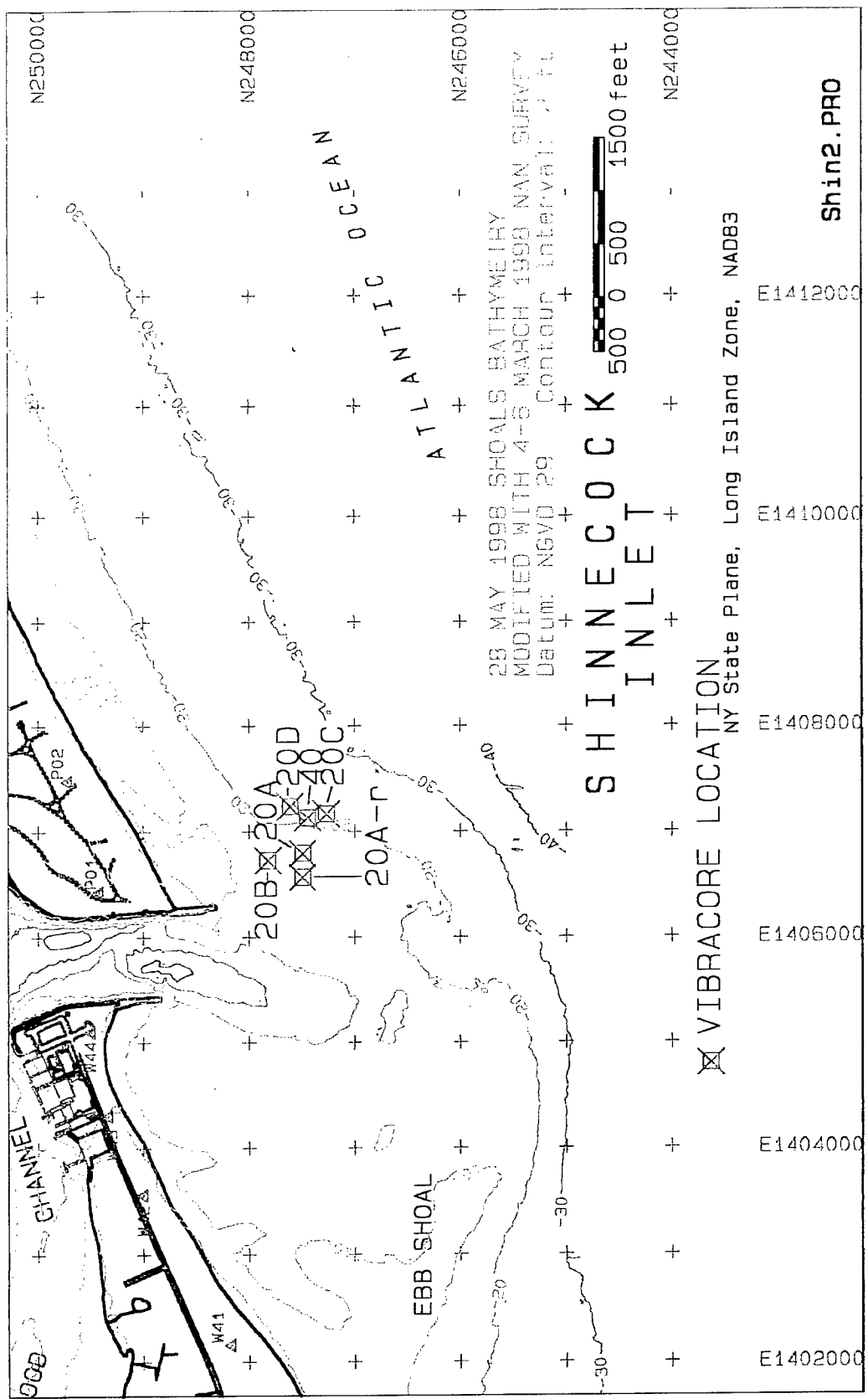


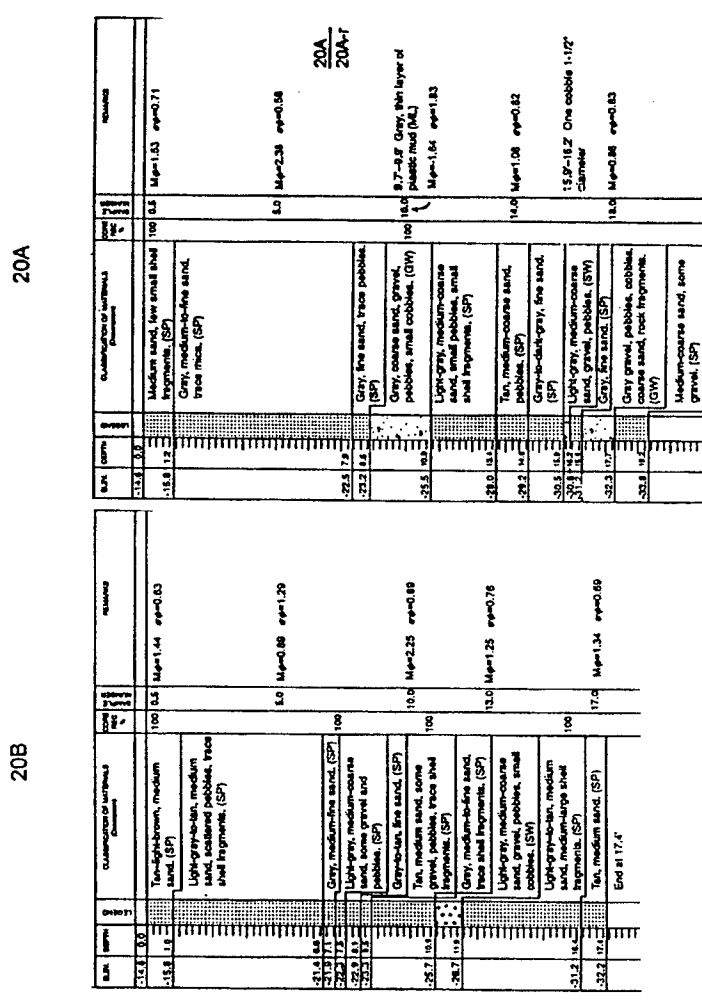
Figure 12. Ebb shoal vibracone locations

## SHINNECOCK INLET

### East Ebb Shoal - Vibracores

Core Logs after Alpine (1997)  
Logs use NAVD88 Datum  
-1 ft = NGVD29

20B



Core Logs after Alpine (1997)  
Logs use NAVD88 Datum  
-1 ft = NGVD29

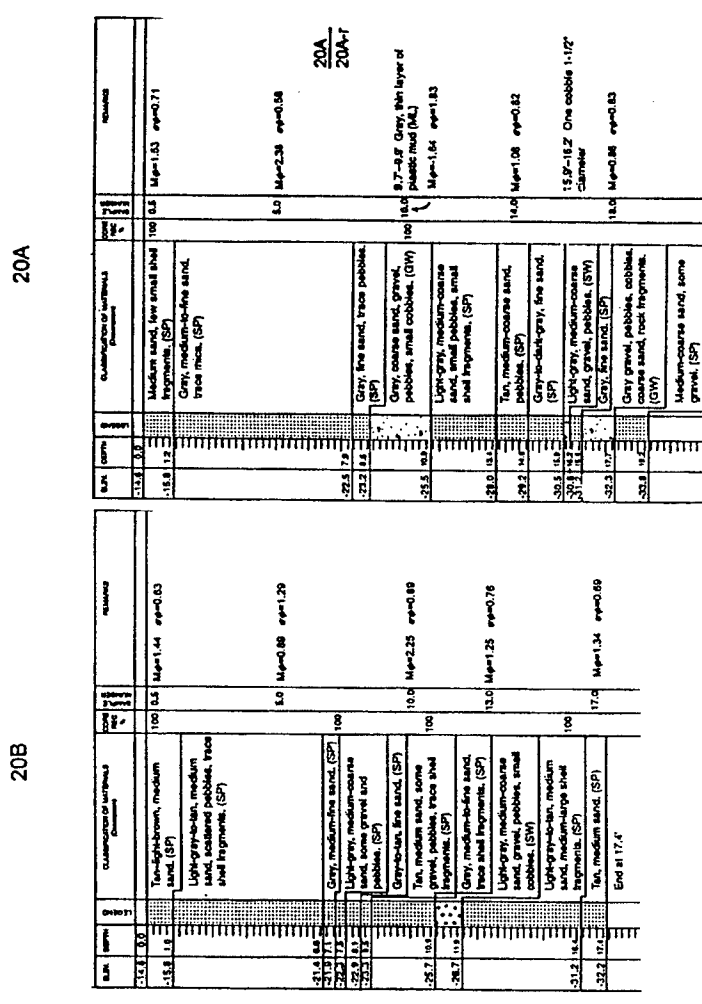


Figure 13. Ebb Shoal vibracore logs (continued)

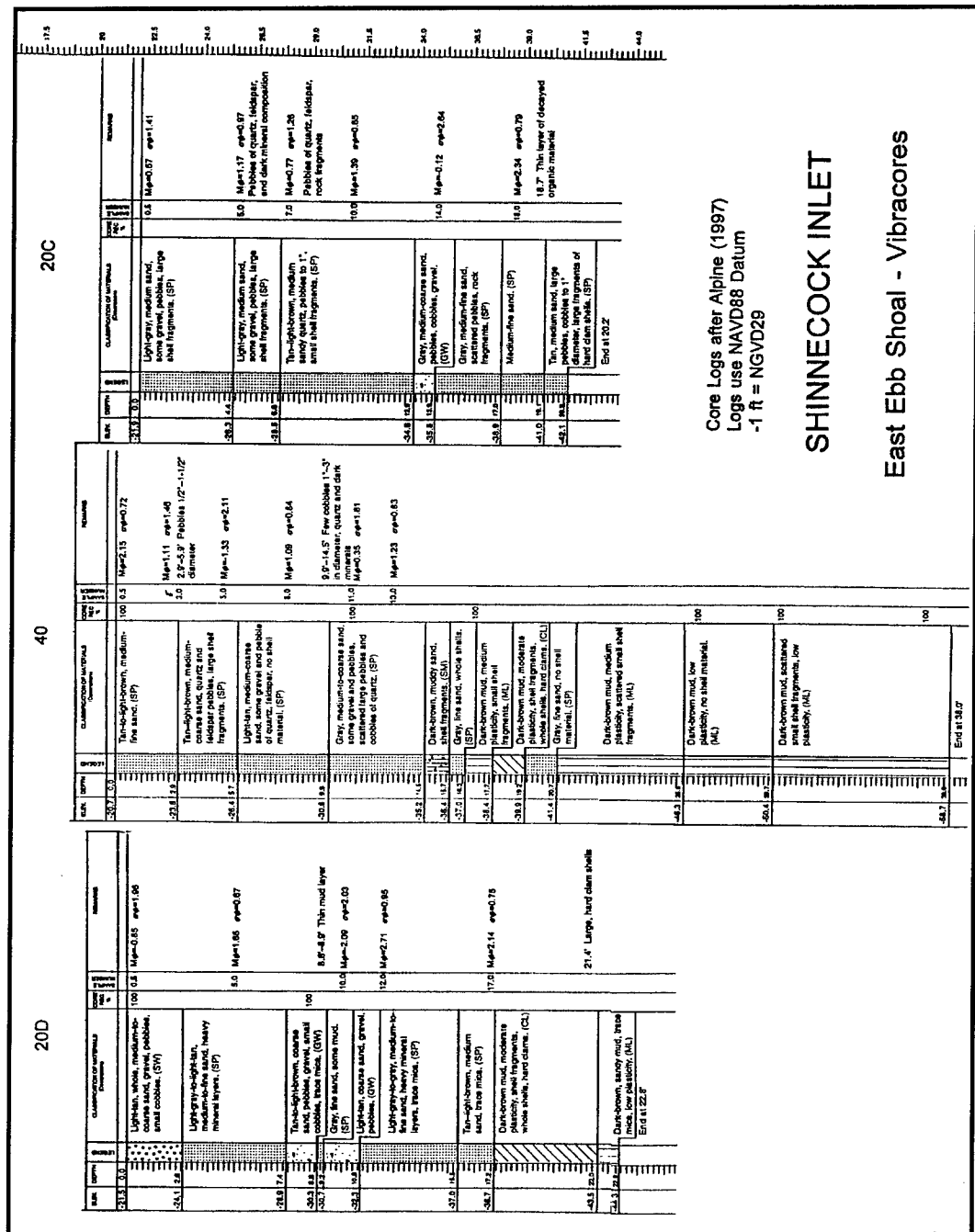


Figure 13. (concluded)

# SHINNECOCK INLET

## COMPOSITE BEACH MEANS

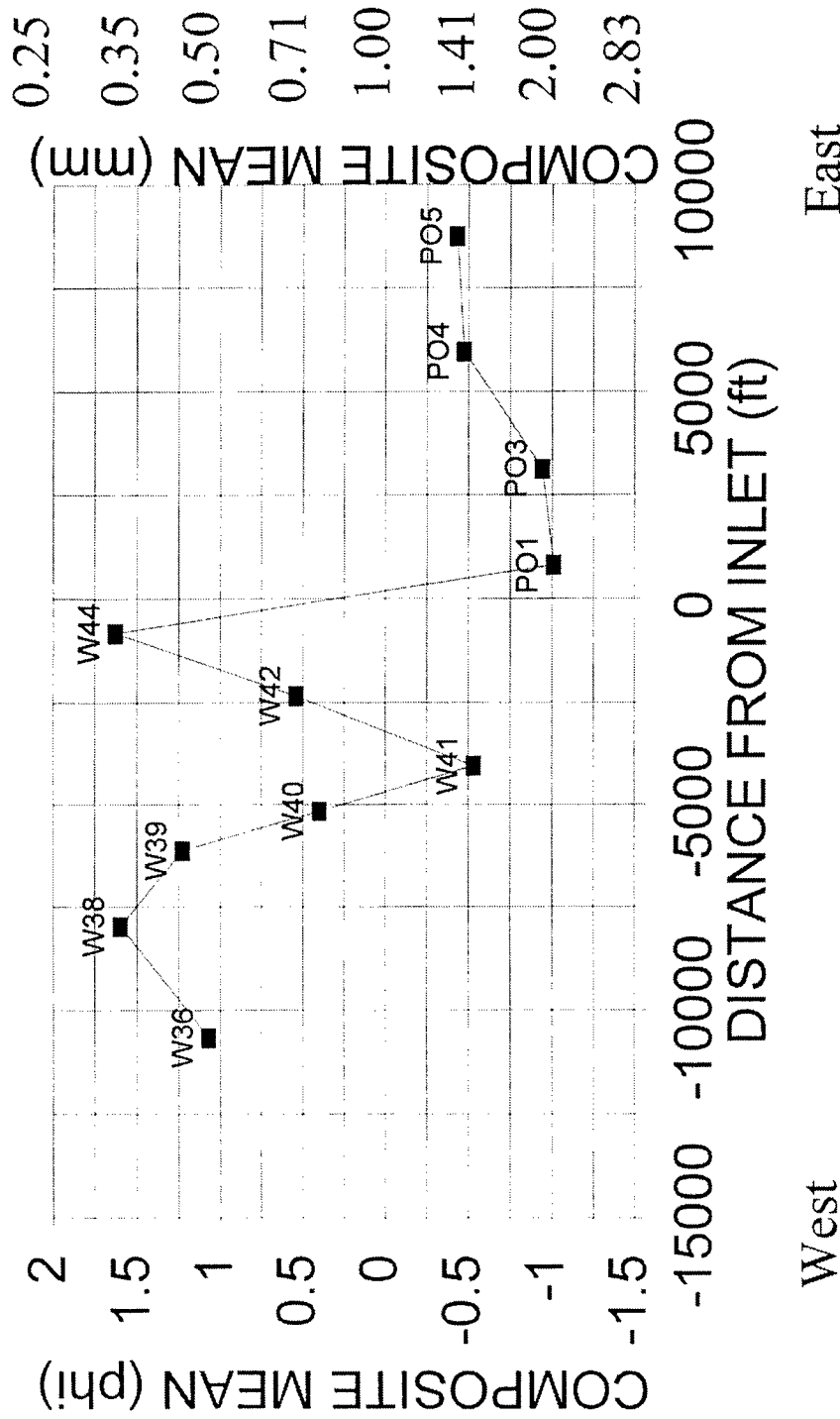


Figure 14. Composite mean grain size of east and west inlet adjacent beach samples. Mathematical composite of high tide, mid tide, low tide and nearshore samples

# SHINNECOCK INLET

## Mean vs. Sorting

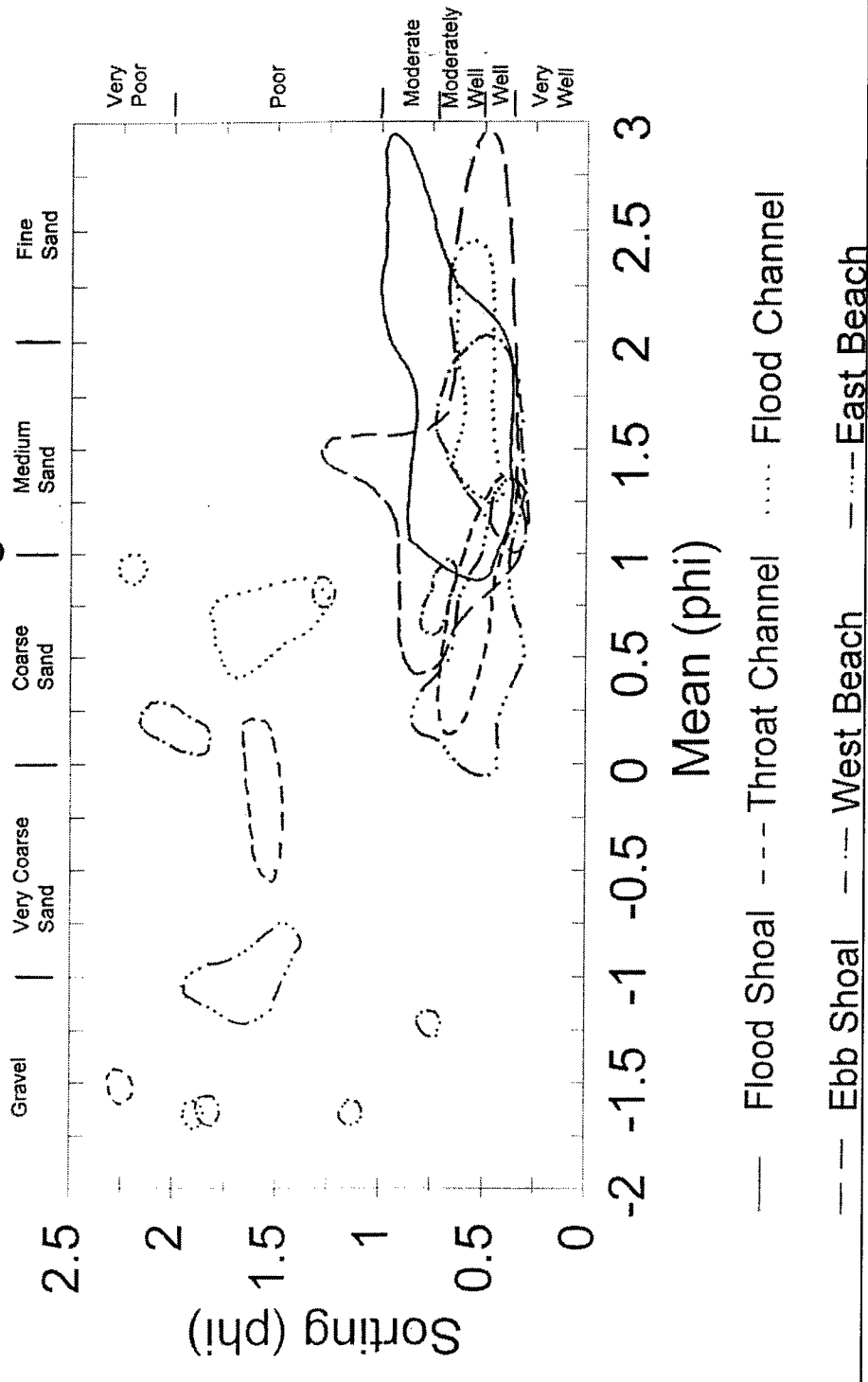


Figure 15. Mean versus sorting plot showing the differential zonation of the sediments of Shinnecock Inlet

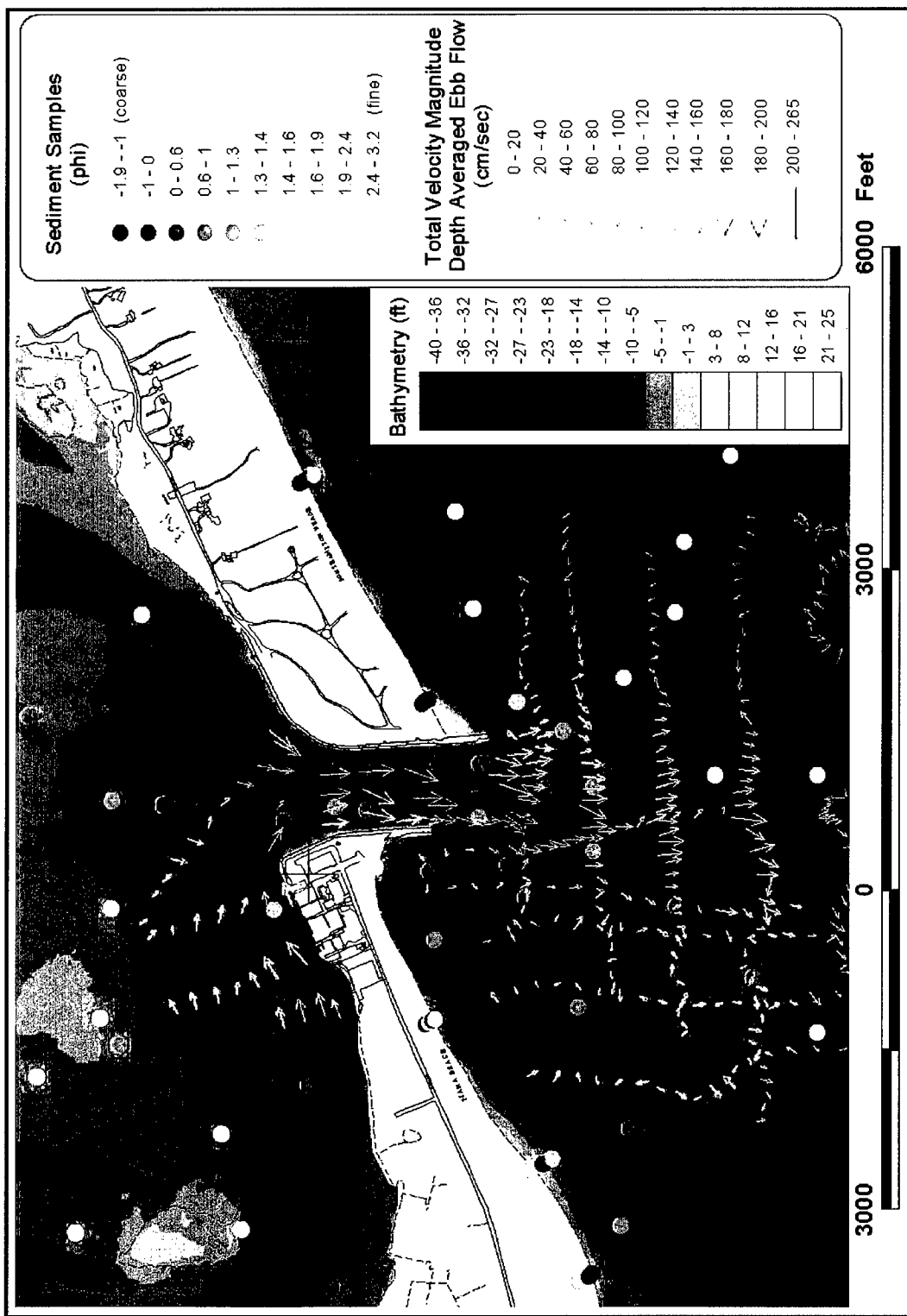


Figure 16. Relationship of sediment particle mean grain size, bathymetry, and ebb velocities

**Table 1****Shinnecock Inlet Sediment Samples**

Sample Location	Mean, phi	Sorting, phi	Skewness phi	Kurtosis phi	Location ft	Mean mm
<b>Channel</b>						
CHA1	0.9	0.5	-1.57	11.05		0.54
CHA2	1.29	0.42	-0.48	7.23		0.41
CHB1	0.26	0.65	-0.89	4.66		0.84
CHB2	-0.47	1.54	-0.68	2.30		1.39
CHC1	-1.47	2.25	-0.43	1.29		2.77
CHC2	0.89	0.58	-2.09	9.36		0.54
CHD1	0.58	0.52	-1.21	6.86		0.67
CHD2	1.16	0.50	-3.93	25.87		0.45
CHE1	0.16	1.59	-0.95	3.77		0.90
CHE2	1.00	0.54	-1.76	11.74		0.50
<b>Ebb Shoal</b>						
E1	1.33	0.58	-0.49	4.69		0.40
E2	2.20	0.58	-0.49	4.69		0.22
E3	2.93	0.51	-3.32	30.71		0.13
SE1	1.21	0.42	-0.28	4.9		0.43
SE2	1.64	-0.39	-0.33	5.62		0.32
SE3	1.99	0.51	0.07	3.91		0.25
SE4	2.54	0.59	-0.79	6.65		0.17
SE5	2.76	0.49	-0.69	4.89		0.15
CL1	1.02	0.37	-0.38	5.58		0.49
CL2	1.17	0.33	-0.28	8.37		0.44
CL3	1.71	0.55	-0.32	4.05		0.31
CL4	2.19	0.40	-0.76	10.62		0.22
CL5	0.86	0.60	0.30	4.87		0.55
CL6	2.24	0.61	-0.80	4.60		0.21
SW1	1.16	0.42	-1.20	8.63		0.45
SW2	0.73	0.85	-0.89	3.38		0.60
SW3	0.98	0.63	-0.18	3.49		0.51
SW4	2.30	0.45	-0.62	7.17		0.20
SW5	1.53	1.24	-0.36	2.16		0.35
W1	1.02	0.51	-0.43	5.08		0.49
W2	0.87	0.78	-1.24	5.49		0.55
W3	0.47	0.79	-0.47	3.55		0.72
W4	1.28	0.79	-0.88	3.43		0.41
W5	0.79	0.60	-0.20	3.96		0.58
W6	1.19	0.51	-0.14	3.51		0.44
W7	2.77	0.54	-0.96	7.21		0.15
WB1	0.85	0.85	-0.08	2.33		0.55
WB2	1.28	0.65	-0.07	3.58		0.41
<b>Flood Channel</b>						
FCCL	-1.61	1.89	0.88	2.50		3.05
FCE1	1.45	0.57	-1.62	10.71		0.37
FCE2	0.94	2.20	-1.04	2.55		0.52
FCE3	1.65	0.53	-0.32	4.47		0.32
FCE4	2.39	0.56	-0.95	7.64		0.19
FCW1	1.35	0.48	-0.72	5.17		0.39
FCW2	0.47	1.70	-2.00	6.11		0.72
FCW3	0.82	1.30	-2.06	7.51		0.57
FCW4	0.73	1.75	-1.05	3.58		0.60
<b>Flood Shoal</b>						
FS1-1	1.55	0.74	-1.74	9.70		0.34
FS1-9	1.68	0.40	-0.56	7.55		0.31
FS1-2	0.98	0.49	-0.45	4.75		0.51
FS1-3	1.16	0.73	-0.96	4.57		0.45

(Sheet 1 of 3)

**Table 1 (Continued)**

Sample Location	Mean, phi	Sorting, phi	Skewness phi	Kurtosis phi	Location ft	Mean mm
<b>Flood Shoal (continued)</b>						
FS1-4	1.66	0.58	-0.54	3.52		0.32
FS1-8	1.95	0.40	-0.26	6.60		0.26
FS1-5	1.18	0.71	-0.86	5.03		0.44
FS1-6	1.77	0.45	-0.73	5.76		0.29
FS1-7	1.52	0.66	-0.61	5.24		0.35
FS2-1	1.84	0.77	0.60	4.15		0.28
FS2-2	1.64	0.73	-0.57	3.00		0.32
FS2-3	1.24	0.42	-0.13	4.67		0.42
FS2-4	1.26	0.47	-0.26	4.53		0.42
FS2-5	1.60	0.42	0.17	5.26		0.33
FS2-6	1.75	0.57	1.50	7.19		0.30
FS3-1	2.92	0.94	-2.07	9.46		0.13
FS3-2	2.23	0.94	-0.04	2.50		0.21
FS3-3	1.10	0.80	-0.89	4.59		0.47
FS3-4	2.22	0.83	0.29	2.64		0.21
FS3-5	2.34	0.69	-0.04	3.63		0.20
FS3-6	1.98	0.58	0.57	4.97		0.25
<b>East Beach (Ponds Reach)</b>						
PO1HT	0.93	0.44	-0.56	6.50		0.53
PO1MT	0.55	0.38	-0.06	4.47		0.68
PO1LT	-1.61	1.10	-0.22	2.51		3.05
PO1OS1	-1.01	1.85	-0.50	1.77		2.01
PO3HT	0.58	0.35	-0.45	3.84		0.67
PO3MT	0.05	0.46	-0.94	6.85		0.97
PO3LT	-1.18	0.72	-0.78	5.02		2.27
PO3OS1	-1.11	1.57	-0.32	1.65		2.16
PO3OS2	1.34	0.37	-0.87	6.32		0.40
PO4HT	0.40	0.69	-0.29	2.84		0.76
PO4MT	1.12	0.44	-1.40	7.21		0.46
PO4LT	0.40	0.55	-0.09	3.25		0.76
PO4OS1	-1.00	1.52	-0.16	1.97		2.00
PO5HT	0.27	0.47	0.24	4.85		0.83
PO5MT	0.21	0.78	0.08	2.74		0.86
PO5LT	0.23	0.80	-0.12	2.54		0.85
PO5OS1	-0.80	1.41	-0.12	2.51		1.74
<b>West Beach (Westhampton Reach)</b>						
W36HT	0.68	0.75	-0.14	2.38		0.62
W36MT	1.53	0.39	-0.35	5.39		0.35
W36LT	1.29	0.57	-0.96	5.53		0.41
W36OS1	0.82	1.28	-0.98	2.86		0.57
W36OS2	1.78	0.68	-1.97	11.28		0.30
W38HT	1.36	0.46	-0.33	4.64		0.39
W38MT	1.39	0.35	0.80	3.98		0.38
W38RC	1.66	0.48	-0.47	4.20		0.32
W38LT	1.61	0.66	-1.30	5.93		0.33
W38OS1	1.99	0.47	-0.63	4.99		0.25
W39HT	1.08	0.37	-0.14	4.75		0.47
W39MT	1.22	0.34	0.15	7.28		0.43
W39LT	0.94	0.69	-1.11	5.02		0.52
W39OS1	1.64	0.43	-0.29	5.96		0.32
W39OS2	1.68	0.47	-0.02	2.87		0.31
W40HT	1.53	0.60	-0.60	6.50		0.35
W40MT	1.65	0.41	-0.59	4.68		0.32
W40LT	0.13	1.89	-1.09	3.31		0.91
W40OS1	0.20	2.09	-1.40	3.46		0.87
W41HT	1.59	0.75	-0.64	3.31		0.33

(Sheet 2 of 3)

**Table 1 (Concluded)**

Sample Location	Mean, phi	Sorting, phi	Skewness phi	Kurtosis phi	Location ft <sup>5</sup>	Mean mm
<b>West Beach (Westhampton Reach) (continued)</b>						
W41MT	1.61	0.40	-0.64	3.92		0.33
W41LT	-1.62	1.83	0.04	2.24		3.07
W41OS1	1.43	0.59	-0.37	3.47		0.37
W42HT	0.91	0.68	-0.45	3.55		0.53
W42MT	1.65	0.40	-0.14	4.01		0.32
W42LT	0.10	1.86	-0.78	2.06		0.93
W42OS1	1.87	0.53	-1.11	7.65		0.27
W44HT	1.46	0.38	0.10	4.72		0.36
W44MT	1.68	0.45	-0.12	4.67		0.31
W44LT	1.48	0.59	-0.17	2.80		0.36
W44OS1	1.91	0.62	-1.83	10.38		0.27
<b>Eastern Long Island Regional Beaches (mid tide)</b>						
MPMT <sup>1</sup>	-3.18	1.28	0.33	1.57		9.06
DPMT <sup>2</sup>	1.42	0.50	-0.52	3.86		0.37
MEIMT <sup>3</sup>	1.54	0.35	0.13	4.18		0.34
MOIMT <sup>4</sup>	1.88	0.38	-0.30	7.60		0.27
<b>Shinnecock Inlet Adjacent Beaches – Composites (Composite of HT,MT,LT,OS1 &amp; OS2 if taken)</b>						
W36	1.07	0.90	-1.37	5.06	-10657	0.48
W38	1.60	0.55	-0.46	4.68	-7957	0.33
W39	1.23	0.54	-0.84	6.66	-6121	0.43
W40	0.40	1.89	-1.46	4.11	-5.153	0.76
W41	-0.53	2.14	-0.41	1.98	-4038	1.45
W42	0.54	1.71	-1.20	3.12	-2333	0.69
W44	1.63	0.54	-0.50	5.33	-827	0.32
PO1	-1.01	1.60	-0.36	2.04	808	2.01
PO3	-0.94	1.21	-0.48	2.66	3143	1.92
PO4	-0.47	1.51	-0.61	2.31	5981	1.38
PO5	-0.43	1.31	-0.55	2.95	8740	1.35

<sup>1</sup> Montock Point.<sup>2</sup> Ditch Plains.<sup>3</sup> Mecox Inlet (closed).<sup>4</sup> Moriches Inlet (east side).<sup>5</sup> Note: To convert feet to meters, multiply by 0.3048.

(Sheet 3 of 3)

**Table 2**  
**Shinnecock Inlet - ADCP Data - 4 December 1997**

Date	Line No.	Time EST	Total Area sq m	Average Velocity cm/sec	Velocity Direction deg	Discharge cu m/sec
12/4/97	1	812	1,498.5	134.84	39	2,020.6
		923	2,192.0	93.63	43	2,052.5
	2	1029	2,338.2	32.32	41	755.7
		814	1,404.4	120.12	33	1,687.0
		927	1,855.7	91.06	34	1,689.9
		1032	2,000.1	36.51	38	730.3
		1129	1,767.7	40.88	209	722.6
	3	816	1,965.3	102.94	29	2,023.1
		930	2,023.6	88.30	34	1,786.9
		1034	1,958.3	32.68	31	640.1
		1131	1,791.7	62.37	253	1,117.4
	4	819	2,143.3	109.75	14	2,352.3
		934	1,948.0	88.90	10	1,731.8
		1037	1,813.5	32.38	2	587.3
		1135	1,703.5	46.51	194	792.3
		1223	1,799.4	91.04	202	1,638.2
		1314	1,374.6	105.17	202	1,445.6
		1412	1,571.9	108.44	199	1,704.6
		1510	1,575.8	112.55	196	1,773.5
	5	824	2,964.4	76.87	14	2,278.6
		937	3,123.7	60.20	21	1,880.5
		1039	3,484.8	11.25	5	392.2
		1137	3,148.2	28.11	199	885.1
		1227	3,561.8	37.70	199	1,342.7
		1316	3,400.1	46.37	190	1,576.8
		1415	2,834.3	62.48	194	1,770.9
		1512	3,211.7	50.09	187	1,608.9
	6	800	3,565.3	69.11	2	2,463.9
		910	3,863.5	58.96	5	2,277.8
		1020	3,937.5	27.62	8	1,087.6
	6	1120	3,554.3	19.96	149	709.3
		1215	4,174.7	37.47	166	1,564.4
		1307	3,667.1	54.41	186	1,995.4
		1405	3,610.2	59.09	186	2,133.1
		1503	3,456.3	57.27	341	1,979.3
	7	748	3,225.7	43.38	6	1,399.3
		855	3,727.6	41.68	12	1,553.6
		1005	4,822.5	20.94	347	1,010.1
		1110	3,704.0	11.15	231	412.8
		1205	3,426.1	23.37	214	800.8
		1258	3,493.6	29.18	210	1,019.6
		1356	3,181.0	30.64	211	974.7
		1454	3,006.0	29.09	211	874.4
	8	755	1,829.7	66.91	298	1,224.2
		904	1,912.7	55.91	309	1,069.5
		1015	2,098.7	31.03	317	651.3
		1116	1,827.7	13.55	146	247.6
		1211	1,801.2	39.87	138	718.1
		1304	1,492.9	61.98	135	925.4
		1402	1,521.6	58.03	127	883.0
	9	1459	1,480.8	61.38	124	908.9
		831	1,884.7	62.24	264	1,173.1
		943	2,110.0	39.41	264	931.5
		1045	2,112.2	10.58	207	223.5
		1143	2,186.6	24.84	110	543.2
		1235	2,240.7	41.58	109	931.6

*(Continued)*

**Table 2 (Continued)**

Date	Line No.	Time EST	Total Area sq m	Average Velocity cm/sec	Velocity Direction deg	Discharge cu m/sec
12/4/97	9	1327	2,053.9	58.16	105	1,194.6
		1425	2,109.4	60.42	104	1,274.5
		1521	1,870.2	60.54	103	1,132.2
	10	842	1,809.7	35.18	284	636.6
		953	1,938.6	22.79	290	441.8
		1056	1,890.9	2.67	145	50.5
		1154	1,891.1	20.78	108	393.0
		1247	1,785.0	39.98	110	713.6
		1340	1,763.0	50.84	114	896.3
		1439	1,688.7	55.36	113	934.8
		1533	1,629.5	56.13	114	914.6

**Table 3**  
**Shinnecock Inlet - ADCP Data - 20-22 July 1998**

Date	Range/Line No.	Time EST	Total Area sq m	Average Velocity cm/sec	Velocity Direction, deg	Discharge cu m/sec
7/20/98	Peconic Bay	1130	429.5	33.90	195	145.6
		1138	401.1	35.90	198	144.0
		1145	425.4	33.46	197	142.4
		1150	397.5	33.37	199	132.6
		1154	395.4	32.63	204	129.0
		1159	391.4	26.78	197	104.8
		1203	381.7	30.67	187	117.1
		1208	362.5	32.17	184	116.6
		1212	375.1	31.79	211	119.3
		1216	369.7	29.07	225	107.5
		1220	371.3	26.20	212	97.3
		1224	343.8	27.44	212	94.4
		1228	353.5	22.26	198	78.7
		1233	319.0	25.58	179	81.6
		1237	307.1	23.63	181	72.6
		1247	373.0	14.83	202	55.3
		1251	299.1	13.30	215	39.8
		1254	310.7	11.09	213	34.4
		1258	302.9	8.72	208	26.4
	Ponquogue Bridge	1357	1144.4	66.34	261	759.2
7/21/98	20 Ebb	0703	6728.0	9.06	211	609.8
		0718	6078.0	2.11	211	128.3
		0730	5951.3	6.00	244	356.9
		0744	4731.5	3.42	106	161.9
		0756	4504.1	4.82	263	217.2
		1604	9348.1	11.61	49	1084.9
		1614	6057.2	19.61	78	1188.0
		1630	5199.6	15.68	45	815.1
		1641	4814.5	20.18	69	971.4
		1656	3647.2	19.13	76	697.8
		1705	4817.6	18.32	76	882.4
		1718	4418.0	20.16	87	890.8
7/21/98	27 Flood	1728	2775.2	20.74	77	575.7
		1737	2543.9	17.55	85	446.5
		0703	3842.8	3.73	164	143.2
		0756	3604.7	37.53	175	1352.8
7/22/98	1	0858	3440.0	50.84	181	1748.9
		0959	3737.1	54.22	184	2026.3
		1058	3455.0	58.00	184	2003.8
		1204	3428.7	34.84	169	1194.5
		1310	3880.9	2.10	134	81.7
		1401	3563.2	39.49	32	1407.2
		1454	3581.5	50.69	23	1815.3
		1545	3949.2	62.48	15	2467.4
		1640	4254.2	63.20	18	2688.8
		1734	4056.0	58.96	19	2391.5
		0707	2076.8	16.57	203	344.0
		0803	2090.6	68.80	215	1438.4
		0902	2097.0	100.56	201	2108.8
		1002	2056.7	98.50	199	2025.9
		1102	1928.1	86.70	197	1671.8
		1207	1966.7	73.34	196	1442.3
		1315	2038.4	11.38	360	231.9
		1407	2060.9	65.76	17	1355.3
		1459	2007.5	90.36	20	1813.9
		1551	2182.1	107.45	19	2344.6

**Table 3 (Continued)**

Date	Range/Line No.	Time EST	Total Area sq m	Average Velocity cm/sec	Velocity Direction, deg	Discharge cu m/sec
7/22/98	3	1646	2534.6	102.91	19	2608.4
		1740	2516.1	99.50	19	2503.5
		0711	1566.2	26.37	207	413.0
		0806	1522.0	73.63	206	1120.7
		0905	1729.6	101.86	201	1761.8
		1007	1168.3	117.18	201	1369.0
		1106	1369.8	114.82	206	1572.7
		1210	1288.3	73.15	209	942.4
		1320	1462.4	17.03	41	249.1
		1411	1783.4	74.39	20	1326.7
		1503	1768.9	103.85	13	1837.0
		1555	1805.9	115.15	26	2079.5
		1651	1330.7	116.91	17	1555.8
		1744	1615.0	119.58	22	1931.2
	4	0714	2027.8	20.35	206	412.7
		0809	2292.0	58.66	216	1344.4
		0909	1964.1	84.08	201	1651.4
		1011	2003.7	96.52	212	1934.0
		1110	1969.7	95.36	209	1878.4
		1214	1966.4	56.69	232	1114.8
		1324	1864.2	18.64	28	347.5
		1416	1766.9	81.59	22	1441.5
		1506	1783.0	109.44	29	1951.3
		1559	1957.5	105.91	32	2073.3
		1655	1568.3	113.65	24	1782.4
		1746	1922.2	104.79	27	2014.2
	5	0716	2888.0	12.28	193	354.5
		0811	3848.5	33.69	211	1296.6
		0911	3219.8	54.13	212	1742.9
		1014	2301.6	43.26	206	995.7
		1112	3633.1	44.42	219	1613.7
		1215	3326.2	30.54	210	1015.8
		1326	2864.0	22.01	50	630.3
		1418	3072.0	50.13	40	1540.1
		1509	2845.4	70.51	42	2006.3
		1602	3250.8	57.58	33	1871.9
		1700	3370.4	57.95	33	1953.1
		1750	3109.1	61.90	28	1924.5
	6	0720	1642.8	20.25	127	332.6
		0816	1690.0	56.19	201	949.5
		0915	1769.2	65.69	217	1162.2
		1017	1566.7	61.73	203	967.1
		1115	1609.5	56.63	207	911.5
		1220	1664.6	26.99	210	449.3
		1330	1625.2	6.67	295	108.4
		1424	1445.1	23.30	314	336.7
		1513	1559.7	41.98	341	654.8
		1605	1732.2	50.40	358	873.1
		1704	1978.4	46.89	347	927.7
		1755	2277.2	34.73	350	790.8
	7	0724	2977.9	14.97	247	445.7
		0820	4040.2	11.22	211	453.1
		0918	3809.6	22.30	226	849.5
		1020	4032.4	21.15	216	853.0
		1119	3993.8	13.66	214	545.4
		1222	4324.2	14.21	218	614.6
		1333	3955.3	7.12	26	281.6

**Table 3 (Concluded)**

Date	Range/Line No.	Time EST	Total Area sq m	Average Velocity cm/sec	Velocity Direction, deg	Discharge cu m/sec
7/22/98	7	1426	4041.2	20.92	55	845.6
		1515	3810.3	22.59	37	860.9
		1610	3801.3	31.63	40	1202.4
		1707	3116.5	39.86	53	1242.3
		1756	2780.1	26.62	45	740.2
	8	0732	3820.5	14.50	192	554.1
		0828	3627.8	21.33	198	773.7
		0929	3190.6	32.24	203	1028.6
		1031	3281.8	28.04	190	920.2
		1129	3251.6	21.73	184	706.4
		1231	2901.2	10.61	187	307.7
	8	1340	3330.5	19.75	21	657.6
		1430	3164.6	27.32	348	864.5
		1521	3848.2	32.00	356	1231.5
		1615	3915.0	41.72	352	1633.3
		1711	4117.9	41.26	359	1698.9
		1759	3684.0	31.81	358	1171.9
		0740	1929.5	27.70	118	534.5
	9	0835	1935.8	48.54	116	939.6
		0935	1862.4	63.50	107	1182.6
		1038	1454.8	72.18	102	1050.1
		1135	1754.1	49.83	104	874.1
		1239	1558.9	26.43	109	412.0
		1345	1576.2	19.66	311	309.9
		1438	1537.4	48.56	279	746.6
		1526	1660.2	60.55	284	1005.3
		1620	1874.4	54.80	284	1027.1
		1712	1976.5	49.70	283	982.3
		1805	1942.5	37.06	298	719.9
		0746	1138.6	30.73	82	349.9
		0841	1048.7	60.10	77	630.2
		0941	1652.3	70.35	99	1162.3
	10	1044	923.6	93.15	93	860.3
		1144	940.6	80.20	88	754.4
		1244	837.2	49.82	90	417.1
		1351	821.0	25.85	257	212.2
		1444	910.7	47.38	264	431.5
		1531	1160.7	54.26	254	629.8
		1628	1211.7	50.82	258	615.8
		1724	1531.0	39.96	261	611.8
		1810	1178.2	39.22	255	462.1
		0751	1282.4	30.26	95	388.1
		0845	1174.2	51.01	104	598.9
	11	0953	971.0	77.15	95	749.1
		1054	931.1	83.33	99	775.9
1154		848.9	72.42	101	614.8	
1250		870.1	36.27	104	315.5	
1355		974.5	22.11	271	215.5	
1448		934.8	48.26	277	451.1	
1540		879.8	53.36	280	469.5	
1634		923.4	41.15	280	380.0	
1730		978.7	33.88	271	331.6	
1815		974.5	23.44	270	228.4	

(Sheet 3 of 3)

**Table 4**  
**Shinnecock Inlet - ADCP Data - 28-29 July 1999**

Date	Line No.	Time EDT	Total Area sq m	Average Velocity cm/sec	Velocity Direction deg	Discharge cu m/sec
7/28/99	1	2054	5,716	5.94	78	340
		2214	7,335	24.30	164	1,782
	2	2123	10,846	6.18	133	670
		2227	10,196	21.66	219	2,208
	3	2140	10,600	2.16	102	229
		2239	10,457	22.15	176	2,316
	4	2154	13,642	6.47	127	883
		2300	14,918	16.83	227	2,511
	5	2106	17,460	2.84	79	496
		2159	16,162	0.29	288	47
		2243	22,499	12.39	53	2,788
		2339	42,692	1.28	247	546
	6	2123	20,342	5.77	111	1,175
		2213	21,911	2.10	108	460
		2306	20,718	6.76	109	1,401
		2350	98,860	0.70	107	688
	7	2137	28,994	0.81	289	236
		2225	27,096	1.14	289	309
		2317	24,554	8.86	284	2,176
	8	2324	12,620	22.27	201	2,811
	9	2338	8,302	7.30	305	606
	10	2346	10,781	23.60	227	2,544
	11	2209	2,288	3.61	43	83
		2350	3,733	0.01	52	1
7/29/99	1	0008	7,766	35.35	195	2,745
	2	0026	9,591	27.12	230	2,601
		0144	9,660	21.83	244	2,108
	3	0046	9,603	27.98	194	2,687
		0124	9,047	24.36	207	2,204
	4	0106	12,467	28.02	246	3,493
	5	0030	16,306	22.79	277	3,716
		0125	23,477	14.11	259	3,312
	6	0042	31,161	7.10	110	2,213
		0137	21,675	5.78	122	1,253
	7	0005	30,089	13.48	301	4,056
		0056	36,620	12.63	279	4,626

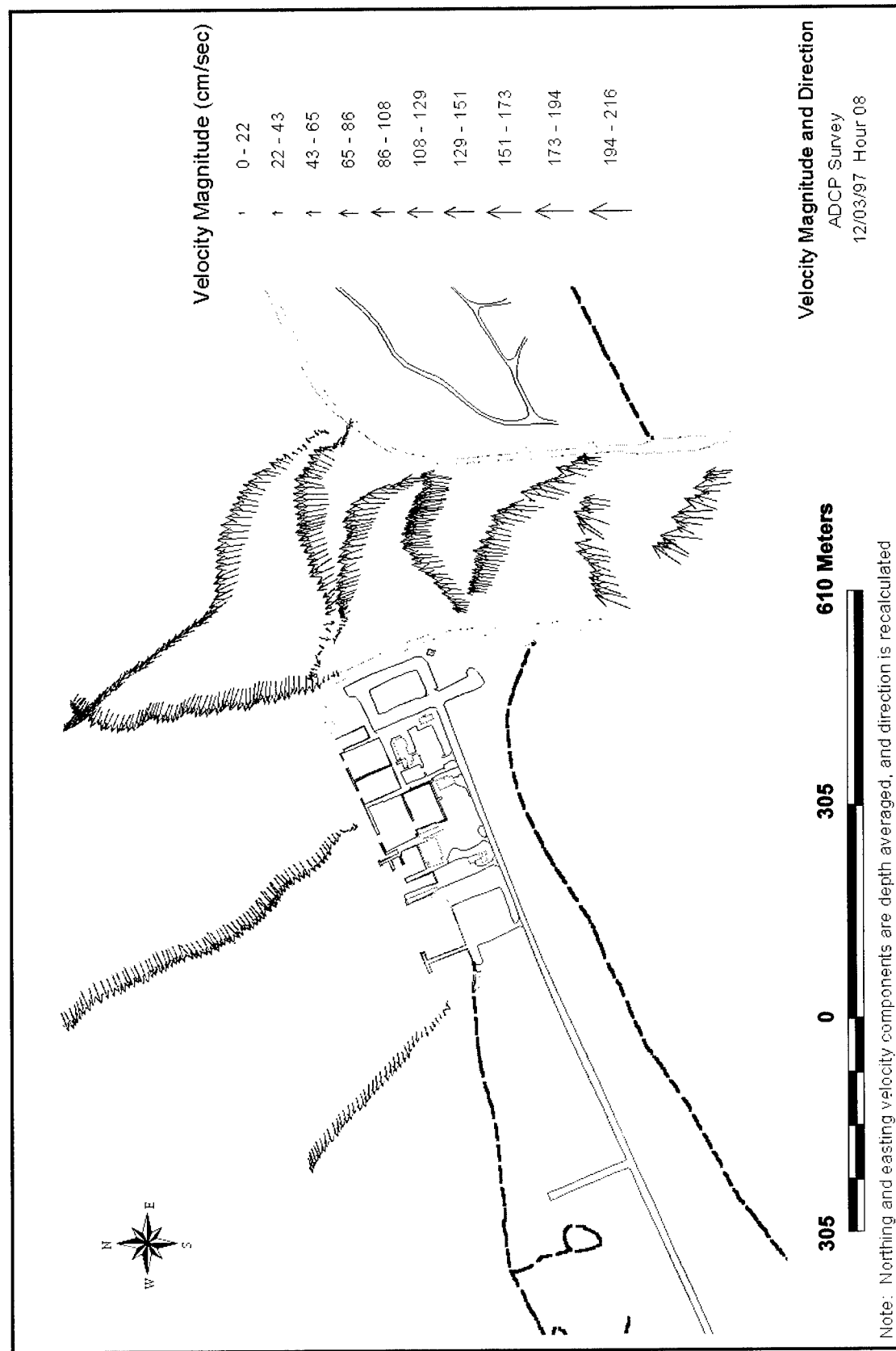
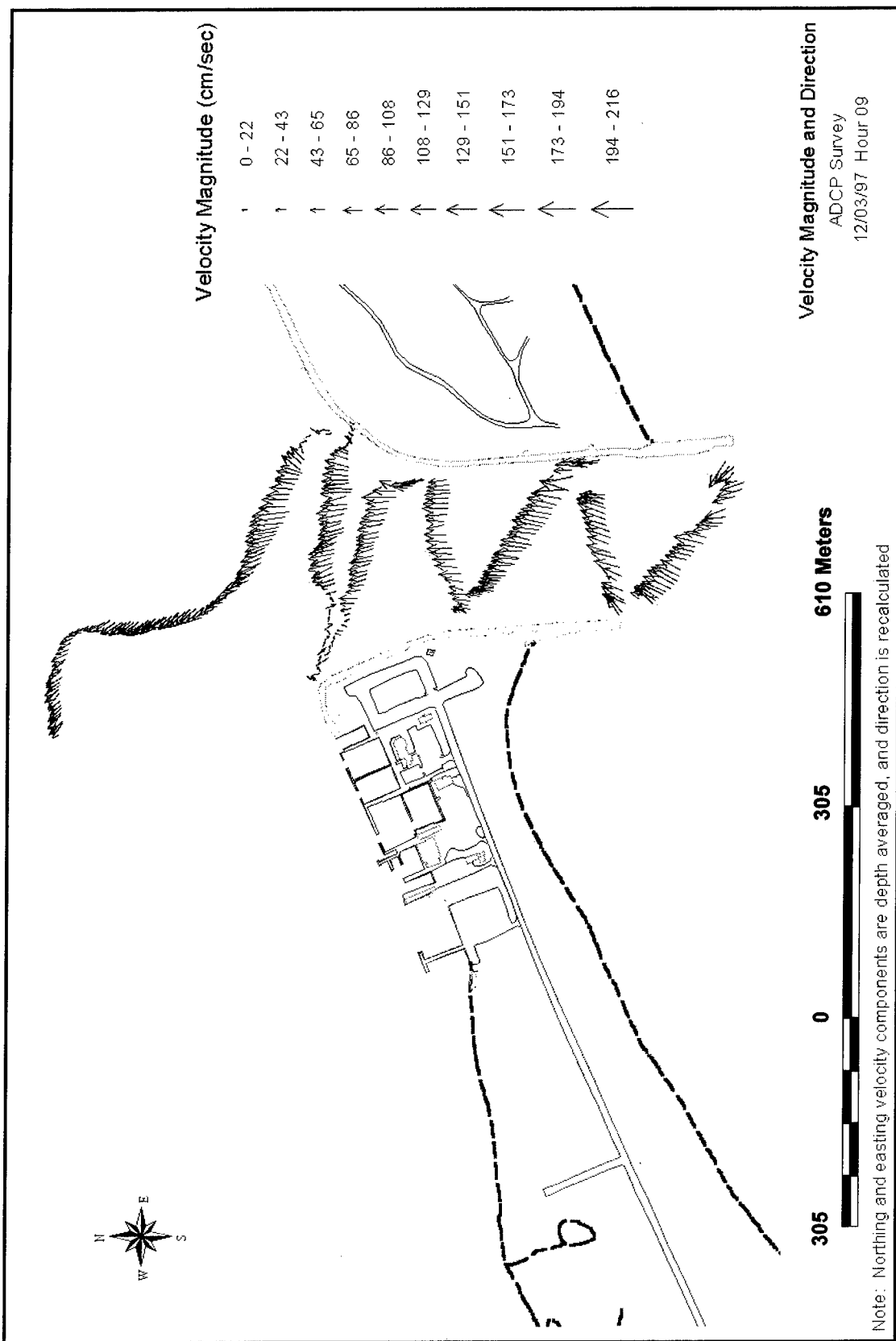
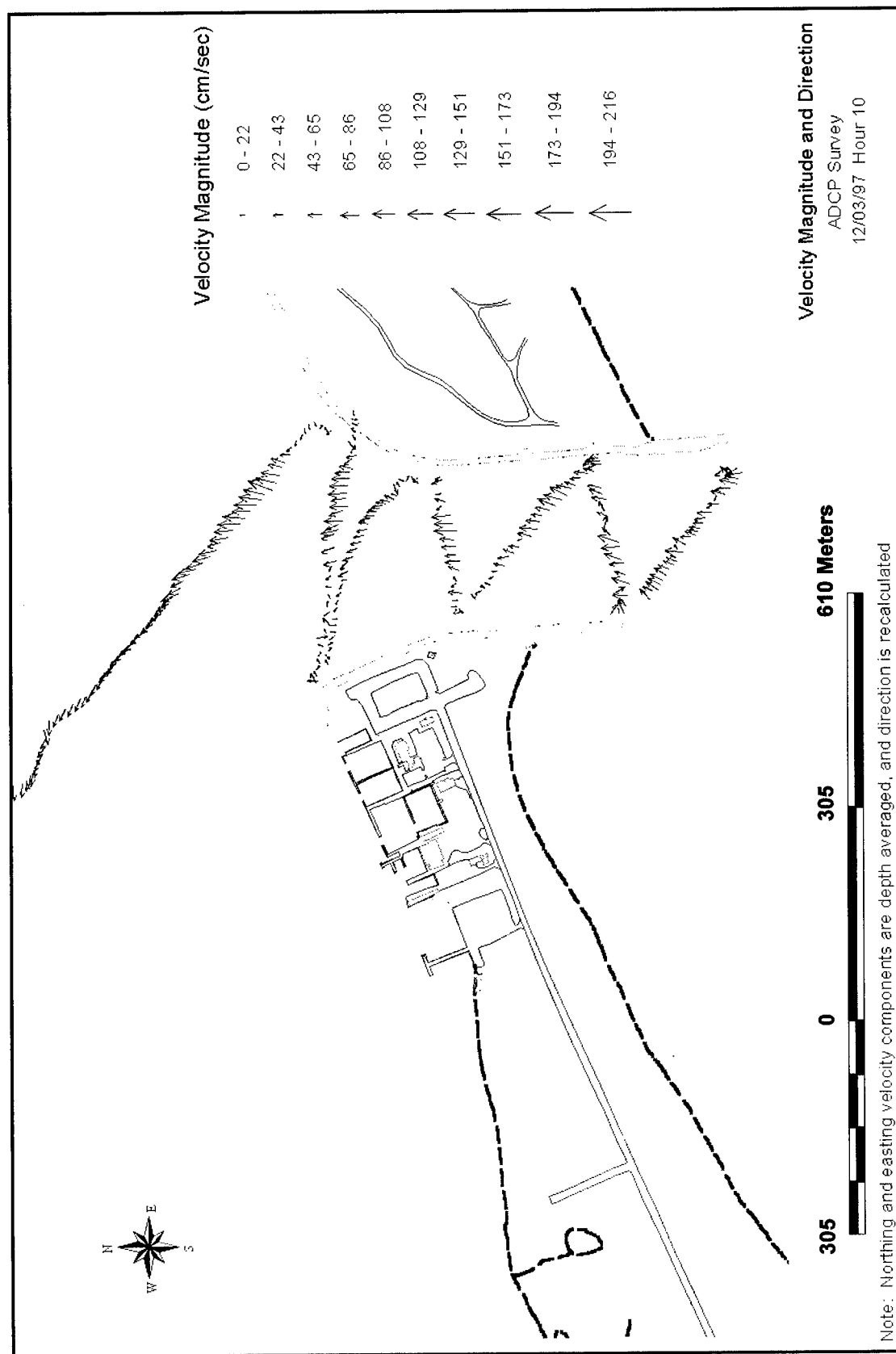


Plate 1



**Plate 2**



**Plate 3**

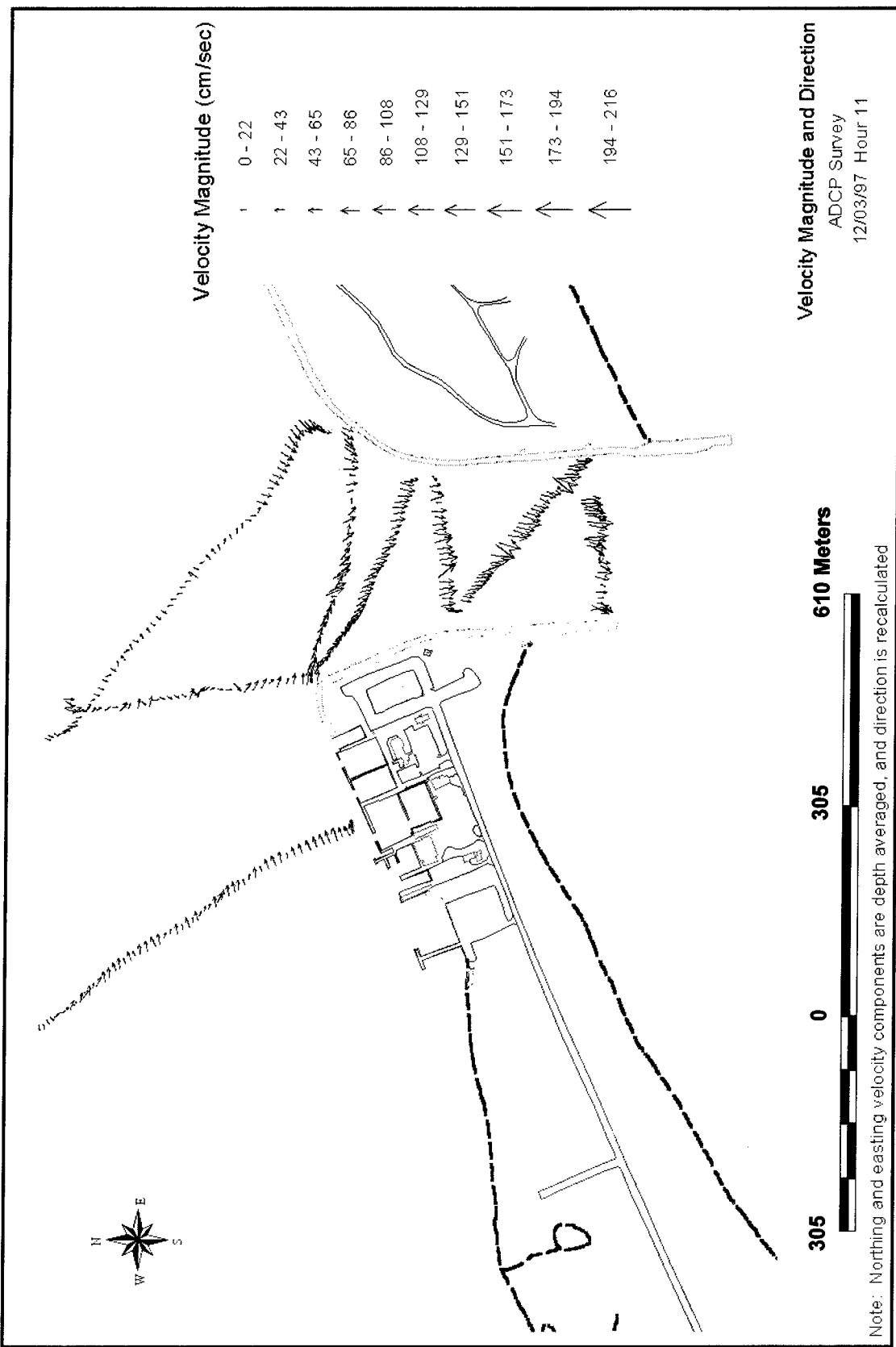
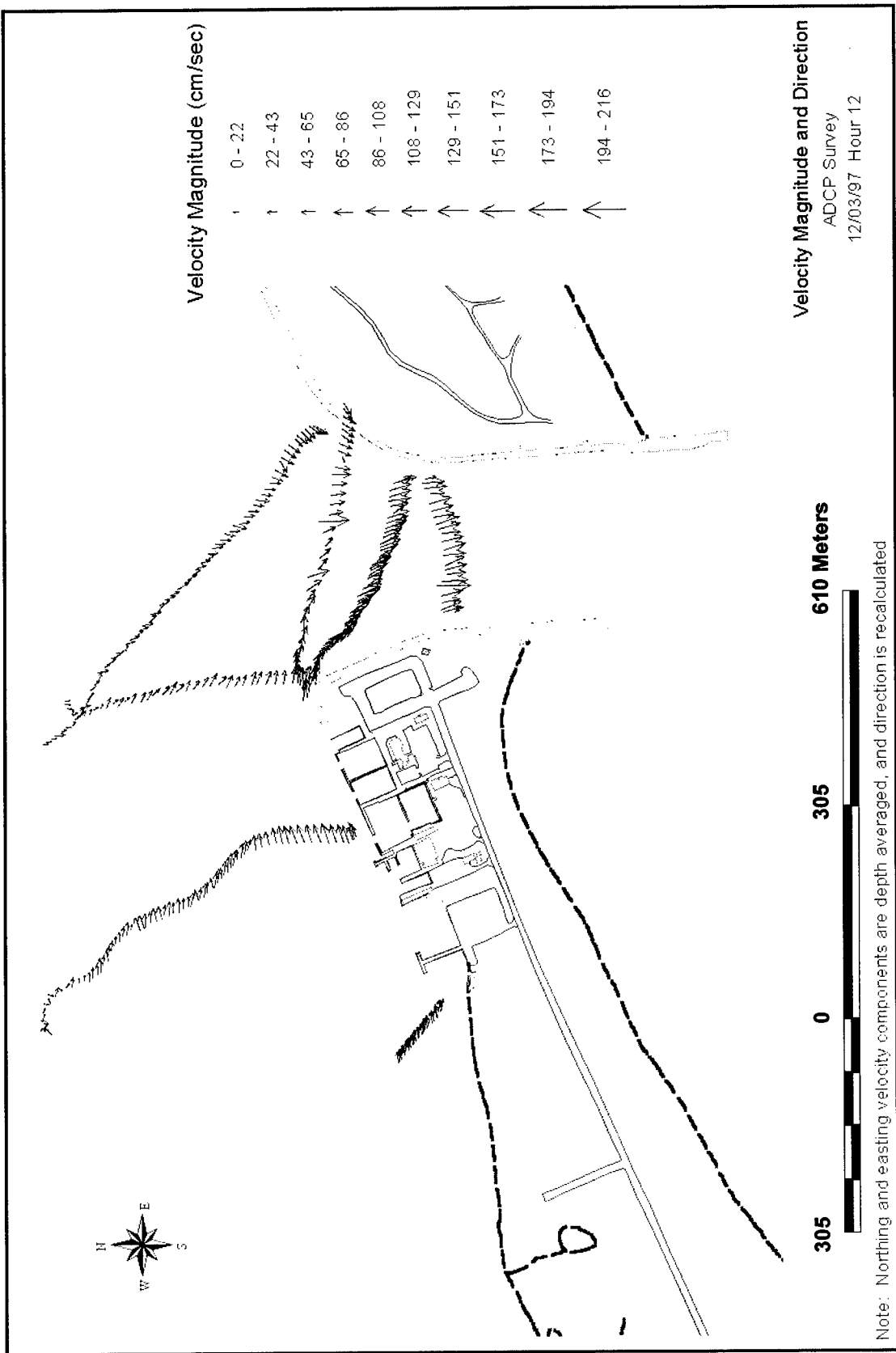
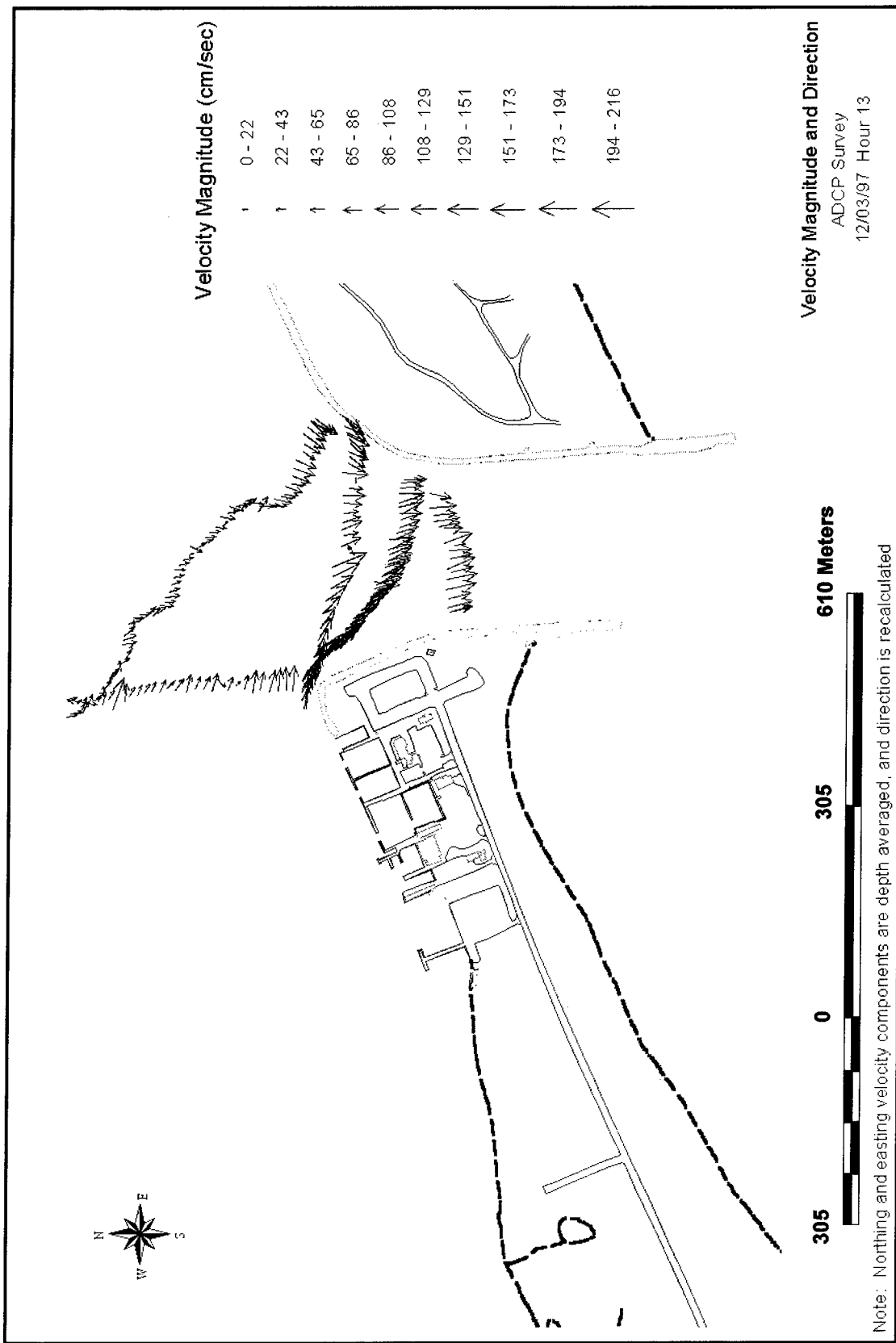


Plate 4



## Plate 5



**Plate 6**

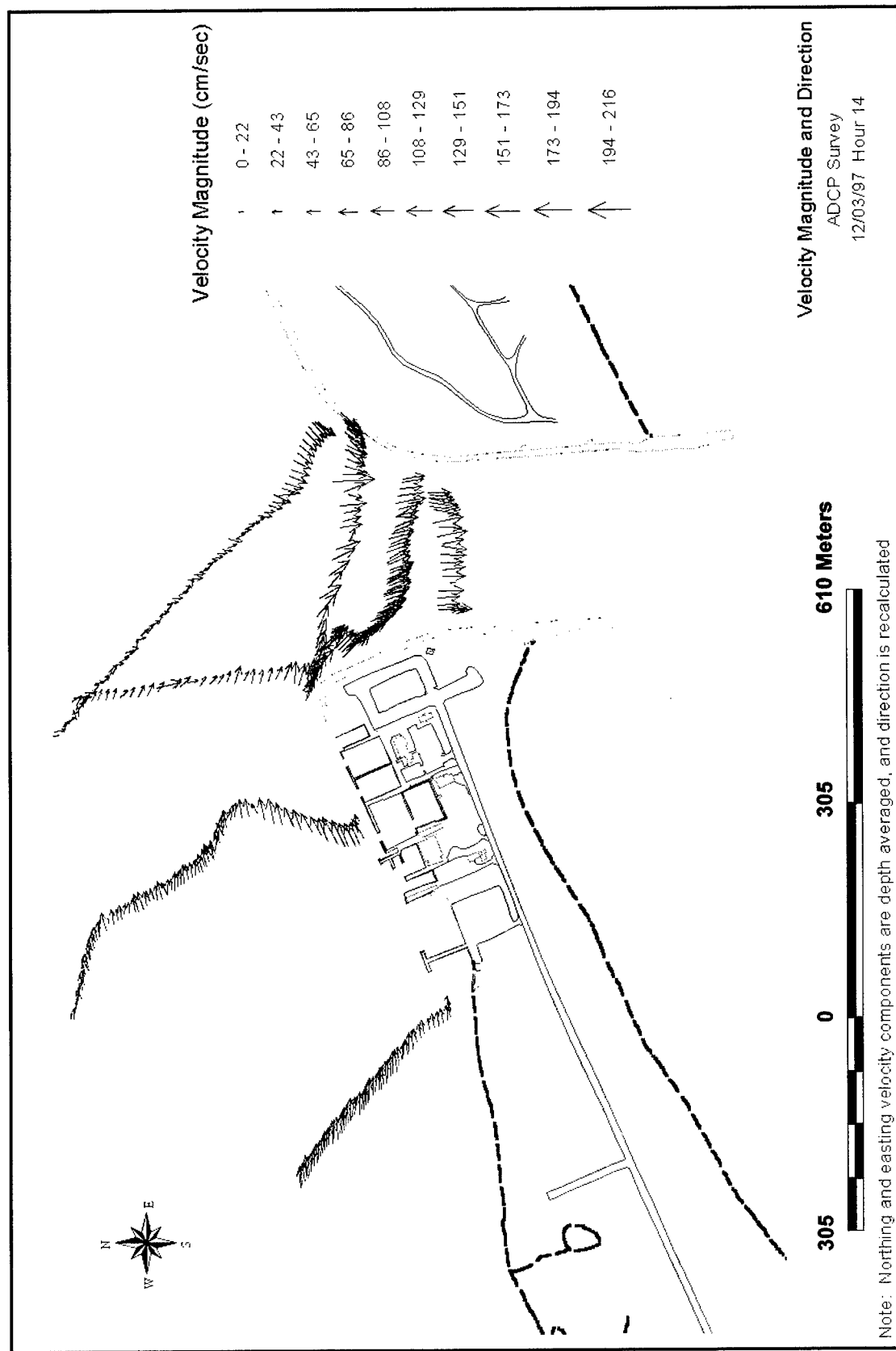
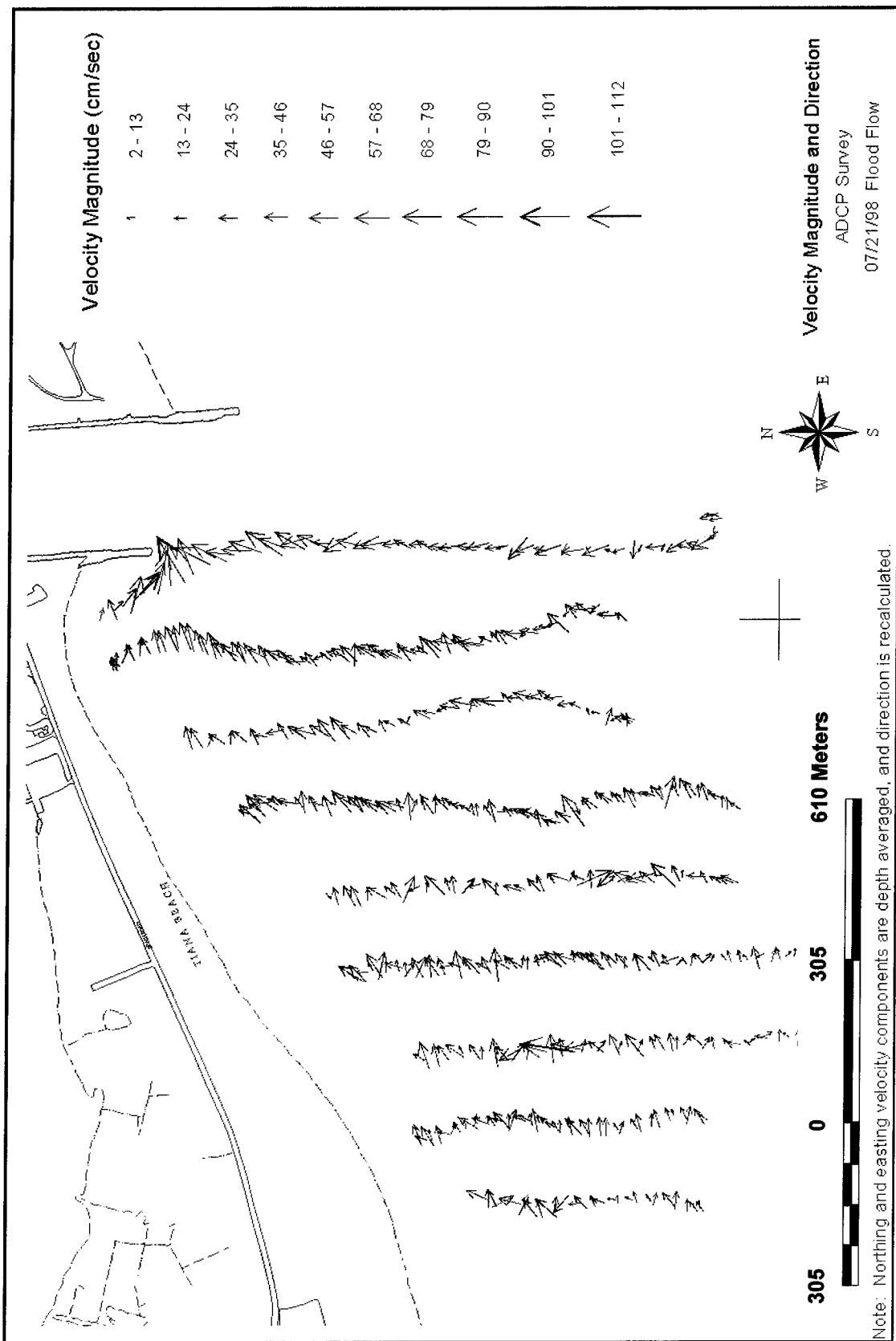


Plate 7



**Plate 8**

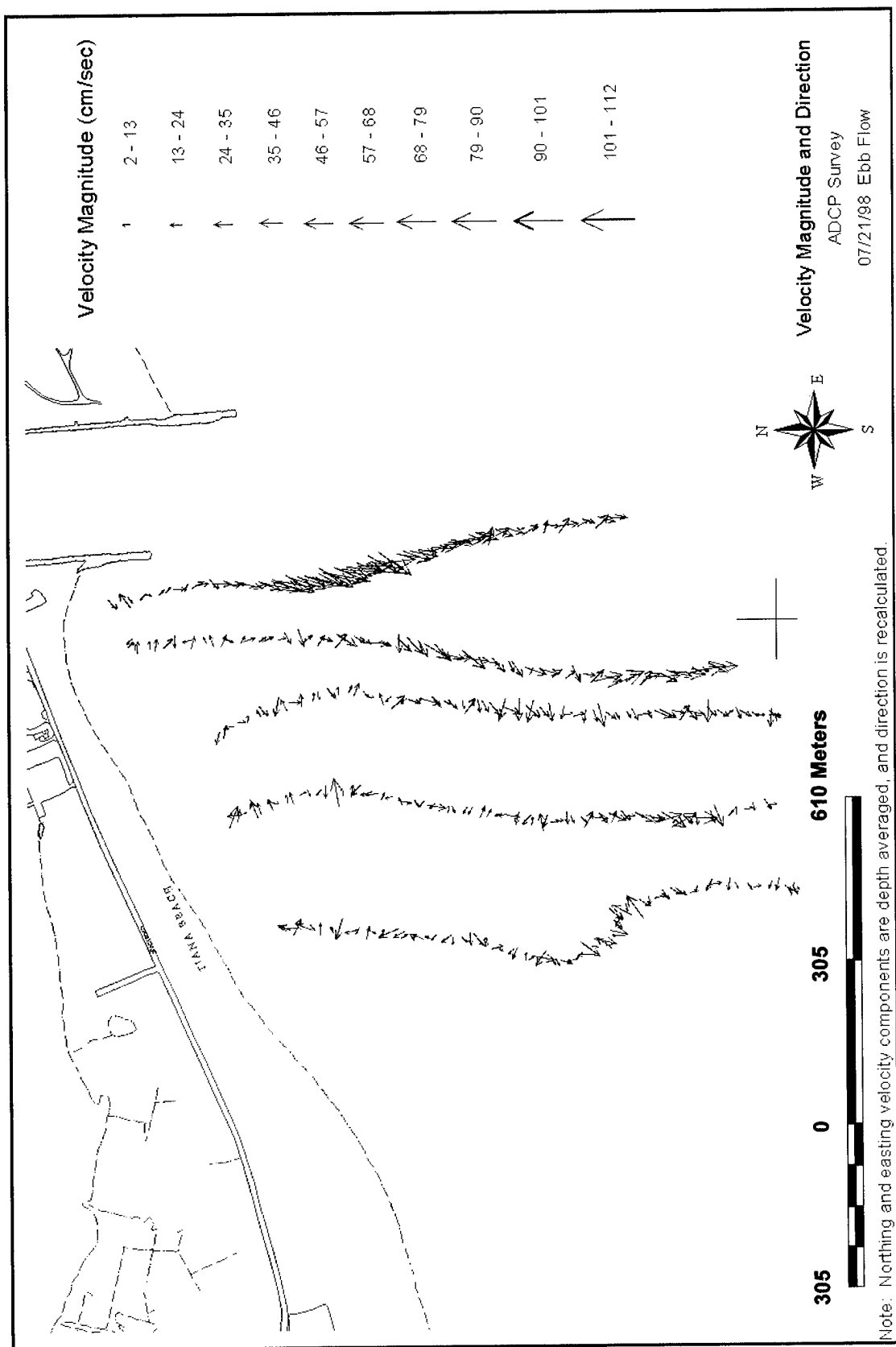
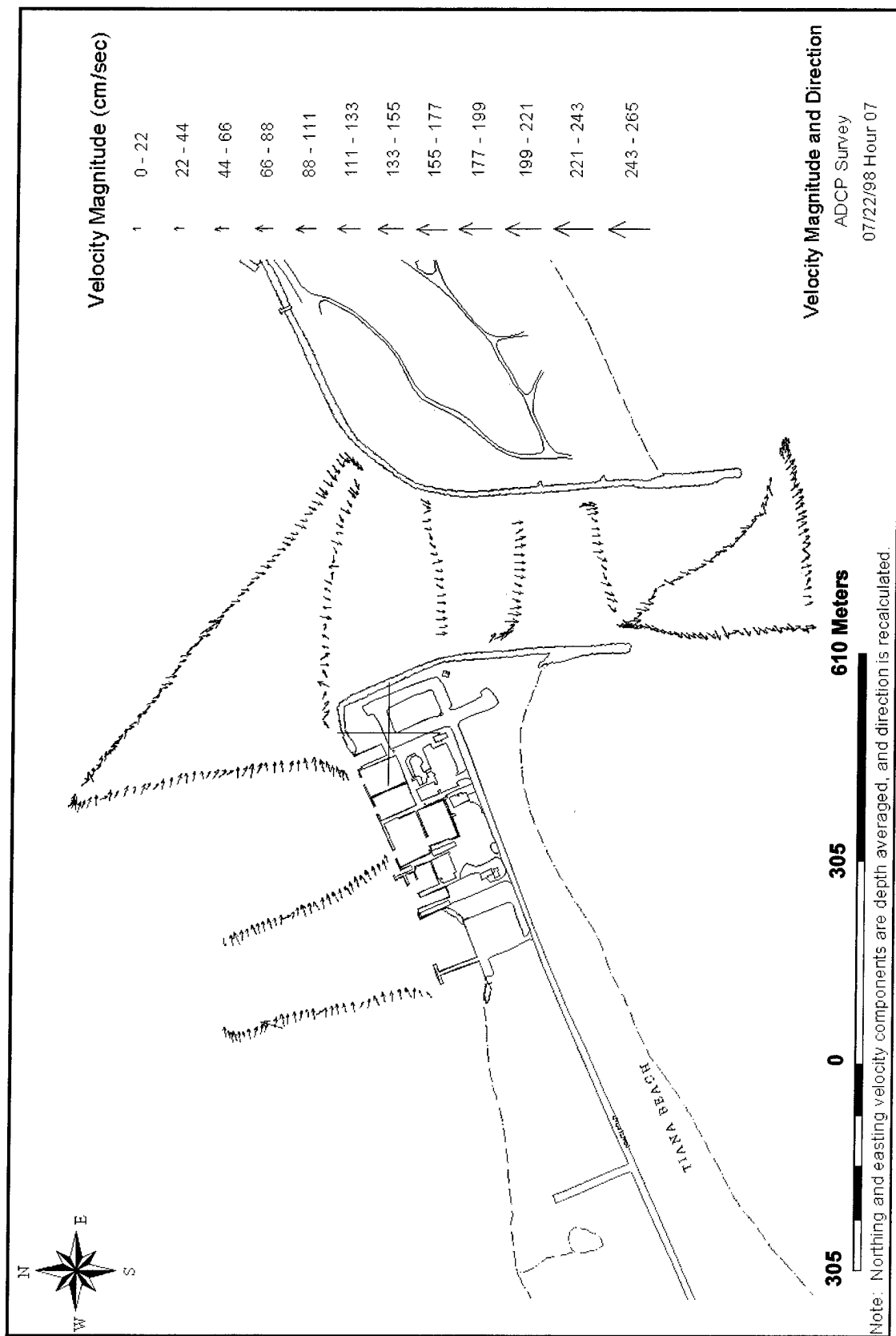


Plate 9



## Plate 10

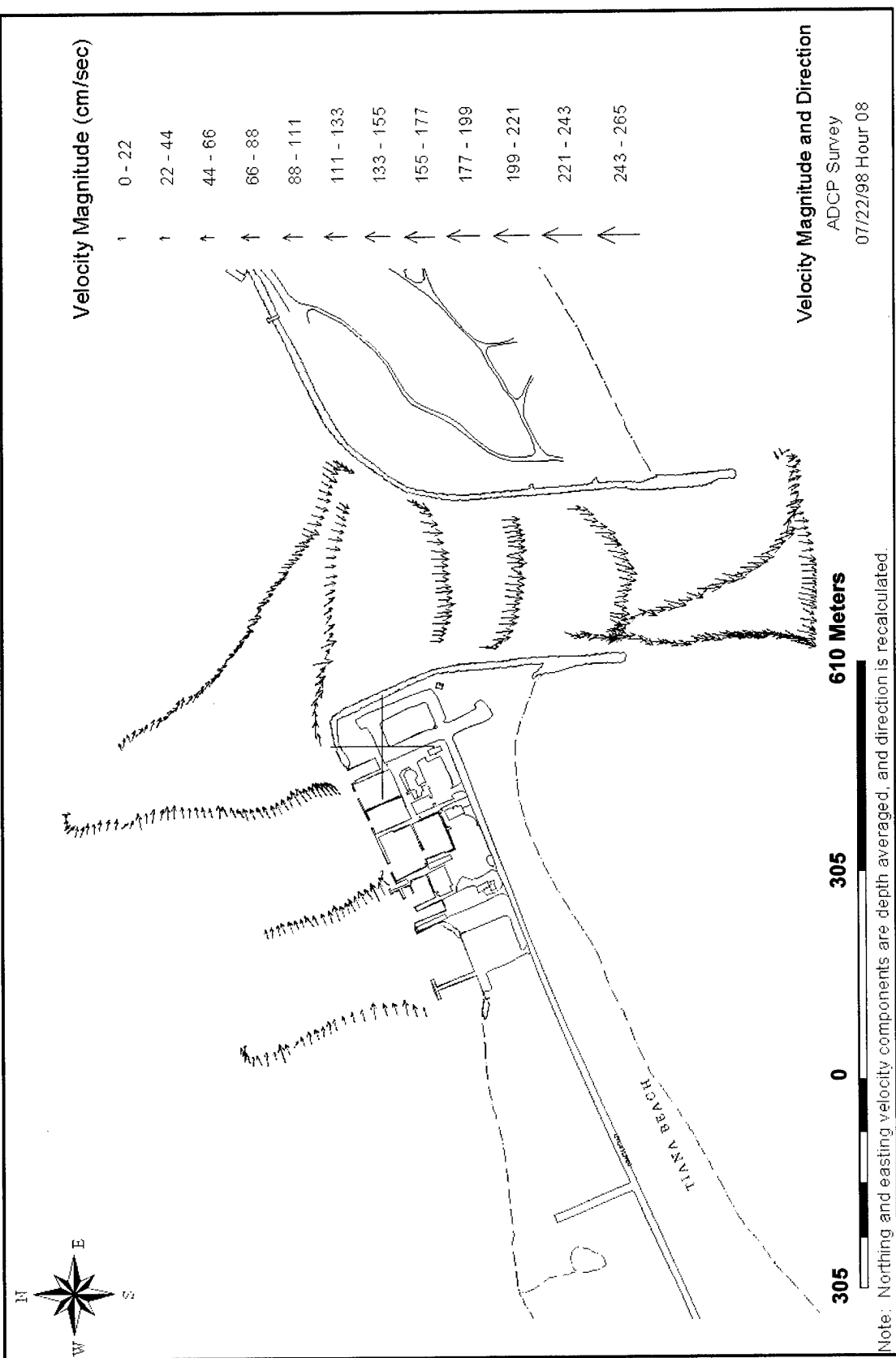
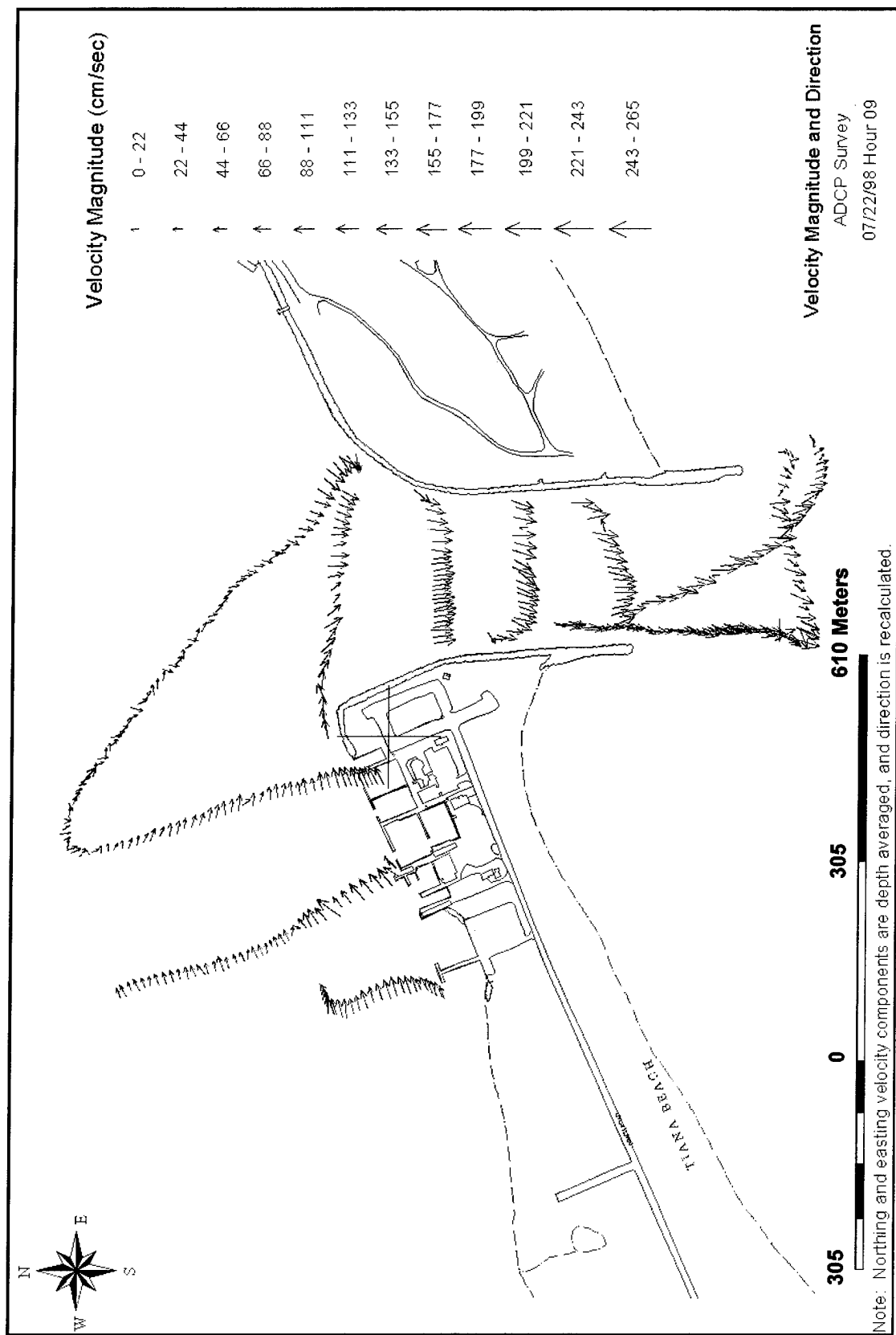
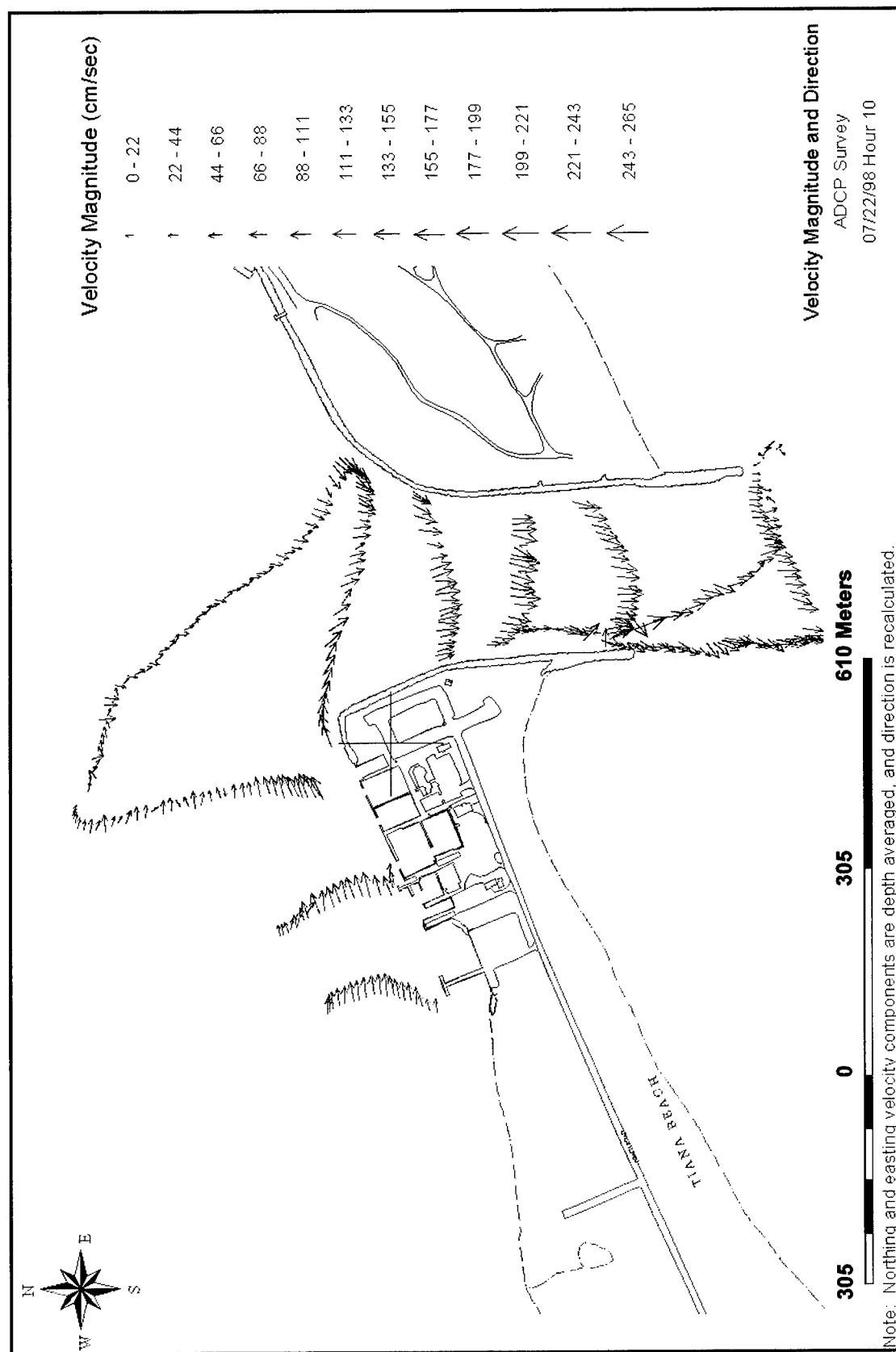


Plate 11



**Plate 12**



## Plate 13

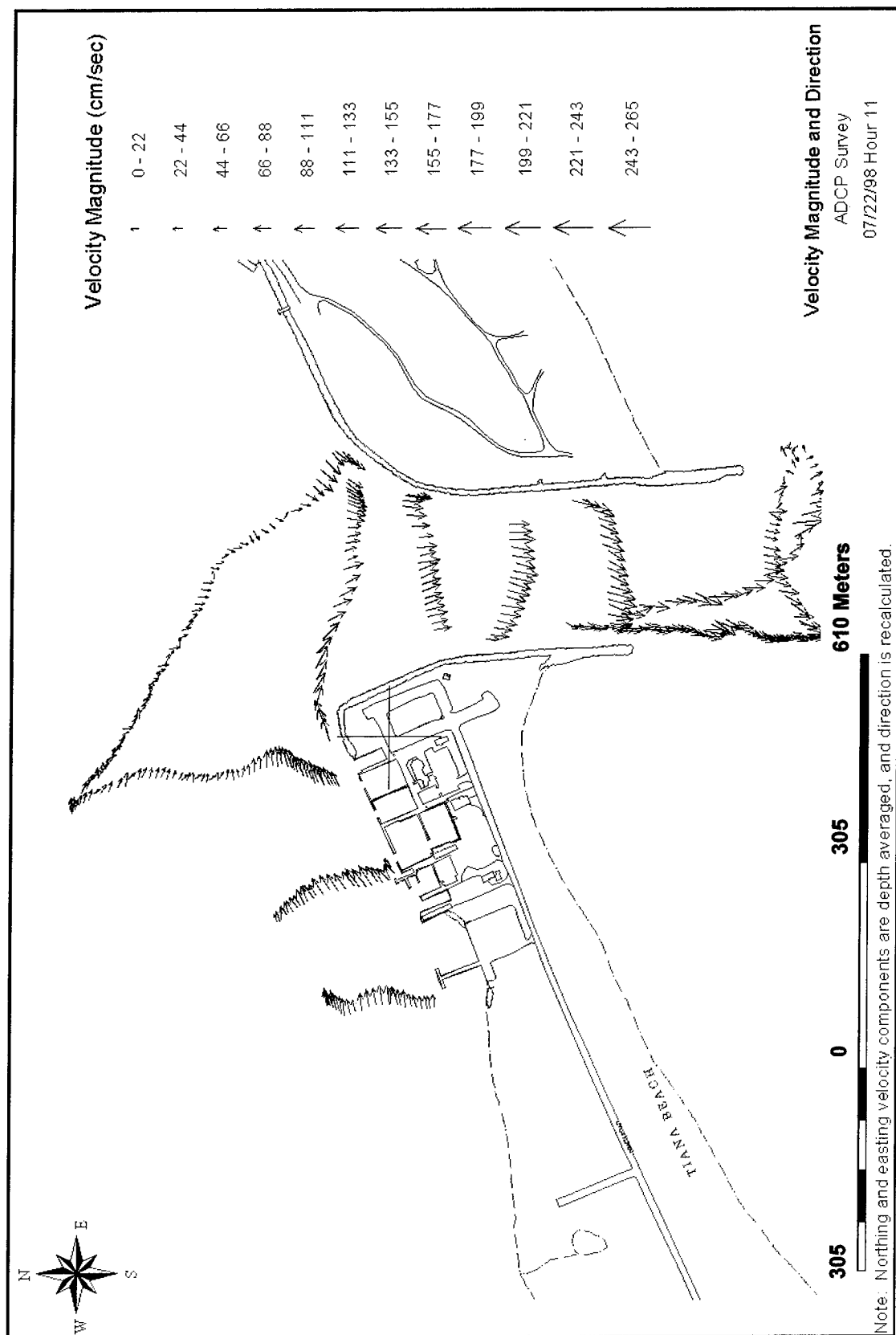


## Plate 14

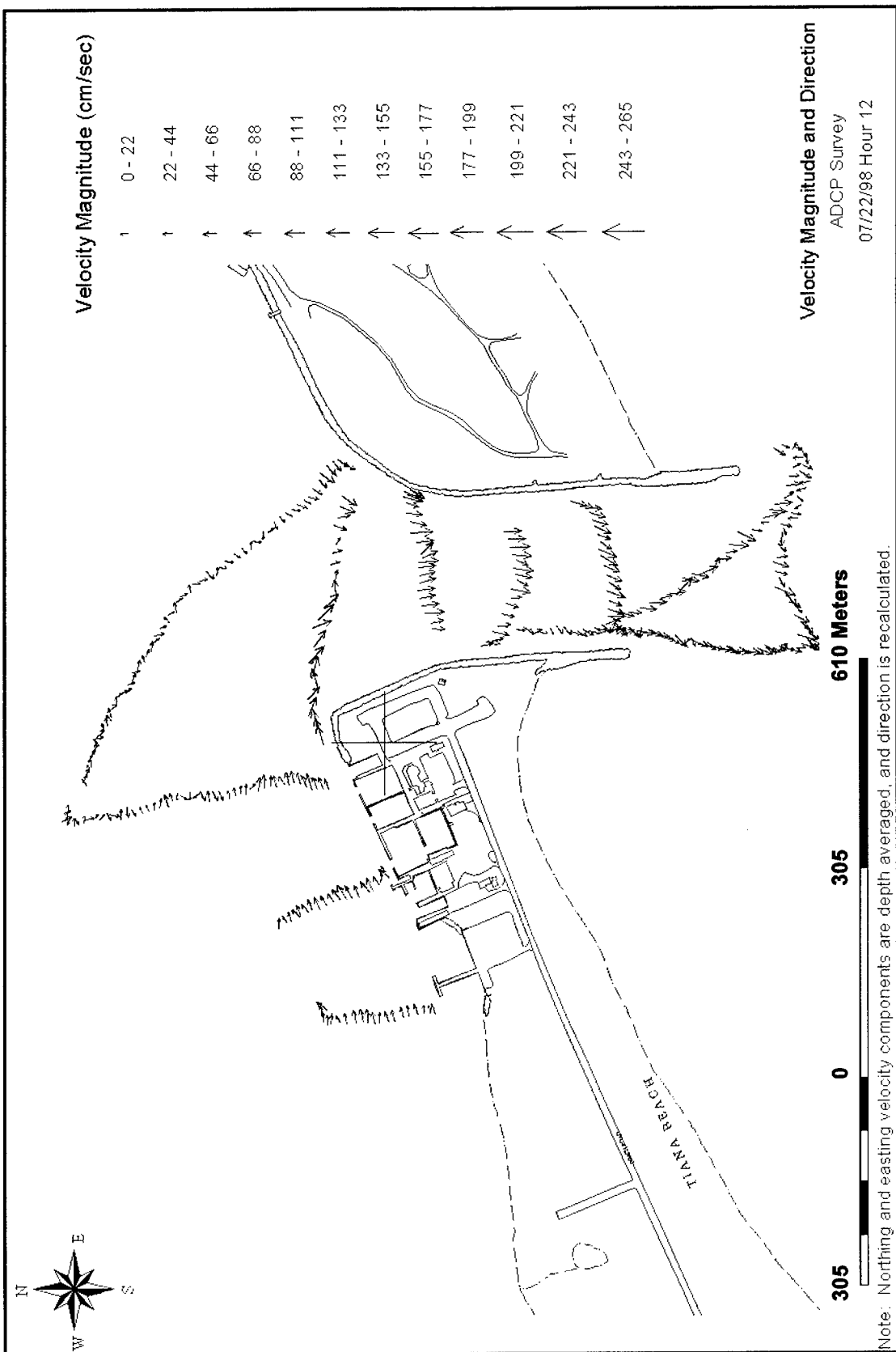


Plate 15

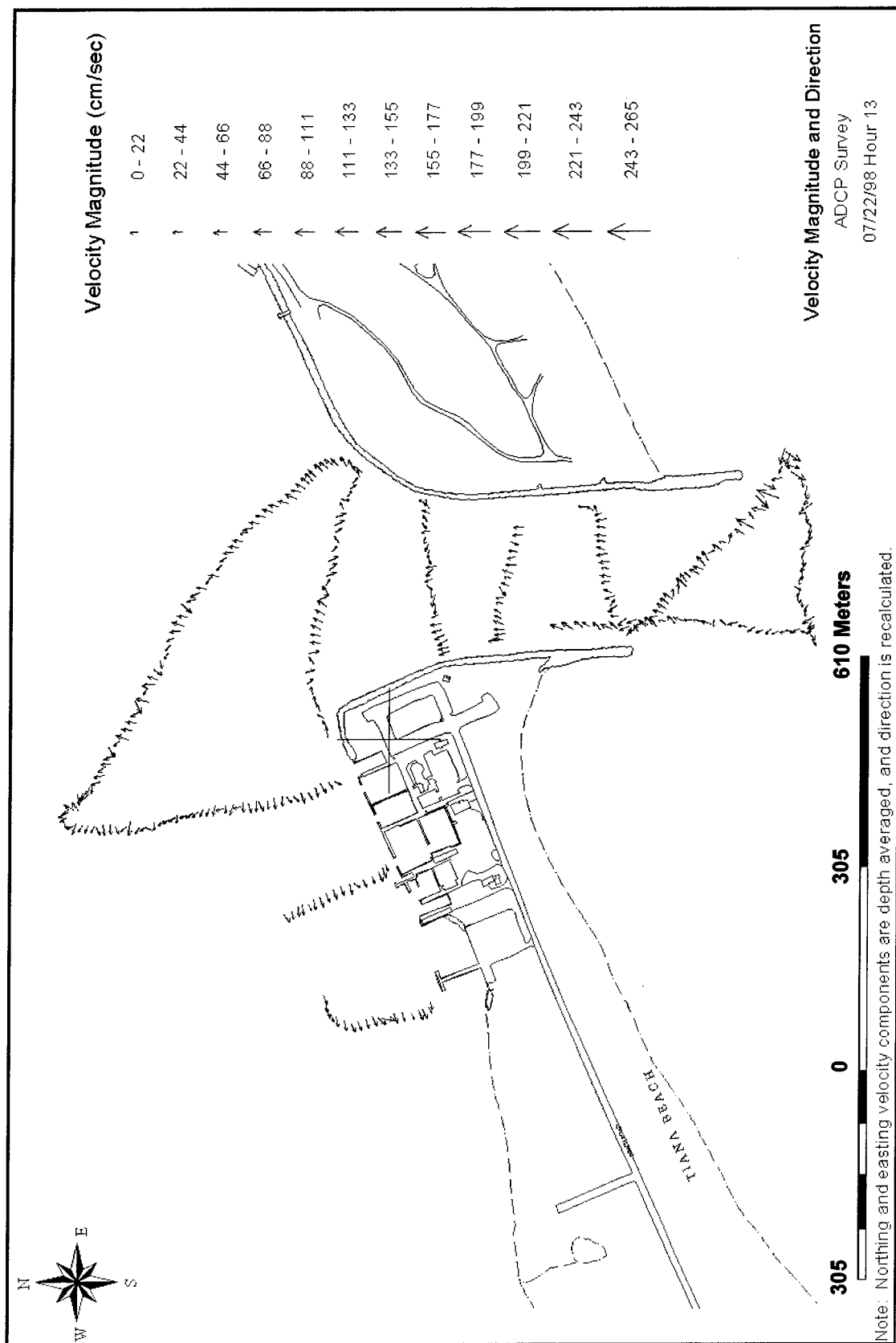


Plate 16

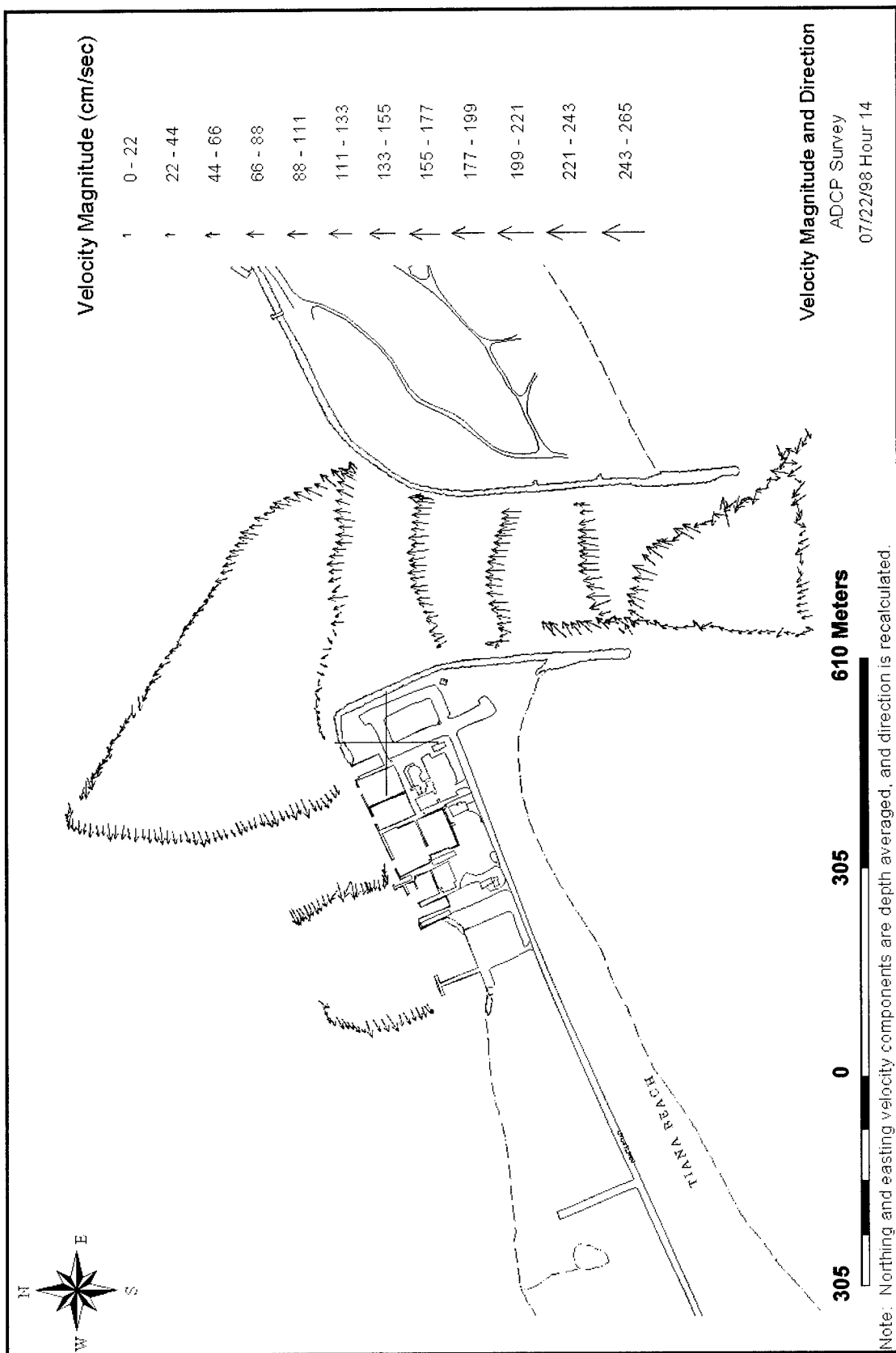


Plate 17

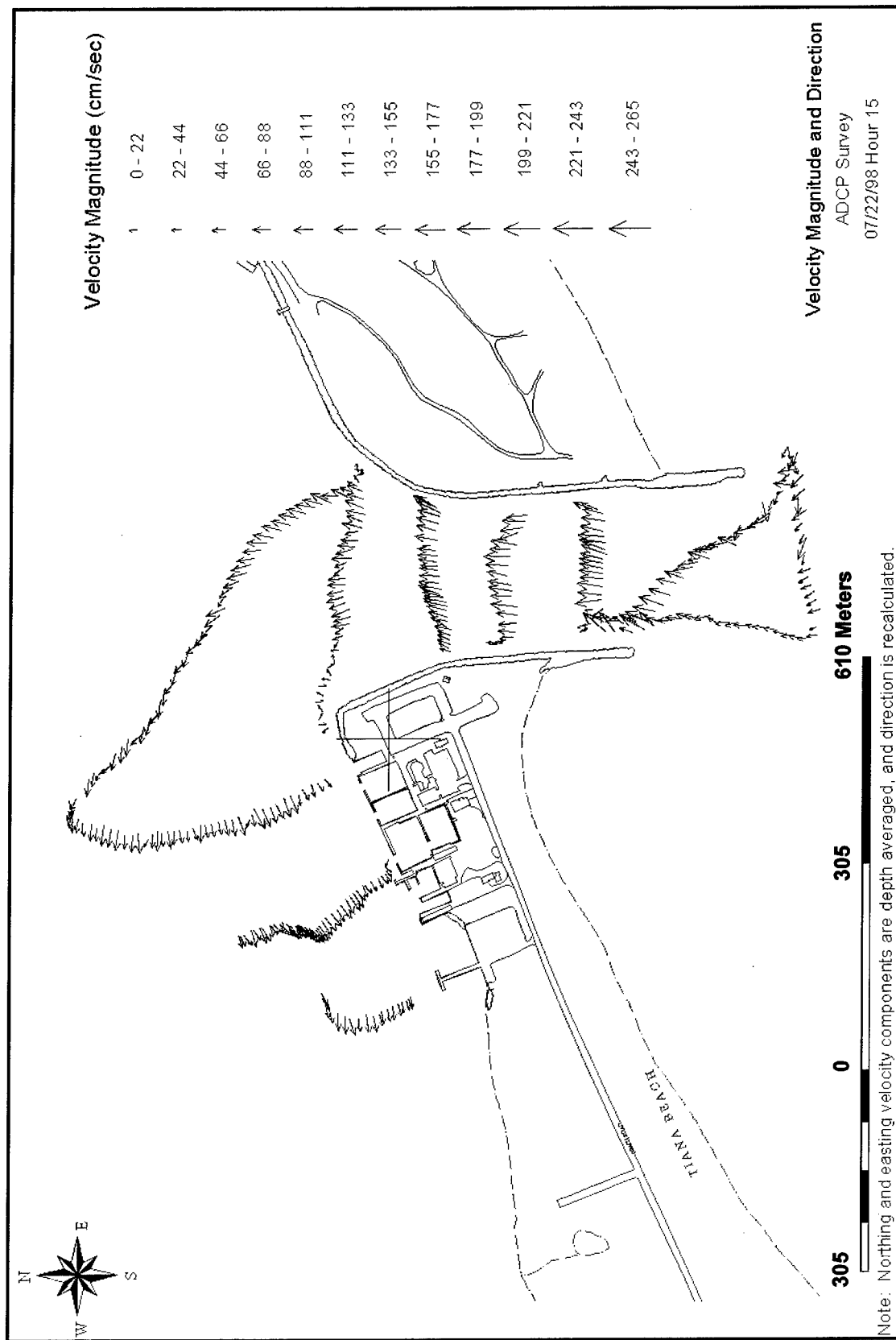
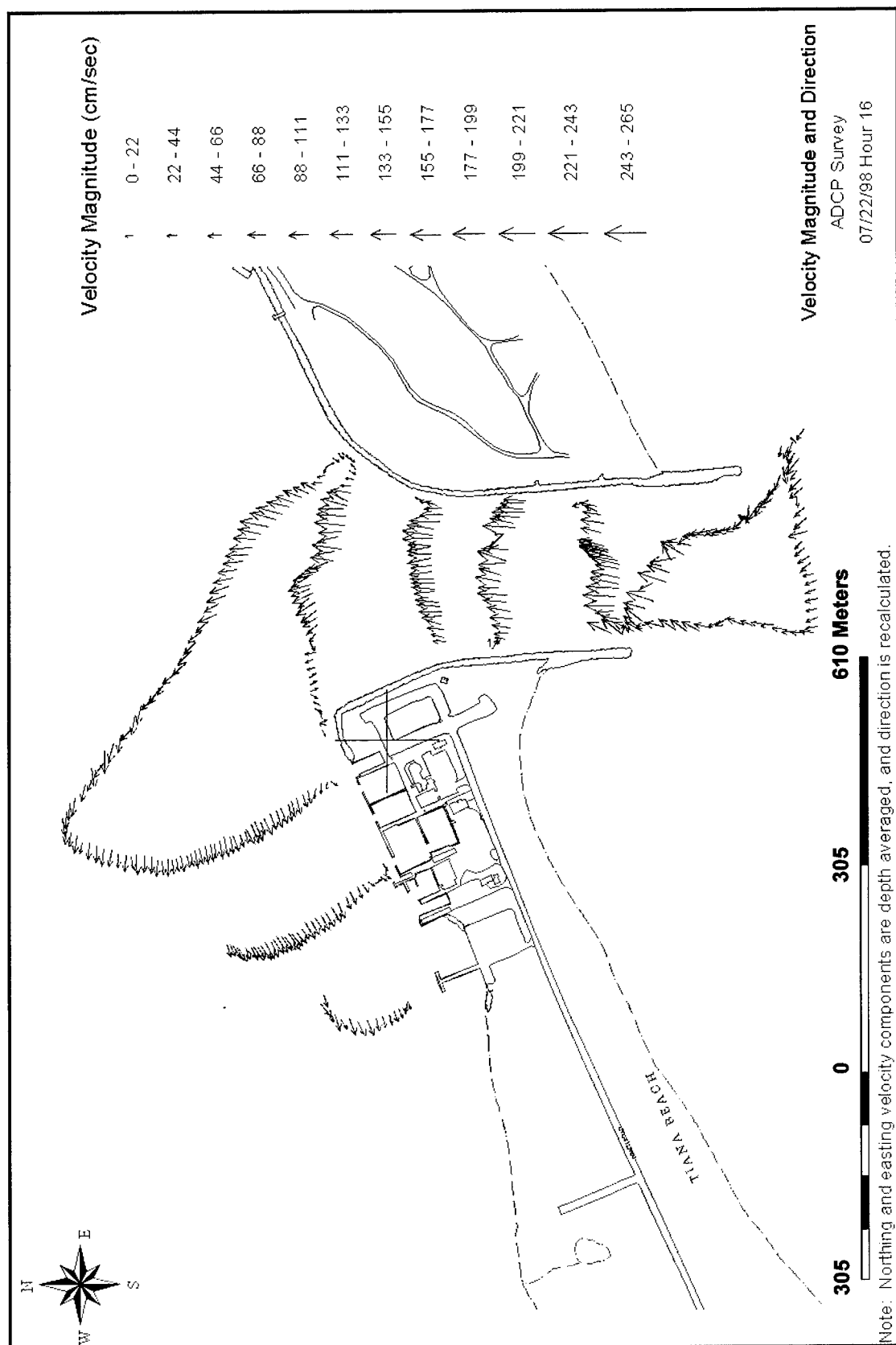
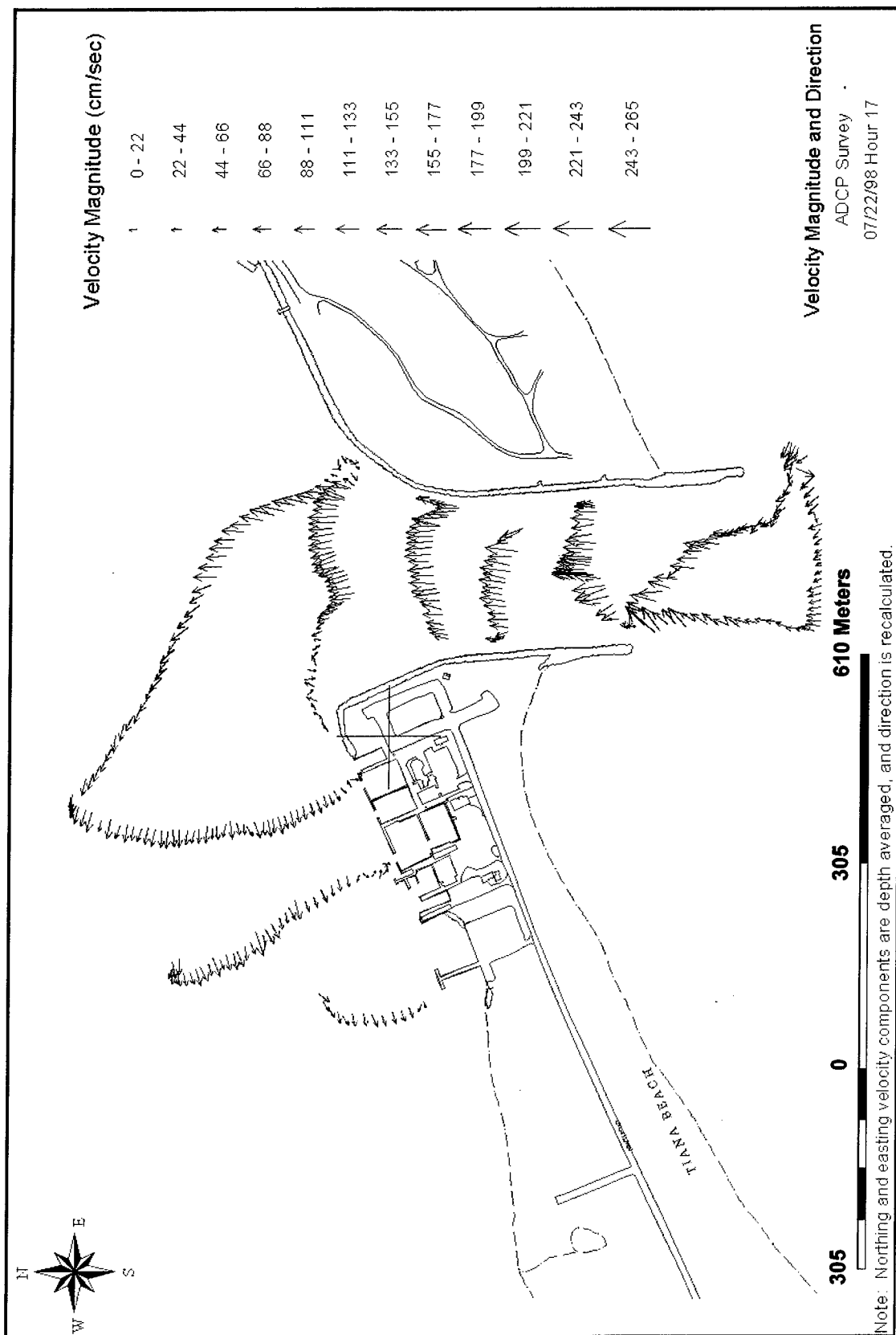


Plate 18



## Plate 19



## Plate 20

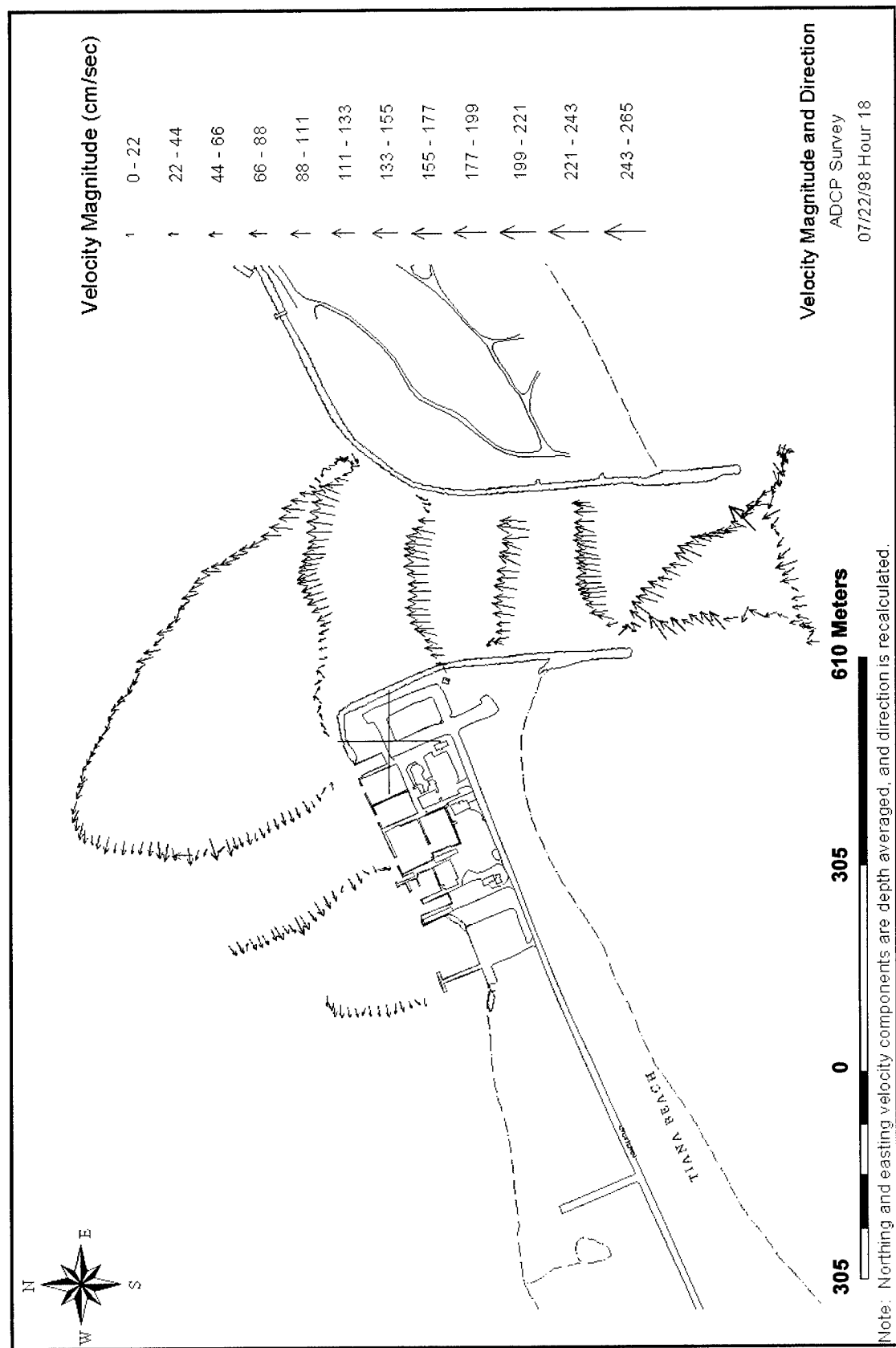


## Plate 21

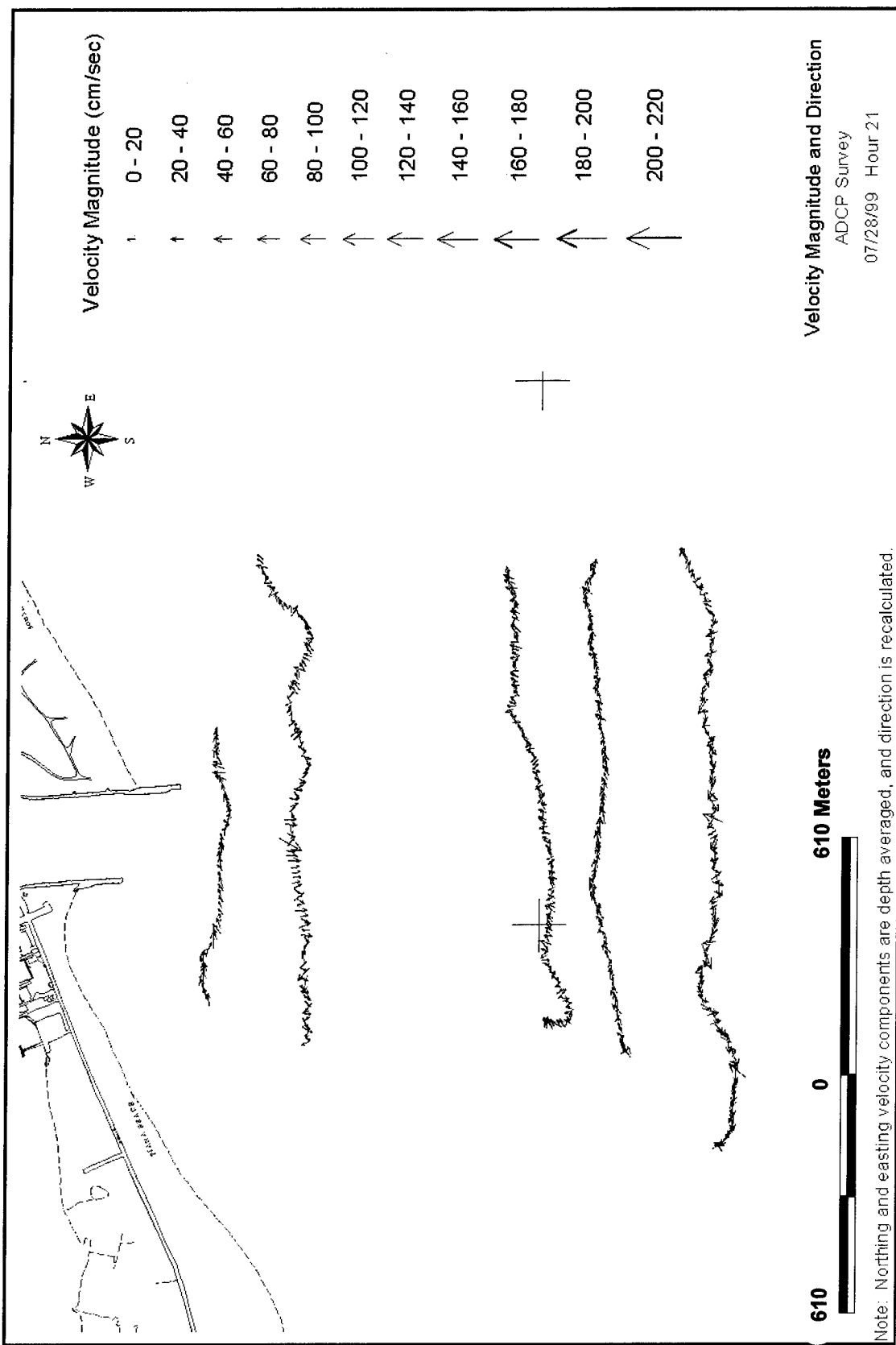


Plate 22

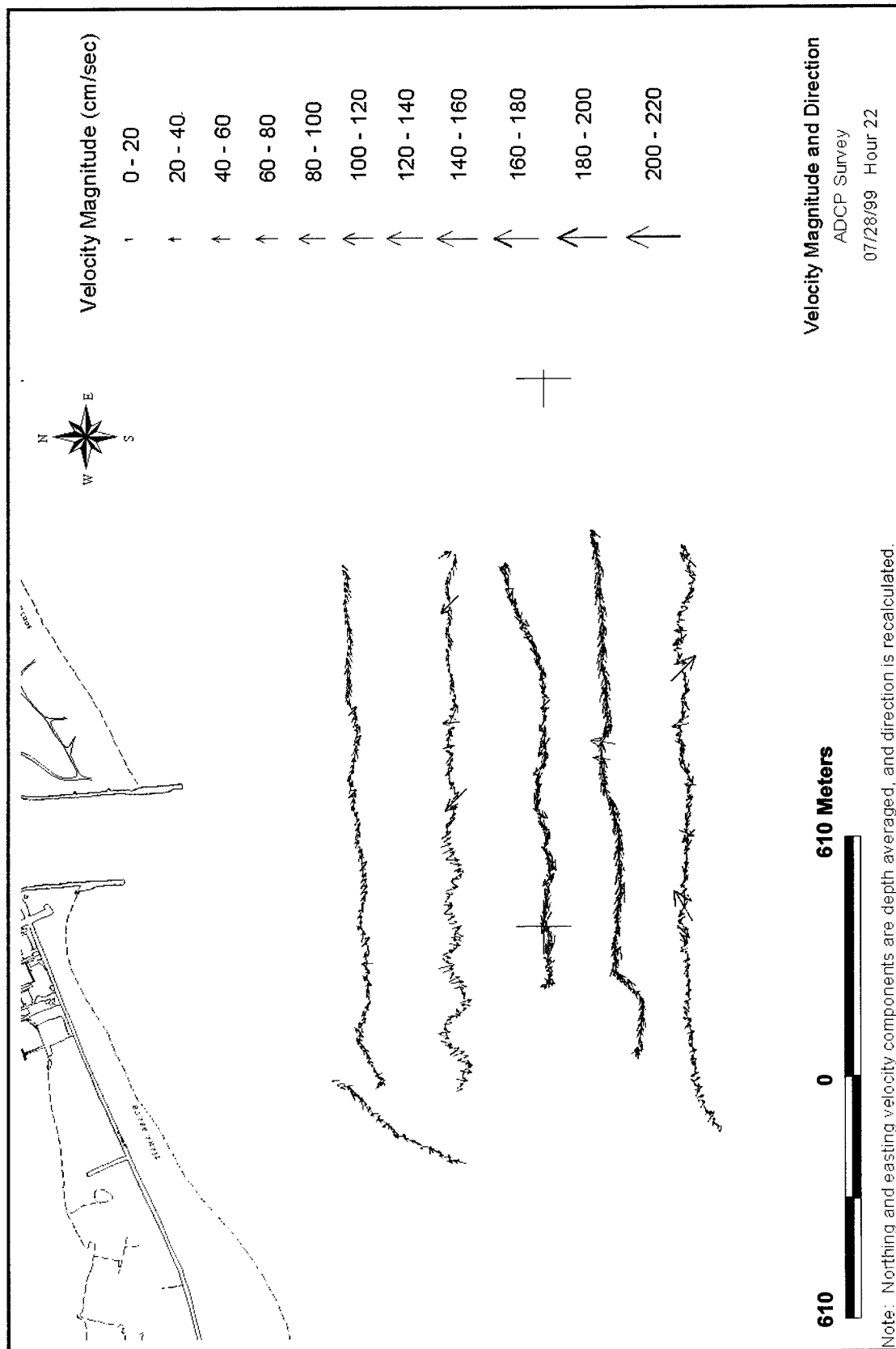
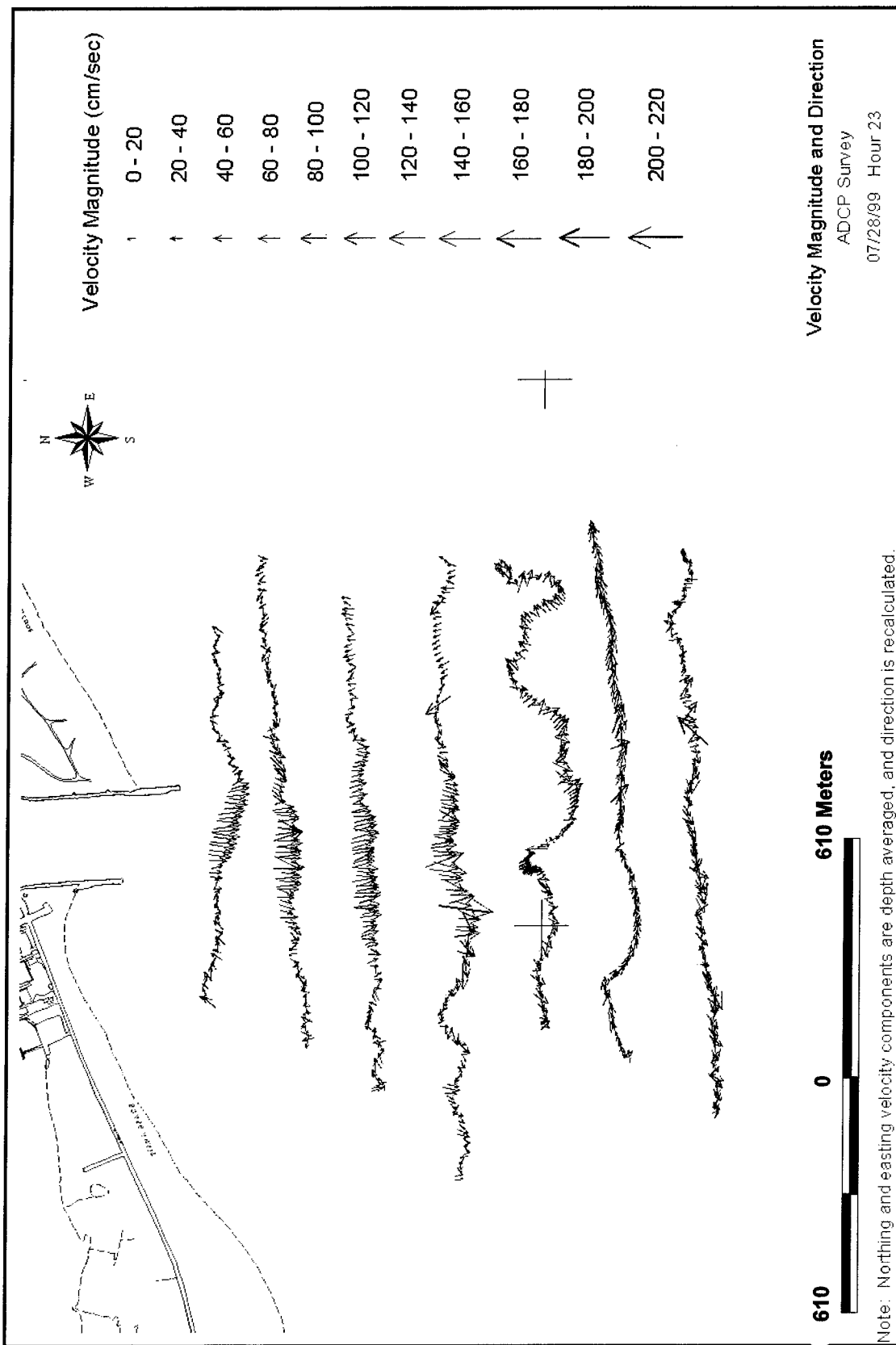


Plate 23



**Plate 24**

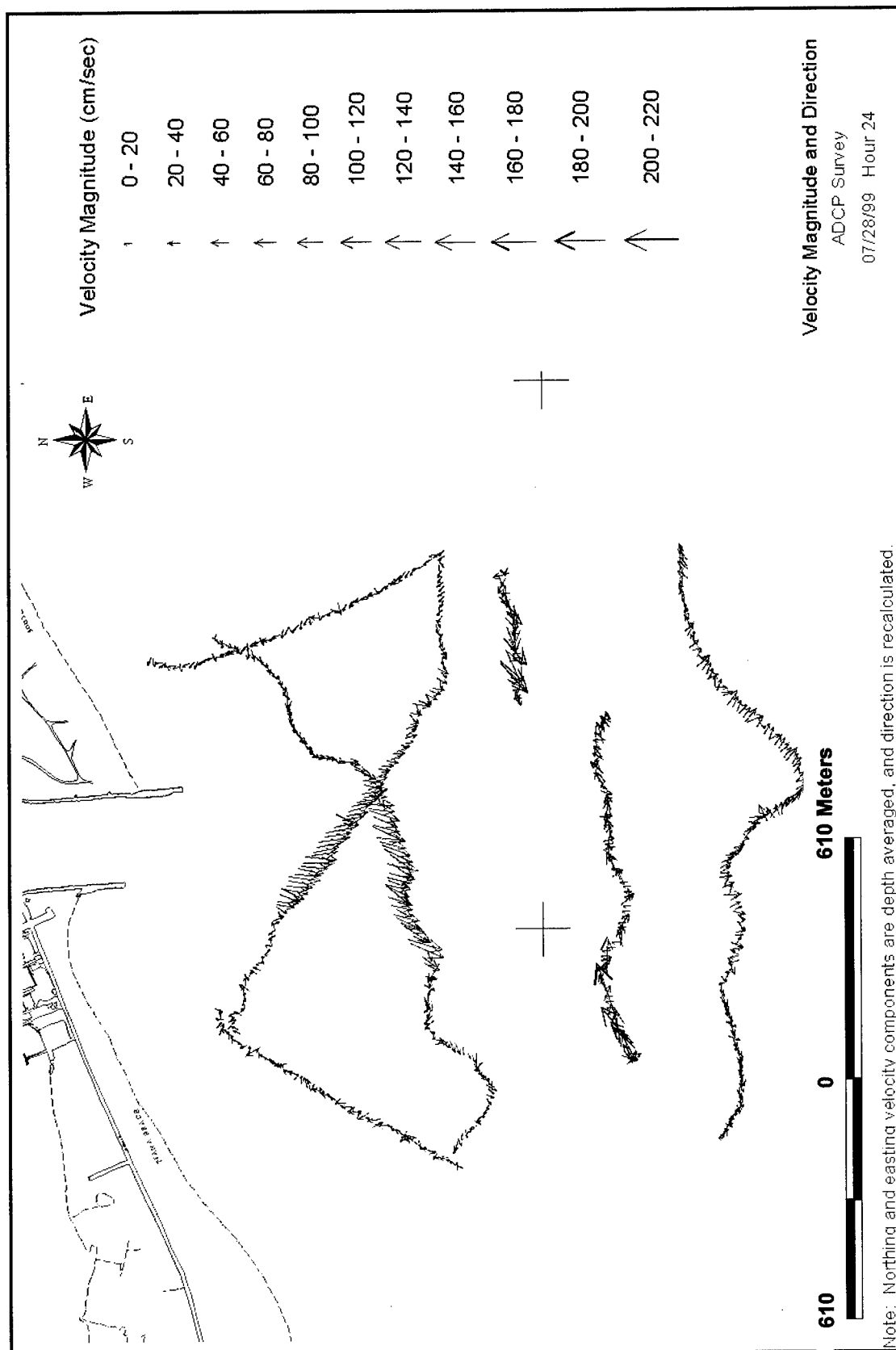


Plate 25

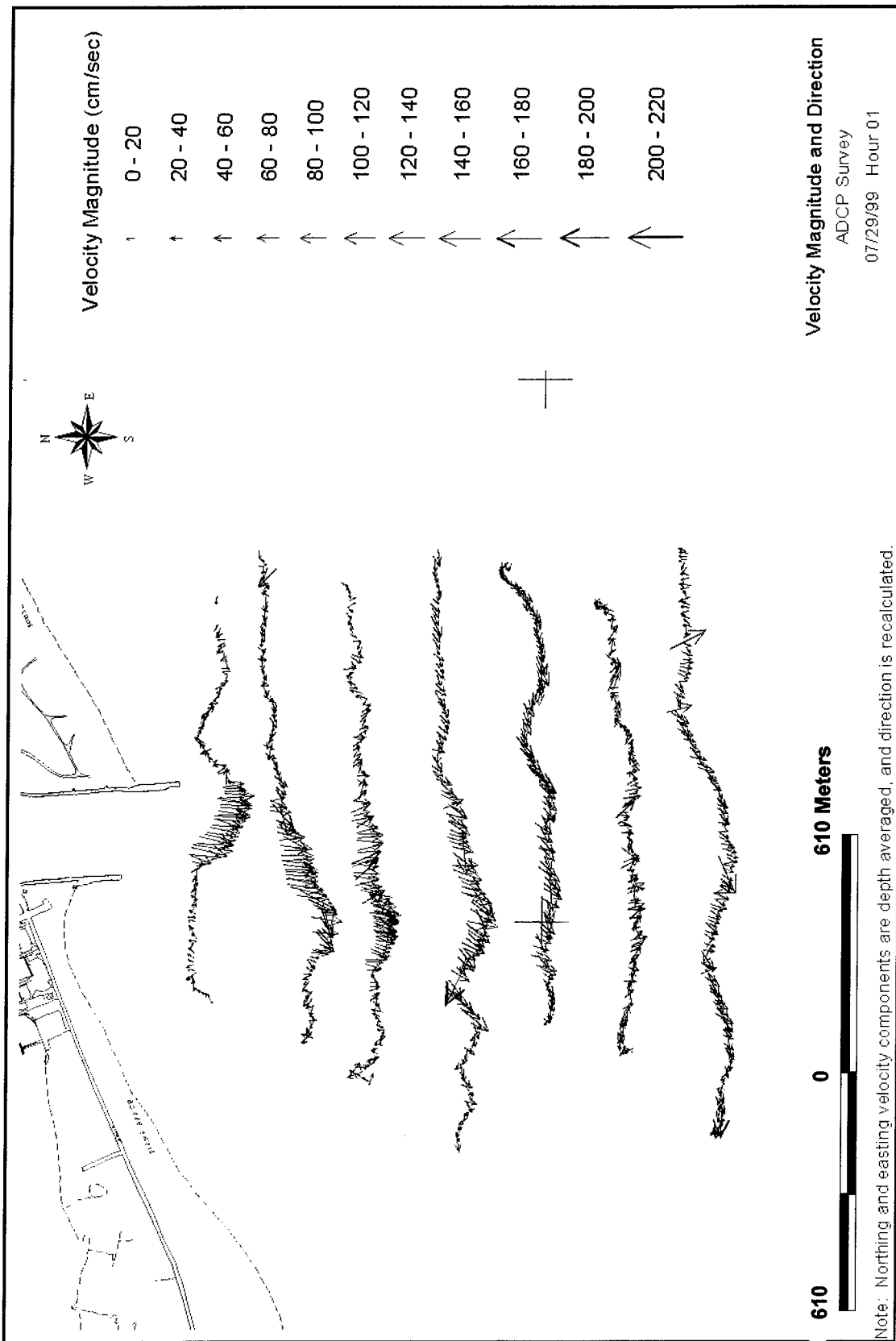


Plate 26

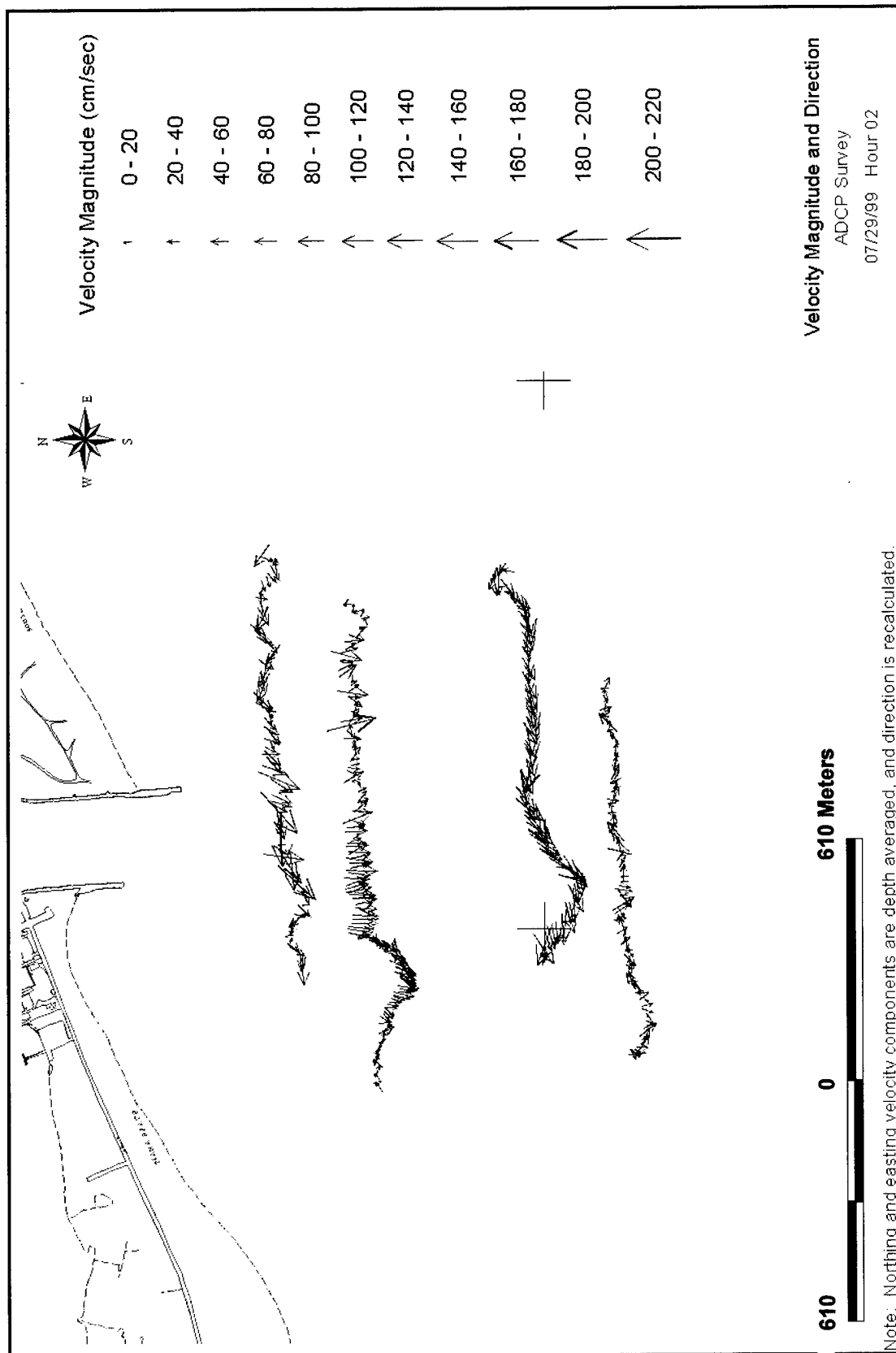


Plate 27

# REPORT DOCUMENTATION PAGE

Form Approved  
OMB No. 0704-0188

Public reporting burden for this collection of information is estimated to average 1 hour per response, including the time for reviewing instructions, searching existing data sources, gathering and maintaining the data needed, and completing and reviewing this collection of information. Send comments regarding this burden estimate or any other aspect of this collection of information, including suggestions for reducing this burden to Department of Defense, Washington Headquarters Services, Directorate for Information Operations and Reports (0704-0188), 1215 Jefferson Davis Highway, Suite 1204, Arlington, VA 22202-4302. Respondents should be aware that notwithstanding any other provision of law, no person shall be subject to any penalty for failing to comply with a collection of information if it does not display a currently valid OMB control number. PLEASE DO NOT RETURN YOUR FORM TO THE ABOVE ADDRESS.

1. REPORT DATE (DD-MM-YYYY) February 2001		2. REPORT TYPE Final Report		3. DATES COVERED (From - To)	
4. TITLE AND SUBTITLE Shinnecock Inlet, New York, Site Investigation Report 3, Selected Field Data Report for 1997, 1998, 1999 Velocity and Sediment Surveys				5a. CONTRACT NUMBER	
				5b. GRANT NUMBER	
				5c. PROGRAM ELEMENT NUMBER	
6. AUTHOR(S) Thad C. Pratt, Donald K. Stauble				5d. PROJECT NUMBER	
				5e. TASK NUMBER	
				5f. WORK UNIT NUMBER	
7. PERFORMING ORGANIZATION NAME(S) AND ADDRESS(ES) U.S. Army Engineer Research and Development Center Coastal and Hydraulics Laboratory 3909 Halls Ferry Road Vicksburg, MS 39180-6199				8. PERFORMING ORGANIZATION REPORT NUMBER Technical Report CHL-98-32	
9. SPONSORING / MONITORING AGENCY NAME(S) AND ADDRESS(ES) U.S. Army Corps of Engineers Washington, DC 20314-1000				10. SPONSOR/MONITOR'S ACRONYM(S)	
				11. SPONSOR/MONITOR'S REPORT NUMBER(S)	
12. DISTRIBUTION / AVAILABILITY STATEMENT Approved for public release; distribution is unlimited.					
13. SUPPLEMENTARY NOTES					
14. ABSTRACT As part of a site investigation of Shinnecock Inlet, Long Island, NY, for the Coastal Inlets Research Program, field-monitoring was conducted during 1997, 1998, and 1999. This fieldwork included ADCP current measurements and sediment sampling in the inlet channel, the Atlantic Ocean encompassing the ebb shoal, and Shinnecock Bay including the navigation channels and flood shoal. The 1997 ADCP surveys focused on the interior channel between the jetties and entrance into the bay. The majority of flood flow went into the west channel and over the flood shoal. On ebb the flow comes predominately from the west channel and impinges on the east jetty creating the interior scour hole. The 1998 and 1999 survey focused more on the ocean side of the jetties. The ebb jet follows the direction of the navigation channel cut through the ebb shoal. In the ocean area west of the west jetty a large-scale eddy seems to rotate clockwise on both phases of the tide. The end of the west jetty has a deep scour hole where the throat flow interacts with this eddy flow. Analysis of the sediment grain size distributions indicated a wide variety of depositional environments, with the coarsest material found in the high energy wave/current interaction between the jetties. Finer material was found on the seaward edge of the ebb shoal and on the landward side of the flood shoal. This combined study of currents and sediment distributions and their relationships to the inlet bathymetry provides a picture of the wave and current-induced circulation and depositional patterns active at Shinnecock Inlet.					
15. SUBJECT TERMS ADCP Data      Sediment samples      Shoals Surveys Inlet              Shinnecock Inlet					
16. SECURITY CLASSIFICATION OF:		17. LIMITATION OF ABSTRACT	18. NUMBER OF PAGES	19a. NAME OF RESPONSIBLE PERSON	
a. REPORT UNCLASSIFIED	b. ABSTRACT	c. THIS PAGE UNCLASSIFIED	83	19b. TELEPHONE NUMBER (include area code)	